



VALIDATION OF THE IONOSPHERIC FORECAST
MODEL (IFM) VERSION 3

THESIS

Michael D. Scott, Captain, USAF

AFIT/GAP/ENP/00M-04

DEPARTMENT OF THE AIR FORCE
AIR UNIVERSITY

AIR FORCE INSTITUTE OF TECHNOLOGY

Wright-Patterson Air Force Base, Ohio

20001113 031

APPROVED FOR PUBLIC RELEASE; DISTRIBUTION UNLIMITED.

The views expressed in this thesis are those of the author and do not reflect the official policy or position of the Department of Defense or the U. S. Government

AFIT/GAP/ENP/00M-04

VALIDATION OF THE IONOSPHERIC FORECAST
MODEL (IFM) VERSION 3

THESIS

Presented to the Faculty
Department of Engineering Physics
Graduate School of Engineering and Management
Air Force Institute of Technology
Air University
Air Education and Training Command
In Partial Fulfillment of the Requirements for the
Degree of Master of Science in Physics

Michael D. Scott, B.S.,
Captain, USAF

March 2000

APPROVED FOR PUBLIC RELEASE; DISTRIBUTION UNLIMITED

VALIDATION OF THE IONOSPHERIC FORECAST
MODEL (IFM) VERSION 3

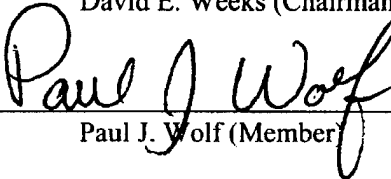
Michael D. Scott, B.S.
Captain, USAF

Approved:



David E. Weeks (Chairman)

2 Mar 00
date



Paul J. Wolf (Member)

2 Mar 00
date



Devin J. Della-Rose (Member)

2 Mar 00
date

Acknowledgments

Thanks go first to my faculty advisor, Dr. David Weeks. His knowledge and experience and his willingness to share them was indispensable. Thanks too go to my committee members, Lt Col Paul Wolf and Maj Devin Della-Rose whose interest, encouragement and sound advice helped to smooth many of the bumps along the way.

A special thanks to Maj Pete Citrone and Mr Kevin Scro at SMC Det 11 and to Maj Kathleen Dowdy at Space Command DOW for their assistance getting this project off the ground. On several occasions it appeared as though this project would never even get started, but the folks out in Colorado Springs always came through. Though I don't know their names, I know there were many other people whose assistance and expertise was tapped on my behalf. A hearty thanks to them as well.

I would like to thank my fellow students, Captains Ariel Acebal and Kelly Doser. Ariel's good humor often provided welcome relief, and helped to keep things in perspective. Thanks to Kelly for taking time away from his own research to get me up and running with the PRISM model, and for answering all of my annoying computer questions.

On a more personal note, I want to thank my mother, Nancy, for her constant encouragement in everything I've attempted. Finally, I must thank my wife Cathy and my children Andrew and Cristina. They more than anyone have suffered through my tour here at AFIT. Their Support and encouragement, not to mention their tolerance of my frequent bad moods, has been greatly appreciated.

Michael D. Scott

Table of Contents

	Page
Acknowledgments	iv
List of Figures	vii
List of Tables	ix
Abstract	xi
1. Introduction	1
1.1 Background	1
1.2 The Ionosphere	2
1.3 Air Force Impact	4
2. The Ionospheric Forecast Model	6
2.1 Initialization Programs	7
2.2 Core Programs	8
2.3 Utility Programs	9
2.4 IFM Physics	9
3. Methodology	11
3.1 Overall Concept of Research	11
3.2 Methodology of IFM Runs	11
3.3 Selection of Stations and Comparison Data	13
3.4 Statistical Methodology	15
3.5 Display and Analysis of Data	17
4. Results and Analysis	19
4.1 Analysis of foF2	19
4.1.1 Seasonal and Geographic Variations	22
4.1.2 Period 1 foF2	24
4.1.3 Period 2 foF2	27
4.1.4 Period 3 foF2	30
4.1.5 Period 4 foF2	34
4.1.6 Period 5 foF2	37
4.1.7 IFM vs. IFMP Error	41
4.2 Analysis of hmF2	43
4.2.1 Period 1 hmF2	46

4.2.2	Period 2 hmF2	49
4.2.3	Period 3 hmF2	52
4.2.4	Period 4 hmF2	55
4.2.5	Period 5 hmF2	59
5.	Conclusions and Recommendations	63
5.1	Conclusions	63
5.1.1	Summary	63
5.1.2	Validation of foF2 Forecasts	63
5.1.3	Validation of hmF2 Forecasts	65
5.2	Recommendations	65
Appendix A	Space Environment Corporation Validation Results.....	67
Appendix B	The Ionosphere	69
Appendix C	PRISM	73
Appendix D	DISS Station Information	74
Appendix E	Additional Charts and Tables.....	77
Appendix F	Glossary of Terms	91
Bibliography.....		95
Vita.....		96

List of Figures

Figure	Page
1. IFM Program Flow.....	6
2. Location of DISS Stations used in validation	13
3. Example Data Comparison Chart.....	17
4. Tashkent 18-19 March foF2 data	24
5. Chung-Li 17-18 March foF2 data	26
6. Chilton 11-12 May foF2 data.....	27
7. Hobart 13-14 May foF2 data.....	30
8. Lerwick 10-11 July foF2 data	32
9. Chung-Li 9-10 July foF2 data	33
10. Tashkent 16-17 September foF2 data.....	34
11. Chung-Li 16-17 September foF2 data.....	36
12. Learmonth 14-15 December foF2 data	38
13. Eglin AFB 13-14 December foF2 data	41
14. Average Absolute Errors (IFM vs. IFMP)	42
15. Chung-Li 18-19 March hmF2 data.....	47
16. Chilton 19-20 March hmF2 data	48
17. Grahamstown 11-12 May hmF2 data.....	50
18. Lerwick 13-14 May hmF2 data	51
19. Grahamstown 10-11 July hmF2 data	52
20. Lerwick 10-11 July hmF2 data.....	55

21. Dixon Island 18-19 September hmF2 data.....	56
22. Tashkent 17-18 September hmF2 data.....	57
23. Chung-Li 13-14 December hmF2 data.....	59
24. Grahamstown 12-13 December hmF2 data.....	61
25. Chilton 10-11 May foF2 data.....	78
26. Chung-Li 18-19 March foF2 data	79
27. Chung-Li 14-15 September foF2 data.....	80
28. Eglin AFB 15-16 September foF2 data.....	81
29. Grahamstown 10-11 July foF2 data	82
30. Grahamstown 13-14 December foF2 data	83
31. Learmonth 14-15 September foF2 data.....	84
32. Learmonth 13-14 December foF2 data	85
33. Lerwick 10-11 July foF2 data	86
34. Tashkent 13-14 May foF2.data	87
35. Townsville 17-18 September foF2 data	88
36. Chung-Li 18-19 September hmF2 data.....	89
37. Grahamstown 18-19 September hmF2 data	90
38. Lerwick 11-12 May hmF2 data.....	91
39. Tashkent 11-12 May hmF2 data.....	92

List of Tables

Table	Page
1. Example Data Comparison Table	18
2. Global Indices Used to Initialize the IFM	20
3. foF2 Statistics (averaged over all stations and periods).....	20
4. foF2 Statistics (averaged over each period for each station)	21
5. Average Statistics Grouped By Region.....	23
6. Tashkent 18-19 March foF2 data	25
7. Chung-Li 17-18 March foF2 data	26
8. Chilton 11-12 May foF2 data	28
9. Hobart 13-14 May foF2 data.....	29
10. Lerwick 10-11 July foF2 data	31
11. Chung-Li 9-10 July foF2 data	33
12. Tashkent 16-17 September foF2 data.....	35
13. Chung-Li 16-17 September foF2 data.....	37
14. Learmonth 14-15 December foF2 data	39
15. Eglin AFB 13-14 December foF2 data	40
16. hmF2 Statistics (averaged over each period for all stations)	44
17. hmF2 Statistics (averaged over each period for each station).....	45
18. Chung-Li 18-19 March hmF2 data.....	46
19. Chilton 19-20 March hmF2 data	48
20. Grahamstown 11-12 May hmF2 data.....	49

21. Lerwick 13-14 May hmF2 data	51
22. Grahamstown 10-11 July hmF2 data	53
23. Lerwick 10-11 July hmF2 data.....	54
24. Dixon Island 18-19 September hmF2 data.....	56
25. Tashkent 17-18 September hmF2 data.....	58
26. Chung-Li 13-14 December hmF2 data.....	60
27. Grahamstown 12-13 December hmF2 data.....	61
28. Chilton 10-11 May foF2 data.....	78
29. Chung-Li 18-19 March foF2 data	79
30. Chung-Li 14-15 September foF2 data.....	80
31. Eglin AFB 15-16 September foF2 data.....	81
32. Grahamstown 10-11 July foF2 data	82
33. Grahamstown 13-14 December foF2 data	83
34. Learmonth 14-15 September foF2 data.....	84
35. Learmonth 13-14 December foF2 data	85
36. Lerwick 10-11 July foF2 data	86
37. Tashkent 13-14 May foF2.data	87
38. Townsville 17-18 September foF2 data	88
39. Chung-Li 18-19 September hmF2 data.....	89
40. Grahamstown 18-19 September hmF2 data	90
41. Lerwick 11-12 May hmF2 data.....	91
42. Tashkent 11-12 May hmF2 data.....	92

Abstract

The purpose of this research was to validate the Ionospheric Forecast Model (IFM) Version 3 to assess its suitability and usefulness as an operational tool. The Ionospheric forecast model is a first principles computer model designed to forecast the state of the global ionosphere to 24 hours. The scope was limited to a comparison of the F2 layer critical frequency ($foF2$) and peak electron density ($hmF2$) against observed ionosonde data. The model was run with global solar and geomagnetic indices and Information from Digital Ionospheric Sounding System (DISS) observations as inputs. The DISS observations were input through the Parameterized Real-Time Ionospheric Specification Model (PRISM). The IFM was run for a total of 25 days. It was run twice for each 24-hour period: once by starting with only an initial specification of the ionosphere from an empirical model, and again, with an initial specification from the PRISM model with DISS data as an input. As many as 50 DISS stations were used as inputs to the PRISM model, and IFM output was compared against the observations from 10 of the 50 stations. Analysis of the $foF2$ showed that the IFM output was, on average, was within 1 MHz of observed values, and showed a slight bias to over forecast. Correlation between predictions and observations was generally about 0.8. Analysis of the $hmF2$ data showed a tendency for the model to under forecast the values. $hmF2$ forecasts were characterized by large errors and poor correlation between predicted and observed values. There was surprisingly little difference between the results with DISS input and without. The model does not seem to heavily weight the observed data input through PRISM.

Validation of the Ionospheric Forecast Model (IFM) Version 3

1. Introduction

1.1 Background

The Ionospheric Forecast Model (IFM) is a first principles computer model designed to forecast the state of the ionosphere on a global scale. This model has existed in various versions for several years, but is not used operationally at this time. The IFM is a global ionospheric model. It provides up to a 24-hour forecast in increments as small as 30 minutes for the global distribution of N_2^+ , O_2^+ , NO^+ and O^+ densities, electron and ion temperatures, heights and plasma frequencies of electron density peaks, and Total Electron Content (TEC) between 90 and 1600 km. Additionally, the model contains simple algorithms for predicting H^+ density in the F region and a magnetic Kp index. Output from the model is produced on a user-specified grid. Some outputs can be obtained for specific locations based on user-input latitude and longitude coordinates. The IFM requires as inputs the neutral gas parameters such as temperature, density and winds; electric fields; magnetic fields; auroral electron precipitation; and topside electron heat flux. (Schunk et al, 1997: v-1)

The IFM has a vertical spatial resolution of 4 km in the E region and 20 km in the F region; it calculates and produces output data at each of these levels. IFM takes into account all important ionospheric processes, including field-aligned diffusion, cross-field electrodynamic drifts, thermospheric winds, protonospheric exchange fluxes, energy dependent chemical reactions, neutral composition changes, major ion production

sources, electron thermal conduction, many local heating and cooling processes, and the offset between geomagnetic and geographic poles. (Schunk et al, 1997: 1)

The IFM differs from most other ionospheric models in that it is a physics based forecast model and not a climatologically or empirically based specification model. The IFM represents an attempt to forecast the state of the ionosphere based on the actual physics and chemistry believed to shape that region of the atmosphere. The IFM requires as user inputs some of the global parameters that define solar and geomagnetic activity, and an initial specification of the ionosphere either from a specification model, observed data, or a combination of both. Details of the IFM are discussed in Chapter 2.

1.2 The Ionosphere

The ionosphere is that region of the atmosphere where incident solar radiation causes photoionization leading to a weakly ionized gas. In polar latitudes, high-energy particle collisions also contribute to the ionization process. The ionosphere is roughly defined as the region between 70 km and 2000 km altitude. Ionization persists in this region, even at night, due to the relatively low gas density that inhibits the recombination process. The ionosphere is further subdivided into regions of peak ion concentration. IFM recognizes the E, and F regions which roughly correspond to altitudes of 110 km and 300 km respectively. (Tascione, 1994: 89-92 and Rees, 1989: 1-4)

The ionosphere is a very dynamic region with ion concentrations being highly dependent on solar energy and particle fluxes. Time evolution of the ionosphere follows a regular diurnal cycle with other variations due to solar and geomagnetic activity superimposed on this diurnal pattern. Typical ion concentrations within the ionosphere

range between 10^4 and 10^6 cm^{-3} depending on altitude as well as other factors already mentioned. (Tascione, 1994: 99-100) The primary neutral species that make up the ionosphere are N₂, O₂ and O. The primary ions are N₂⁺, O₂⁺, NO⁺ and O⁺. Ionospheric plasma is quasi-neutral with the number of free electrons approximately equal to the number of positive ions. Ionospheric parameters are measured in many ways. A relatively dense network of ionosondes provides a vertical profile of electron densities by vertically transmitting pulses of RF energy in the frequency range from 1 to 20 MHz. Density and height are then determined from the frequency of the signal and the time delay between transmission and when the reflected signal is received back at the earth's surface. (Unfortunately, ionosondes can only provide data when electron density is increasing with height). Consequently, ionosondes only give a profile up to the peak within each region, and provide no information beyond the peak in the F region (approximately 300km). Another ground-based method for remotely determining electron density profiles in the ionosphere is by use of incoherent backscatter radar. This method uses a short pulse of microwave energy, and measures the weak backscattered waves from electrons in the ionosphere. The electron density is proportional to the strength of the backscattered signal, and the round trip time of the pulse gives altitude. This method provides a more continuous profile, and yields information beyond the peak in the F region. *In situ* measurements can be made by satellites orbiting within the ionosphere and by rocketsondes. Satellites can also be used to obtain remote soundings from above the ionosphere. (Tascione, 1994: 116-117)

The ionosphere is important for a number of reasons. Neutral gases in the ionosphere filter for solar UV and EUV radiation and prevent much of it from reaching

the earth's surface. The ionized plasma of the ionosphere reflects radio waves in the high frequency (HF) region of the electromagnetic spectrum and refracts radio waves above this range. This makes long range HF communications possible, but can have adverse effects on communications signals between satellites and space vehicles, and the earth. Additionally, heating and cooling of the ionosphere leads to expansion and contraction which causes density variations along the orbital paths of satellites in this region. Unanticipated changes in drag can seriously alter orbital positions and speeds. (Tascione, 1994: 119-128 and Shea, 1998: 34)

1.3 Air Force Impact

The technological evolution of the Air Force has led to an ever increasing dependence on space based platforms for navigation, observations and communication. All of these systems can be dramatically impacted by the state of the ionosphere. A robust capability to forecast ionospheric parameters is essential and will become even more important to the continued exploitation and reliability of these systems. For example, the GPS constellation of satellites has become the dominant source for navigational information. From navigating aircraft and targeting weapons to applications in search and rescue operations, GPS is the most accurate system available. Since GPS signals must penetrate the ionosphere, a detailed knowledge of the electron content of this region is critical to the accuracy of this system. Similarly, long-range communications, once dependent on cables and surface based radio relay stations, are now almost exclusively carried by satellite relays. HF radio communications, an early method of long-range communications which is still widely used, is perhaps the technology most

dependent on the state of the ionosphere since the radio signals are reflected from the ionosphere to reach distant points on the earth's surface. Weather and intelligence gathering satellites, many of which orbit within the region of the ionosphere, are also effected by the ionosphere both with respect to the signals they send back to the surface, and with respect to their physical, orbital characteristics. An increasing dependence on these and other technologies that are strongly influenced by the ionosphere makes a thorough understanding of the environment upon which the technology is dependent critical. Only through a detailed understanding and robust forecast capability of the ionosphere, can existing and emerging technology be fully exploited.

2. The Ionospheric Forecast Model

The first version of the IFM was delivered to the Air Force in September 1994 with the most recent version, version 3, being delivered in September 1997. The IFM was validated by the contractor, Space Environment Corporation, but has not been independently validated by the Air Force. Previous validation efforts have been very spatially and temporally restricted. The current effort is global, and the included times encompass nearly one year. See Appendix A for a summary of Space Environment Corporation's validation results.

The IFM is a set of programs consisting of initialization programs, core programs and utilities. See fig. 1 for a diagram of the programs.

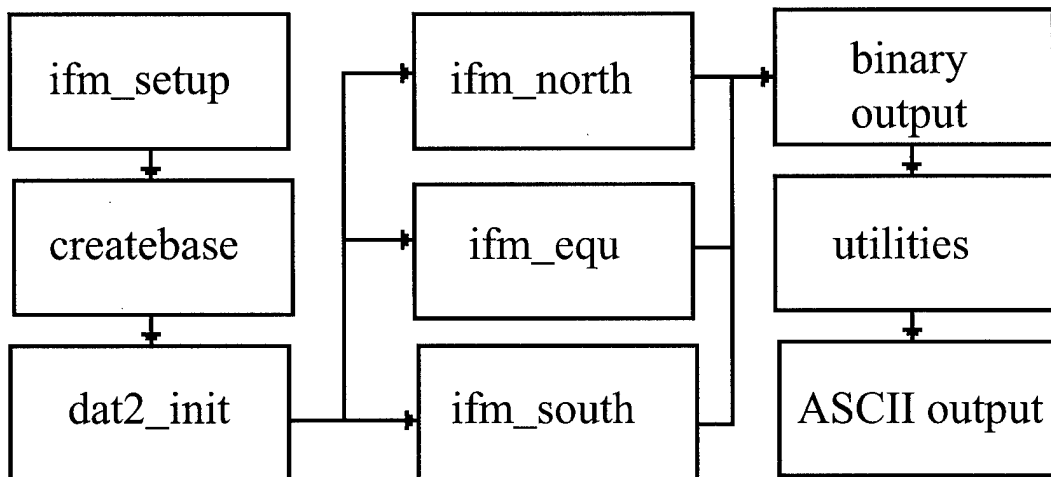


Figure 1. IFM Program Flow

2.1 Initialization Programs

The initialization program, *ifm_setup*, prompts the user for input parameters and creates the files used by the other initialization programs as well as the core and utility programs to run and create output. Inputs required include: date and time of run, type of outputs desired, output grid desired, the region of interest (if not global), name of the gridded output files, duration and interval of the forecast output, most recent value of the magnetic Kp index (and optionally, forecast Kp values for the duration of the run), the y and z components of the interplanetary magnetic field (IMF), the most recent F10.7 value and the previous 90-day average F10.7 value, and the effective sunspot number (SSN).

The initialization program *createbase* creates a best first guess for the ionosphere at the initial hour of the forecast run. It first checks for an output file from the Parameterized Real-time Ionospheric Specification Model (PRISM) to create an initial IFM output file. If a PRISM output file isn't found, *createbase* will look for an IFM output file from a previous run which corresponds to the start time of the current run, and will create an initial IFM output file from this information. If the PRISM or IFM output files do not cover the entire geographic area of interest of the current IFM run, *createbase* will fill in the missing data with information from the International Reference Ionosphere (IRI) empirical model. If neither a PRISM nor an IFM output file is found, *createbase* will produce an initial IFM output file exclusively from the IRI model.

The final initialization program, *dat2_init*, initializes the flux tubes, which correspond to the paths for plasma transport, within the northern, southern and equatorial latitudes.

IFM cannot independently utilize any real time ionospheric observational data. The only data directly acquired by the IFM are the global parameters (SSN, F10.7, K_p, etc.) which are input through the *ifm_setup* program. Observational data (such as ionosonde measurements, DMSP measurements, GPS TEC data and backscatter radar data) can only be used in the IFM model by first using them as inputs to PRISM and then using the PRISM output to initialize the IFM.

2.2 Core Programs

The three core programs of the IFM are *ifm_north*, *ifm_south*, and *ifm_equ*. These three core programs implement the equations governing the physics of the ionosphere to propagate the initial ionospheric specification through the requested forecast period and produce output files at the requested forecast intervals. These three programs can run simultaneously or sequentially.

The *ifm_equ* program calculates ionospheric parameters from -37.5 to $+37.5$ degrees latitude. The programs *ifm_north* and *ifm_south* calculate ionospheric parameters above 27.5 degrees and below -27.5 degrees latitude respectively. For regions where the output solutions from *ifm_equ* overlap with *ifm_north* and *ifm_south*, the results from the core programs are averaged in the output file to create a continuous ionosphere. The division of the core programs illustrates the sometimes radically different processes at work in the ionosphere. The equatorial region is effected by the zonal electric field that leads to vertical plasma drifts in the F region. The earth's magnetic field is approximately horizontal in the equatorial regions so the field aligned plasma drifts are horizontal to the earth's surface. The mid-latitudes lack the large-scale

current systems, and the earth's magnetic field over this region is more inclined causing field aligned currents associated with plasma motions to have a vertical and horizontal component. In polar regions, large-scale current systems are found again, largely due to a coupling with the magnetosphere, and the earth's magnetic field here is nearly vertical. Another latitudinal difference one finds in the ionosphere is the importance of collisional ionization, which can be significant in auroral regions, but decreases in importance as one moves equatorward. The core programs have been modularized to deal best with their particular regions.

Final output of the core programs are binary gridded files for each specified time in the forecast period and for the region define in the files created by *ifm_setup*.

2.3 Utility programs

The utility programs convert the data from the output binary data files into usable ASCII files. *ifm_to_prism* converts data in the IFM binary output files into a PRISM-like gridded output file. It also creates station output files for specific station locations based on user inputs defined in the *ifm_setup* program and a separate station input file edited by the user to define station locations of interest. Several other utility programs allow users to extract various parameters such as critical heights and frequencies, total electron content, and altitude profiles into ASCII gridded data files.

2.4 IFM Physics

The IFM is a first principles, physics based model which evaluates the ionosphere based on the mass continuity equation, the momentum equation and the energy equation

which are discussed in appendix B. It also relies on several internal inputs derived from empirical or climatological models. Assuming no other inputs are present, (such as PRISM or previous IFM output) the IFM initializes with the IRI empirical model contained within the IFM code. For forecasts longer than three hours, Kp values must be specified at increments throughout the forecast period. The user can either forecast the values and enter them through the *ifm_setup* program, or can query the IFM to generate forecast Kp values for the forecast period. The internal Kp forecast algorithm within the IFM is based on the F10.7 value entered and 40 years of Kp data (Schunk et al, 1997: 5). Thus, the Kp forecast algorithm is an empirical model within the IFM. The IFM also uses the Fejer empirical model (Fejer et al, 1995: 5769-5776) to model the equatorial electric fields that result in the vertical plasma drifts used to model the evolution of the ionosphere. In addition, empirical models for plasma convection (Heppner and Mynard, 1987: 4467-4489) and electron precipitation patterns (Hardy et al, 1985: 4229-4238) are used.

3. Methodology

3.1 Overall Concept of Research

The overall intent of this research is to independently validate the IFM's capability to forecast the state of the ionosphere at a variety of geographic locations and under various degrees of solar and geomagnetic activity. Previous validations efforts covered only limited geographic regions, and used data that is not routinely available in real-time. For this validation, an attempt was made to run the model in a manner as similar as possible to how it might be run in an operational environment with respect to available data, and runtime considerations. It is hoped that the results of this research will assist those charged with implementing the IFM as an operational forecast tool, and will be an aid to users of the IFM's output in assessing its reliability and usefulness.

3.2 Methodology of IFM Runs

Based on data and time availability, it was determined that IFM forecasts would be generated for five separate periods consisting of five days each for a total of 25 days of runs. Each five-day period consisted of continuous days, and the periods were spread fairly evenly throughout a year to aid in identifying seasonal dependencies, and to achieve the greatest possible variety of solar and geomagnetic activity. The IFM was run in two different modes to determine the benefit, if any, of biasing the model with real-time observed data versus a cold start of the IFM using only the IRI model. The first mode of operation was to initialize the IFM using the IRI model for the initial run of each five day period and then to make the four subsequent runs initializing with the output

from the previous IFM run. In this mode, the only observed data utilized by the IFM code were the global geomagnetic and solar parameters input through the *ifm_setup* program at the beginning of each run. An initial K_p value was input for each run, and the values generated by the internal K_p forecast algorithm were used for the remainder of the forecast period. The second mode of operation was to start the IFM with the same global parameters as in mode one, but to initialize each day's run with output from a PRISM run which used real-time ionospheric observations. In mode two, the PRISM model (see appendix C) was run using Digital Ionospheric Sounding Station (DISS) data (see appendix D), and essentially the same global parameters as the IFM. Data from 50 different ionosonde stations was used for the PRISM runs, though data wasn't available from every station for every PRISM run. Additionally, PRISM accepts ionosonde data for the hour of the run as well as one hour before and after. All available data within this time window was used for these model runs. The gridded output files from PRISM, which subsequently became the input for the IFM, were generated on a default PRISM grid of a data point every two degrees latitude and every 10 degrees longitude. The default output had a 50 point altitude grid with 5 km spacing from 90 to 150 km, 10 km spacing from 150 to 300 km, 20 km spacing from 300 to 400 km, 50 km spacing from 400 to 900 km, and 100 km spacing from 900 to 1600 km. The PRISM output files included the critical frequencies and heights of the F2 and E layers as well as TEC and an electron density profile for each data point on the grid. IFM runs were made in both modes for each of the 25 days using the IFM default grids and requesting PRISM-like station output for ten station locations. Though gridded output was produced, only the station data was used in

this research. The initial hour for each of the IFM runs was chosen as 1200 UT to maximize the amount of input data available to PRISM.

3.3 Selection of Stations and Comparison Data

Ten ionosonde stations were chosen for comparison with IFM output. The stations were chosen based on reasonably robust data availability good latitude coverage to aid in evaluating each of the core programs of the IFM. The stations chosen were: Chilton, England; Chung Li, Taiwan; Dixon Island, Russia; Eglin AFB, Fl, U.S.; Grahamstown, South Africa; Hobart, Australia; Learmonth Australia; Lerwick, England; Tashkent, Uzbekistan; and Townsville, Australia. See fig. 2 for approximate locations.

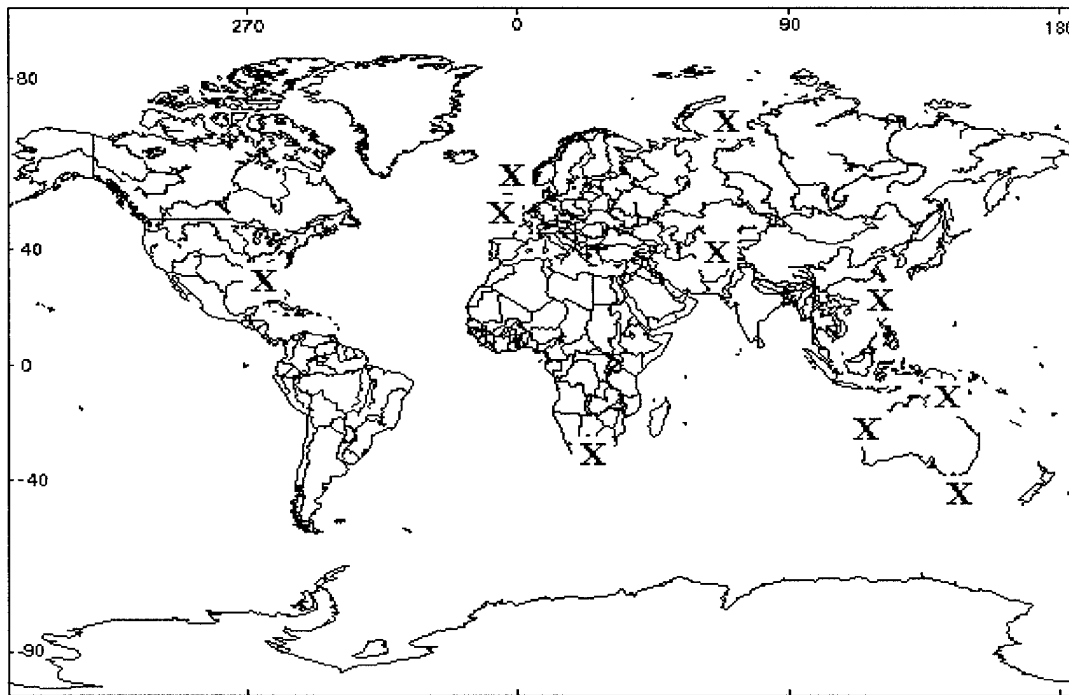


Figure 2. Location of DISS Stations used in validation

Five periods were chosen from 1996 based primarily on data availability. The periods covered are March 16-21, May 10-15, July 7-12, September 14-19, and December 12-17.

The critical frequency (foF2) and height (hmF2) of the F2 layer are the only ionospheric parameters evaluated in this study. The foF2 and hmF2 values are compared with the foF2 and hmF2 values from the corresponding ionosonde stations. Each forecast produced 24 data values for comparison with observed ionosonde data. Only stations with at least eight ionosonde measurement values available were analyzed and used in the calculation of the statistics. Ionosonde values for hmF2 and foF2 are considered accurate within 17 km and 0.4 MHz respectively (Titheridge, 1990: 21-24), and these values were used to evaluate the statistical significance of differences throughout this research. What represents a "good" forecast or specification of the ionosphere is variable depending on the application intended for the data. The prime interest in the F2 layer is HF radio propagation in the band from 3 to 30 MHz. The maximum useable frequency in this band is directly related to the foF2 value. Considering an average foF2 value of 9 MHz, an error of 0.6 MHz represents about a 10% error. The height of the F2 layer effects the maximum single reflection range of an HF signal for a given angle of propagation with the horizon. An error of 20 km in the hmF2 would correspond to an error of about 150 km in the calculation of the maximum single reflection range of a signal assuming an hmF2 near 300km and a radio signal directed at an angle of about 4 deg. with the horizontal. Since the IFM has a vertical resolution of 20 km in the F region, a forecast value within 20 km of the observed value seems a reasonable criteria. For this study,

these values of 0.6 MHz and 20 km, coupled with the inherent uncertainty of the measurements will constitute the criteria for validating the output of the IFM.

3.4 Statistical Methodology

Statistics for this study were chosen to reveal possible model biases and whether the model followed the trend of the observed data, as well as to determine the absolute accuracy of the model output. The three statistics used for this validation are the absolute error, the residual and the correlation, which are defined below.

The absolute error, E , is the absolute value of the difference between a forecast value and an observed value. The absolute error is an indication of the accuracy of the model output compared to observations, and is defined in equation 1 below. A mean absolute error, equation 2, was also used for evaluating time series data. In the following equations, F is the forecast value, O is the observed value, n is the total number of pairs (one forecast and one observed) of values, and i refers to a specific value within a group.

$$E_i = \sqrt{(F_i - O_i)^2} \quad (1)$$

$$\bar{E} = \frac{\sum_{i=1}^n (\sqrt{(F_i - O_i)^2})}{n} \quad (2)$$

The residual (McClave and Dietrich, 1991: 751-753), R , (equation 3) is similar to the absolute error, but retains its sign to show the relation between the forecast and observed data. The residual is positive when the forecast value is greater than the

observed, and negative when the forecast value is less than the observed. Like the absolute error, there is also a mean residual error, equation 4, that is especially useful in determining if the model is biased to consistently produce value higher or lower than the observed values. If forecast values fall nearly equally above and below the observed values, the mean residual will be quite small indicating no trend for the model to consistently over or under forecast values. Even with a small residual, the mean absolute error might still be quite large indicating poor model accuracy. The symbols used in equations 3 and 4 below are the same as those defined above for absolute error.

$$R_i = F_i - O_i \quad (3)$$

$$\bar{R} = \frac{\sum_{i=1}^n (F_i - O_i)}{n} \quad (4)$$

The final statistic used in this study was Spearman's Rank Correlation Coefficient, r_s (McClave and Dietrich, 1991: 576-578), equation 5. This coefficient provides an indication of how well the model output is forecasting the trend of the observed data, even when the absolute values are different. The correlation coefficient will have a value between 1 and -1. A value of 1 indicates perfect positive correlation, a value of -1 indicates perfect negative correlation, and a value near zero indicates poor correlation. The equation for r_s is given below with symbols as defined earlier.

$$r_s = \frac{SS_{FO}}{\sqrt{SS_{FF}SS_{OO}}} \quad (5)$$

Where:

$$SS_{FO} = \sum_{i=1}^n F_i O_i - \frac{(\sum_{i=1}^n F_i)(\sum_{i=1}^n O_i)}{n} \quad (6)$$

$$SS_{FF} = \sum_{i=1}^n F_i^2 - \frac{(\sum_{i=1}^n F_i)^2}{n} \quad (7)$$

$$SS_{OO} = \sum_{i=1}^n O_i^2 - \frac{(\sum_{i=1}^n O_i)^2}{n} \quad (8)$$

3.5 Display and Analysis of Data

Figure 3 and Table 1 represent a typical displayed for analysis. The three traces are IFM output for runs initialized with Prism (IFMP), IFM output for runs initialized without Prism (IFM), and raw data from the ionosonde station (DISS).

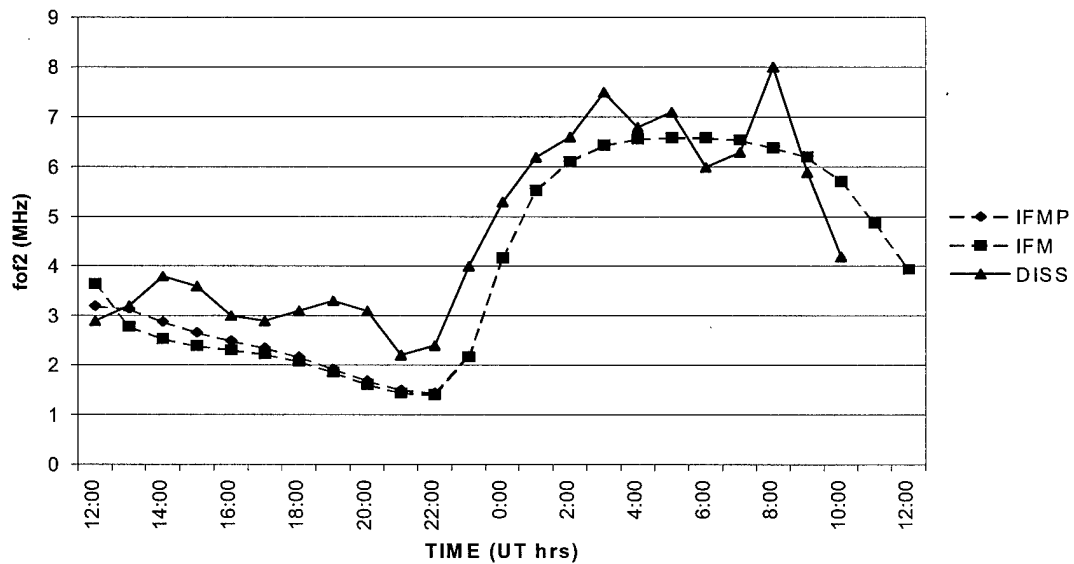


Figure 3. Example Data Comparison Chart

Table 1 Gives the same information as Figure 3, but also provides statistical information for each hour in which an observation is available, and gives mean statistics and the correlation for the entire 24-hour run.

Table 1. Example Data Comparison Table

Data (foF2 in MHz)				Absolute Error		Residual	
TIME	IFMP	IFM	DISS	IFMP	IFM	IFMP	IFM
12:00	3.2	3.65	2.9	0.30	0.75	0.30	0.75
13:00	3.14	2.78	3.2	0.06	0.42	-0.06	-0.42
14:00	2.88	2.53	3.8	0.92	1.27	-0.92	-1.27
15:00	2.66	2.39	3.6	0.94	1.21	-0.94	-1.21
16:00	2.49	2.31	3	0.51	0.69	-0.51	-0.69
17:00	2.35	2.22	2.9	0.55	0.68	-0.55	-0.68
18:00	2.17	2.08	3.1	0.93	1.02	-0.93	-1.02
19:00	1.93	1.86	3.3	1.37	1.44	-1.37	-1.44
20:00	1.69	1.62	3.1	1.41	1.48	-1.41	-1.48
21:00	1.5	1.44	2.2	0.70	0.76	-0.70	-0.76
22:00	1.45	1.41	2.4	0.95	0.99	-0.95	-0.99
23:00	2.18	2.17	4	1.82	1.83	-1.82	-1.83
0:00	4.17	4.17	5.3	1.13	1.13	-1.13	-1.13
1:00	5.54	5.54	6.2	0.66	0.66	-0.66	-0.66
2:00	6.12	6.11	6.6	0.48	0.49	-0.48	-0.49
3:00	6.44	6.44	7.5	1.06	1.06	-1.06	-1.06
4:00	6.57	6.57	6.8	0.23	0.23	-0.23	-0.23
5:00	6.59	6.59	7.1	0.51	0.51	-0.51	-0.51
6:00	6.59	6.59	6	0.59	0.59	0.59	0.59
7:00	6.55	6.55	6.3	0.25	0.25	0.25	0.25
8:00	6.39	6.39	8	1.61	1.61	-1.61	-1.61
9:00	6.21	6.21	5.9	0.31	0.31	0.31	0.31
10:00	5.72	5.72	4.2	1.52	1.52	1.52	1.52
11:00	4.88	4.88					
12:00	3.95	3.95					
				IFM	IFMP	Lat Learmonth (LM42B) -21.90 960510/11 Lon 114.00 E	
Mean Absolute Error				0.92	0.84		
Mean Residual				-0.67	-0.60		
Correlation				0.93	0.93		

4. Results and Analysis

4.1 Analysis of foF2

Table 2 shows the global indices used to initialize each run of the IFM. The statistics from the foF2 forecasts are summarized in Tables 3 and 4. From Table 3, which shows the average statistical comparison results for all stations over each period, one sees that the average absolute error was around 1.0 MHz, and the average residual was approximately 0.5 MHz. Thus, half of the absolute error can be attributed to the IFM's tendency to over forecast foF2 values. The remainder of the absolute error, about 0.5 MHz, is approximately equal to the measurement uncertainty in the ionosonde data, 0.4 MHz. The correlation was about 0.8 for all periods except period five, indicating the IFM models the physical processes well. Table 4 presents the results averaged over each stations for each period. The analysis failed to show any conclusive trends related to season or latitude, but did show some evidence that the model performs better for quiet solar and geomagnetic activity levels. There was no statistically significant difference between the runs initialized with ionosonde data, and those without. The mean differences were 0.07 MHz for absolute error, 0.1 MHz for the residual, and 0.01 for the correlation. The following paragraphs examine the foF2 data in more detail. Additional charts and tables for each period can be found in appendix E.

Table 2. Global Indices Used to Initialize the IFM

PERIOD	DAY	Kp	Bz	By	F10.7a	F10.7	SSN
March	16	2.0	4.1	3.3	72.2	70.4	12
	17	2.3	0.5	-2.5	72.2	71.0	10
	18	2.0	-1.9	-1.8	72.2	70.6	9
	19	2.3	-0.9	-3.1	72.2	70.6	9
	20	2.7	-2.6	-3.0	72.2	70.0	8
May	10	1.0	1.7	-29.8	70.5	76.2	12
	11	1.0	0.5	1.6	70.5	77.5	14
	12	1.0	-2.4	2.8	70.5	76.5	18
	13	2.3	-7.3	0.8	70.5	73.6	16
	14	2.0	0.2	-5.3	70.5	72.7	15
July	7	1.0	2.9	4.6	70.0	70.0	0
	8	2.0	-1.0	2.0	70.0	71.9	14
	9	1.0	0.2	0.6	70.0	81.6	26
	10	0.7	-0.1	-0.4	70.0	83.6	27
	11	0.3	-3.8	1.8	70.0	79.8	26
September	14	3.0	-1.7	2.4	71.1	70.0	0
	15	2.7	1.9	-1.4	71.1	70.0	0
	16	3.0	-4.8	2.4	71.1	70.0	0
	17	1.3	2.0	-1.7	71.1	70.0	0
	18	0.7	-1.6	1.3	71.1	70.0	0
December	12	2.3	2.4	3.2	72.4	77.6	28
	13	1.0	0.7	1.1	72.4	81.1	29
	14	2.0	-0.2	3.6	72.4	81.7	32
	15	2.3	-1.0	2.2	72.4	82.5	27
	16	3.0	0.6	2.9	72.4	85.0	29

Table 3. foF2 Statistics (averaged over all stations and periods)

Period	Period Averages						
	IFM			IFMP			
Period	Abs Error	Residual	Correlation	Abs Error	Residual	Correlation	
March	0.90	0.50	0.87	0.88	0.46	0.88	
May	0.99	0.49	0.82	0.94	0.40	0.84	
July	0.97	0.43	0.85	0.92	0.37	0.86	
September	1.06	0.73	0.80	1.02	0.63	0.80	
December	1.34	0.44	0.67	1.17	0.22	0.67	

Table 4. foF2 Statistics (averaged over each period for each station)

Station	Period	IFM			IFMP		
		Abs Error	Residual	Correlation	Abs Error	Residual	Correlation
Chilton	March	0.58	0.31	0.87	0.64	0.38	0.87
	May	0.44	0.04	0.89	0.50	0.12	0.87
	July	0.48	0.02	0.84	0.55	0.10	0.81
	September	0.74	0.47	0.85	0.78	0.51	0.84
	December	1.21	-0.28	0.69	1.20	-0.29	0.69
Chung-Li	March	1.73	1.36	0.85	1.70	1.16	0.86
	May	2.58	2.53	0.73	2.25	1.93	0.84
	July	3.00	3.00	0.69	2.61	2.27	0.81
	September	2.43	2.27	0.84	2.14	1.51	0.86
	December	2.28	2.03	0.87	1.91	1.52	0.89
Dixon Is	March						
	May	0.93	0.90	0.55	0.89	0.87	0.54
	July						
	September	1.21	1.09	0.27	1.19	1.07	0.25
	December						
Eglin AFB	March	0.80	-0.29	0.85	0.77	-0.16	0.87
	May	0.94	0.66	0.83	0.98	0.74	0.84
	July	0.87	0.53	0.80	0.88	0.64	0.84
	September	0.78	-0.28	0.83	0.75	-0.21	0.86
	December	1.80	-1.26	0.60	1.72	-1.17	0.63
Grahamsto	March	1.08	0.99	0.87	0.76	0.65	0.89
	May	0.88	0.05	0.90	0.83	-0.01	0.90
	July	0.88	0.18	0.92	0.86	0.16	0.92
	September	1.03	0.61	0.88	0.97	0.52	0.87
	December	1.25	1.17	0.90	0.89	0.75	0.88
Hobart	March	0.75	0.50	0.94	0.74	0.35	0.95
	May	1.04	0.10	0.81	1.04	0.08	0.81
	July	1.05	-0.10	0.80	1.01	-0.05	0.80
	September	1.28	1.26	0.95	1.28	1.14	0.95
	December						
Learmonth	March	0.86	0.15	0.75	0.85	0.20	0.76
	May	0.86	-0.51	0.87	0.86	-0.55	0.88
	July	0.78	-0.33	0.85	0.75	-0.29	0.85
	September	1.03	0.61	0.84	0.98	0.60	0.84
	December	0.68	0.15	0.92	0.66	-0.14	0.88
Lerwick	March						
	May	0.52	0.39	0.91	0.56	0.44	0.90
	July	0.50	0.17	0.87	0.54	0.21	0.86
	September	0.75	0.46	0.86	0.80	0.50	0.85
	December	1.37	0.47	0.32	1.33	0.44	0.32
Tashkent	March	0.64	0.56	0.95	0.79	0.72	0.93
	May	1.09	1.04	0.83	0.82	0.75	0.90
	July	0.53	0.44	0.95	0.48	0.34	0.93
	September	0.36	0.19	0.93	0.36	0.04	0.94
	December	0.63	-0.09	0.56	0.63	-0.09	0.56
Townsville	March	0.79	0.39	0.88	0.76	0.39	0.87
	May	0.63	-0.31	0.91	0.68	-0.37	0.91
	July	0.67	-0.07	0.91	0.64	-0.04	0.91
	September	0.99	0.61	0.77	0.99	0.58	0.77
	December	1.49	1.34	0.47	1.03	0.72	0.49

4.1.1 Seasonal and Geographic Variations. Table 4 shows the average statistics grouped by regions defined by the core programs of the IFM. The section titled “North” shows the averages for data calculated by the core program *ifm_north*. The section titled “North/Equ” shows the averages for data calculated by the core programs *ifm_north* and *ifm_equ*. The other sections are for data calculated by *ifm_equ*, *ifm_equ* and *ifm_south*, and by *ifm_south* respectively. The row labeled “ALL” is just the average for all time periods in that region. Stations within a particular region are listed in parenthesis.

The negative residuals that appear in the North/Equ section are the most readily apparent differences in the data since this conflicts with the averages from the other sections. However, since this region is an average of the calculations made by *ifm_equ* and *ifm_north*, a model bias to under forecast values should also appear in the North region, or the Equ region, or in both regions. These negative residuals may be a function of measurement errors from the single station included in this section, or could reflect a shortcoming of the IFM to forecast foF2 values in the region of this station. The largest absolute errors seem to be concentrated consistently in the Equ region along with the largest positive residuals. This suggests that the *ifm_equ* algorithm may be more prone to over forecast foF2 values, and may indicate that the model does not handle the equatorial trough well. Though not in perfect agreement with the data, there is some evidence that the poorest correlation and largest absolute error occurs in the winter season (December for the northern hemisphere and July for the southern hemisphere). In contrast, the absolute error and correlation calculated by *ifm_equ* are nearly constant through all times periods. The limited time available for this study did not allow a large enough sample in

each region to have confidence in these speculations. However, there does seem enough evidence to warrant further study.

Table 5. Average Statistics Grouped by Region

	IFM			IFMP		
	North (Chilton, Dixon Island, Lerwick, Taskent)					
	abs	res	cor	abs	res	cor
March	0.61	0.44	0.91	0.72	0.55	0.90
May	0.75	0.59	0.80	0.69	0.55	0.80
July	0.50	0.21	0.89	0.52	0.22	0.87
September	0.77	0.55	0.73	0.78	0.53	0.72
December	1.07	0.03	0.52	1.05	0.02	0.52
ALL	0.74	0.36	0.77	0.75	0.37	0.76
North/Equ (Eglin)						
	abs	res	cor	abs	res	cor
March	0.80	-0.29	0.85	0.77	-0.16	0.87
May	0.94	0.66	0.83	0.98	0.74	0.84
July	0.87	0.53	0.80	0.88	0.64	0.84
September	0.78	-0.28	0.83	0.75	-0.21	0.86
December	1.80	-1.26	0.60	1.72	-1.17	0.63
ALL	1.04	-0.13	0.78	1.02	-0.03	0.81
Equ (Chung-Li, Learmonth, Townsville)						
	abs	res	cor	abs	res	cor
March	1.13	0.63	0.83	1.10	0.58	0.83
May	1.36	0.57	0.84	1.26	0.34	0.88
July	1.48	0.87	0.82	1.33	0.65	0.86
September	1.48	1.16	0.82	1.37	0.90	0.82
December	1.48	1.17	0.75	1.20	0.70	0.75
ALL	1.39	0.88	0.81	1.25	0.63	0.83
South/Equ (Grahamstown)						
	abs	res	cor	abs	res	cor
March	1.08	0.99	0.87	0.76	0.65	0.89
May	0.88	0.05	0.90	0.83	-0.01	0.90
July	0.88	0.18	0.92	0.86	0.16	0.92
September	1.03	0.61	0.88	0.97	0.52	0.87
December	1.25	1.17	0.90	0.89	0.75	0.88
ALL	1.02	0.60	0.89	0.86	0.41	0.89
South (Hobart)						
	abs	res	cor	abs	res	cor
March	0.75	0.50	0.94	0.74	0.35	0.95
May	1.04	0.10	0.81	1.04	0.08	0.81
July	1.05	-0.10	0.80	1.01	-0.05	0.80
September	1.28	1.26	0.95	1.28	1.14	0.95
December						
ALL	1.03	0.44	0.88	1.02	0.38	0.88

4.1.2 Period 1 foF2. The best agreement between forecast and observed foF2 occurred at Chilton, and Tashkent. At these stations, the average absolute error for the period was 0.61 for IFM and 0.72 for IFMP. The average residual was 0.44 for IFM and 0.55 for IFMP. The average correlation was 0.91 for IFM and 0.90 for IFMP. Figure 4 graphically represents the March 18-19 Data for Tashkent, and Table 6 shows the corresponding data. Note in the graph that the IFMP data is nearly the same as the observation at the initial time, but the IFM and IFMP solutions rapidly converge to nearly identical solutions. This was a common observation in nearly all of the foF2 data analyzed. The model output for these stations is in very good agreement with observations. Though there seems to be a slight tendency for the IFM to overestimate the foF2, the errors are just barely large enough to be statistically significant. The correlation was very high, and there was no statistical difference between the IFM and the IFMP runs.

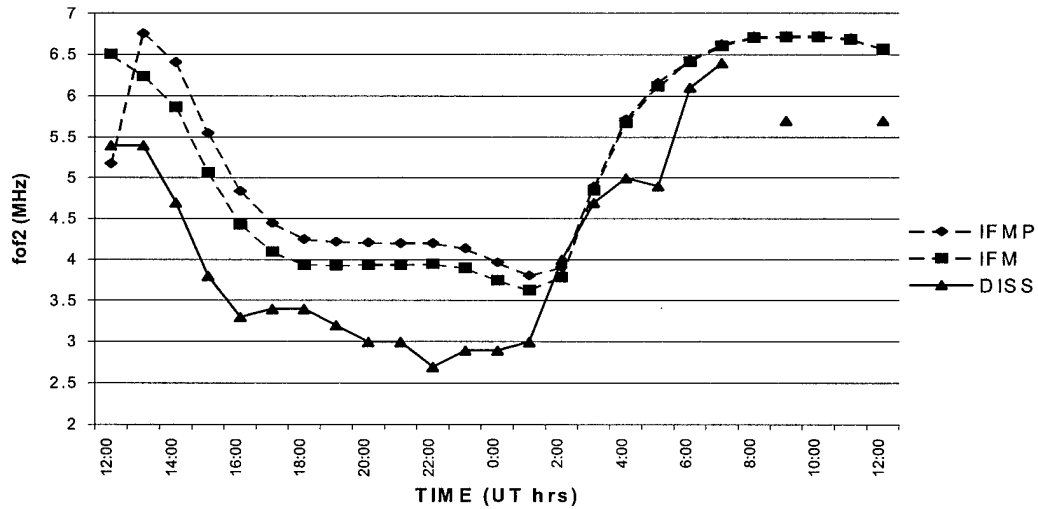


Figure 4. Tashkent 18-19 March foF2 data

Table 6. Tashkent 18-19 March foF2 data

Data (foF2 in MHz)				Absolute Error		Residual	
TIME	IFMP	IFM	DISS	IFMP	IFM	IFMP	IFM
12:00	5.18	6.51	5.4	0.22	1.11	-0.22	1.11
13:00	6.76	6.24	5.4	1.36	0.84	1.36	0.84
14:00	6.41	5.87	4.7	1.71	1.17	1.71	1.17
15:00	5.55	5.07	3.8	1.75	1.27	1.75	1.27
16:00	4.84	4.43	3.3	1.54	1.13	1.54	1.13
17:00	4.45	4.1	3.4	1.05	0.70	1.05	0.70
18:00	4.25	3.94	3.4	0.85	0.54	0.85	0.54
19:00	4.22	3.93	3.2	1.02	0.73	1.02	0.73
20:00	4.21	3.94	3	1.21	0.94	1.21	0.94
21:00	4.2	3.94	3	1.20	0.94	1.20	0.94
22:00	4.2	3.95	2.7	1.50	1.25	1.50	1.25
23:00	4.14	3.9	2.9	1.24	1.00	1.24	1.00
0:00	3.97	3.75	2.9	1.07	0.85	1.07	0.85
1:00	3.81	3.63	3	0.81	0.63	0.81	0.63
2:00	3.91	3.79	4	0.09	0.21	-0.09	-0.21
3:00	4.9	4.85	4.7	0.20	0.15	0.20	0.15
4:00	5.72	5.68	5	0.72	0.68	0.72	0.68
5:00	6.16	6.12	4.9	1.26	1.22	1.26	1.22
6:00	6.44	6.42	6.1	0.34	0.32	0.34	0.32
7:00	6.63	6.61	6.4	0.23	0.21	0.23	0.21
8:00	6.72	6.71					
9:00	6.73	6.72	5.7	1.03	1.02	1.03	1.02
10:00	6.73	6.72					
11:00	6.7	6.69					
12:00	6.57	6.57	5.7	0.87	0.87	0.87	0.87
				IFM	IFMP		
						Lat	
				Tashkent (TQ241)		41.33 N	
				960318/19		Lon	
				Correlation		69.62 E	

The worst agreement for this period was from Grahamstown and Chung-Li. The average absolute error for the period was 1.41 for IFM and 1.23 for IFMP. The average residual was 1.18 for IFM and 0.91 for IFMP. The average correlation was 0.86 for IFM and 0.88 for IFMP. The error for these two stations is quite high, but the large positive residual coupled with the good positive correlation indicates that the IFM is forecasting reasonably well, but is over estimating the foF2 values. Figure 5 and Table 7 show the 17-18 March Chung-Li data. Note that the IFMP trace again starts the period near the observed value, but converges to the IFM solution by 2100 UT.

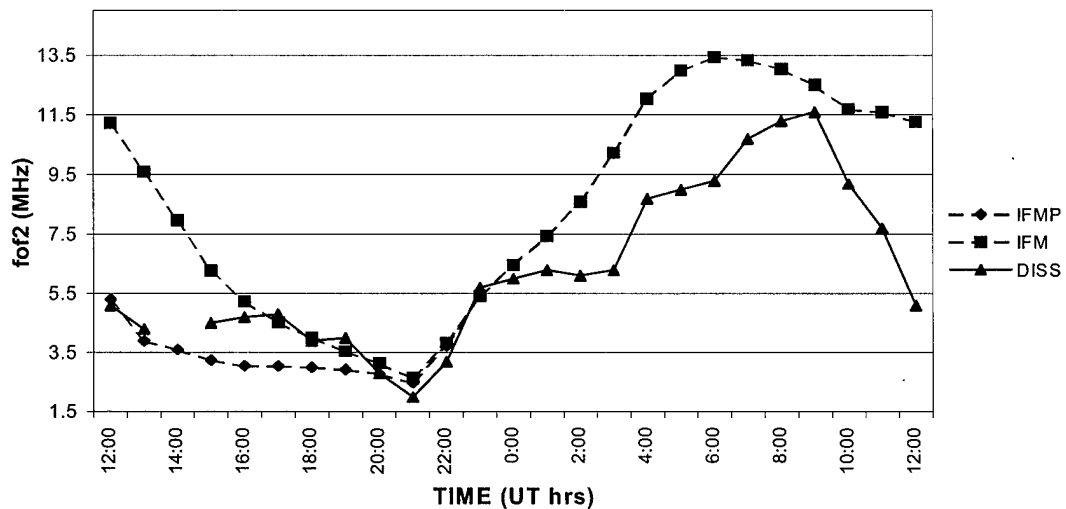


Figure 5. Chung-Li 17-18 March foF2 data

Table 7. Chung-Li 17-18 March foF2 data

TIME	Data (foF2 in MHz)			Absolute Error		Residual	
	IFMP	IFM	DISS	IFMP	IFM	IFMP	IFM
12:00	5.32	11.24	5.1	0.22	6.14	0.22	6.14
13:00	3.9	9.6	4.3	0.40	5.30	-0.40	5.30
14:00	3.6	7.97					
15:00	3.25	6.29	4.5	1.25	1.79	-1.25	1.79
16:00	3.06	5.24	4.7	1.64	0.54	-1.64	0.54
17:00	3.04	4.52	4.8	1.76	0.28	-1.76	-0.28
18:00	3	4	3.9	0.90	0.10	-0.90	0.10
19:00	2.93	3.55	4	1.07	0.45	-1.07	-0.45
20:00	2.79	3.15	2.8	0.01	0.35	-0.01	0.35
21:00	2.48	2.65	2	0.48	0.65	0.48	0.65
22:00	3.73	3.83	3.2	0.53	0.63	0.53	0.63
23:00	5.4	5.42	5.7	0.30	0.28	-0.30	-0.28
0:00	6.45	6.46	6	0.45	0.46	0.45	0.46
1:00	7.43	7.44	6.3	1.13	1.14	1.13	1.14
2:00	8.59	8.59	6.1	2.49	2.49	2.49	2.49
3:00	10.23	10.24	6.3	3.93	3.94	3.93	3.94
4:00	12.03	12.04	8.7	3.33	3.34	3.33	3.34
5:00	13	13	9	4.00	4.00	4.00	4.00
6:00	13.44	13.44	9.3	4.14	4.14	4.14	4.14
7:00	13.34	13.34	10.7	2.64	2.64	2.64	2.64
8:00	13.05	13.05	11.3	1.75	1.75	1.75	1.75
9:00	12.51	12.51	11.6	0.91	0.91	0.91	0.91
10:00	11.7	11.7	9.2	2.50	2.50	2.50	2.50
11:00	11.61	11.61	7.7	3.91	3.91	3.91	3.91
12:00	11.27	11.27	5.1	6.17	6.17	6.17	6.17
		IFM	IFMP			Lat	
Mean Absolute Error		2.08	1.99	Chung-Li (CL424)		24.91 N	
Mean Residual		1.99	1.35	960317/18		Lon	
Correlation		0.88	0.90	121.24 E			

Overall, the IFM did a good job of forecasting foF2 during period one. The best forecasts seemed to be in the mid-latitudes. The average absolute errors were generally at or below 1 MHz. The average residual was almost always positive, but its magnitude was usually much less than one indicating a tendency for the model to slightly overestimate foF2 values. The correlation was generally 0.8 or higher indicating a good correlation between the model and the observations.

4.1.3 Period 2 foF2. The best agreement between forecast and observed foF2 occurred at Chilton, and Lerwick. At these stations, the average absolute error for the period was 0.48 for IFM and 0.53 for IFMP. The average residual was 0.22 for IFM and 0.28 for IFMP. The average correlation was 0.90 for IFM and 0.89 for IFMP. Figure 6 displays the May 11-12 Data for Chilton, and Table 8 lists the corresponding data.

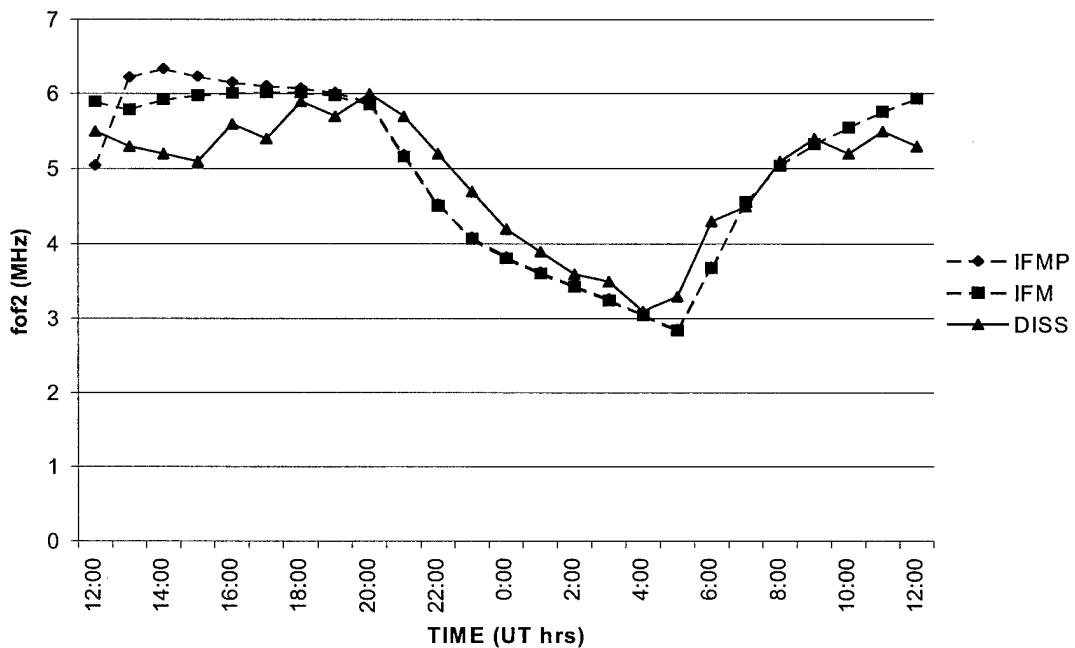


Figure 6. Chilton 11-12 May foF2 data

Table 8. Chilton 11-12 May foF2 data

TIME	Data (foF2 in MHz)			Absolute Error		Residual	
	IFMP	IFM	DISS	IFMP	IFM	IFMP	IFM
12:00	5.05	5.9	5.5	0.45	0.40	-0.45	0.40
13:00	6.23	5.79	5.3	0.93	0.49	0.93	0.49
14:00	6.34	5.93	5.2	1.14	0.73	1.14	0.73
15:00	6.24	5.98	5.1	1.14	0.88	1.14	0.88
16:00	6.16	6.01	5.6	0.56	0.41	0.56	0.41
17:00	6.11	6.02	5.4	0.71	0.62	0.71	0.62
18:00	6.08	6.02	5.9	0.18	0.12	0.18	0.12
19:00	6.02	5.98	5.7	0.32	0.28	0.32	0.28
20:00	5.89	5.86	6	0.11	0.14	-0.11	-0.14
21:00	5.19	5.16	5.7	0.51	0.54	-0.51	-0.54
22:00	4.53	4.51	5.2	0.67	0.69	-0.67	-0.69
23:00	4.09	4.07	4.7	0.61	0.63	-0.61	-0.63
0:00	3.83	3.81	4.2	0.37	0.39	-0.37	-0.39
1:00	3.63	3.61	3.9	0.27	0.29	-0.27	-0.29
2:00	3.45	3.43	3.6	0.15	0.17	-0.15	-0.17
3:00	3.27	3.25	3.5	0.23	0.25	-0.23	-0.25
4:00	3.06	3.05	3.1	0.04	0.05	-0.04	-0.05
5:00	2.86	2.84	3.3	0.44	0.46	-0.44	-0.46
6:00	3.69	3.68	4.3	0.61	0.62	-0.61	-0.62
7:00	4.56	4.56	4.5	0.06	0.06	0.06	0.06
8:00	5.04	5.04	5.1	0.06	0.06	-0.06	-0.06
9:00	5.33	5.33	5.4	0.07	0.07	-0.07	-0.07
10:00	5.55	5.55	5.2	0.35	0.35	0.35	0.35
11:00	5.76	5.76	5.5	0.26	0.26	0.26	0.26
12:00	5.94	5.94	5.3	0.64	0.64	0.64	0.64
		IFM	IFMP			Lat	
Mean Absolute Error		0.38	0.43	Chilton (RL052)		51.60 N	
Mean Residual		0.02	0.09	960511/12		Lon	
Correlation		0.93	0.91			358.70 E	

The model output for these stations is in very good agreement with observations.

The average absolute errors are nearly statistically insignificant, and the residual, though consistently positive, is too small to indicate any strong bias in the model. The correlation was very high, and nearly identical for the IFM and the IFMP runs.

The worst agreement for this period was from Chung-Li and Hobart. The average absolute error for the period was 1.81 for IFM and 1.65 for IFMP. The average residual was 1.32 for IFM and 1.01 for IFMP. The average correlation was 0.77 for IFM and 0.83 for IFMP. The large absolute error and relatively large positive residual indicate a strong

tendency for the model to overestimate the foF2 values. The correlation is still reasonably good indicating again that the model is predicting the trend well, but is over forecasting the foF2 values. Figure 7 and Table 9 show the 13-14 May Hobart data.

Table 9. Hobart 13-14 May foF2 data

Data (foF2 in MHz)				Absolute Error		Residual	
TIME	IFMP	IFM	DISS	IFMP	IFM	IFMP	IFM
12:00	2.81	2.86	2.8	0.01	0.06	0.01	0.06
13:00	2.68	2.69	2.9	0.22	0.21	-0.22	-0.21
14:00	2.42	2.4	3.5	1.08	1.10	-1.08	-1.10
15:00	2.16	2.14	3.4	1.24	1.26	-1.24	-1.26
16:00	1.93	1.9	3	1.07	1.10	-1.07	-1.10
17:00	1.7	1.67					
18:00	1.49	1.46					
19:00	1.29	1.26					
20:00	1.1	1.07					
21:00	0.92	0.9					
22:00	1.77	1.76					
23:00	4.14	4.14					
0:00	5.25	5.25	4.4	0.85	0.85	0.85	0.85
1:00	5.82	5.82	4.9	0.92	0.92	0.92	0.92
2:00	6.13	6.13					
3:00	6.26	6.26					
4:00	6.29	6.29	5.2	1.09	1.09	1.09	1.09
5:00	6.27	6.27	5.5	0.77	0.77	0.77	0.77
6:00	6.2	6.2	5.2	1.00	1.00	1.00	1.00
7:00	6.01	6.01	4.1	1.91	1.91	1.91	1.91
8:00	5.49	5.49	3.7	1.79	1.79	1.79	1.79
9:00	4.3	4.3	2.8	1.50	1.50	1.50	1.50
10:00	3.62	3.62	2.6	1.02	1.02	1.02	1.02
11:00	3.15	3.15					
12:00	2.81	2.81					
				IFM	IFMP	Lat	
Mean Absolute Error				1.12	1.11	Hobart (HO54K) -42.92 N	
Mean Residual				0.55	0.56	960513/14 Lon	
Correlation				0.80	0.80	147.32 E	

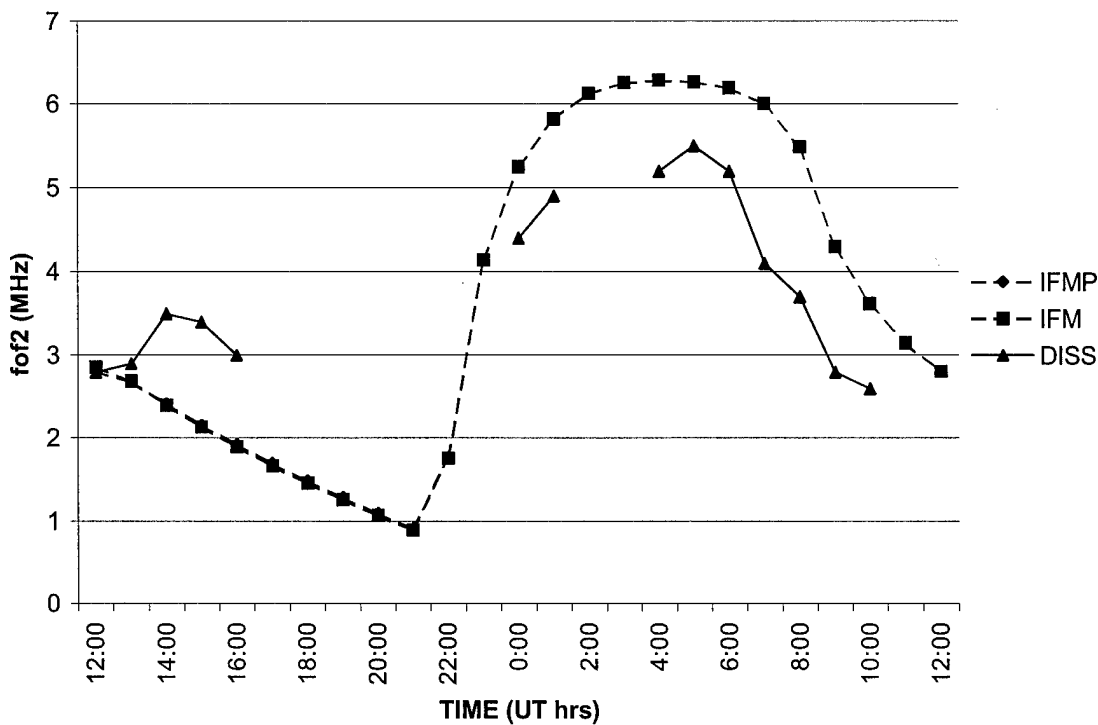


Figure 7. Hobart 13-14 May foF2 data

Overall, the IFM did a good job of forecasting foF2 during period two. There was no clear latitudinal differentiation in how well the model performed. The high latitudes may have fared worse than the mid and low-latitudes. The average absolute errors were generally at or below 1 MHz. The average residual again showed a tendency to over forecast foF2 values at some stations, but was too small to reveal any information at most locations. The correlation was generally 0.8 or higher with Dixon Island being the only station showing poor correlation.

4.1.4 Period 3 foF2. The best agreement between forecast and observed foF2 occurred at Lerwick and Tashkent. At these stations, the average absolute error for the

period was 0.52 for IFM and 0.51 for IFMP. The average residual was 0.31 for IFM and 0.28 for IFMP. The average correlation was 0.91 for IFM and 0.90 for IFMP. Figure 8 shows the July 10-11 data for Lerwick, and Table 10 lists the corresponding data.

Table 10. Lerwick 10-11 July foF2 data

Data (foF2 in MHz)				Absolute Error		Residual	
TIME	IFMP	IFM	DISS	IFMP	IFM	IFMP	IFM
12:00	4.78	5.35	4.9	0.12	0.45	-0.12	0.45
13:00	5.52	5.12	4.6	0.92	0.52	0.92	0.52
14:00	5.64	5.32	4.6	1.04	0.72	1.04	0.72
15:00	5.57	5.38	4.6	0.97	0.78	0.97	0.78
16:00	5.44	5.34	4.6	0.84	0.74	0.84	0.74
17:00	5.32	5.27	4.3	1.02	0.97	1.02	0.97
18:00	5.22	5.19	4.6	0.62	0.59	0.62	0.59
19:00	5.18	5.17	4.9	0.28	0.27	0.28	0.27
20:00	5.2	5.19	4.7	0.50	0.49	0.50	0.49
21:00	5.19	5.19	4.2	0.99	0.99	0.99	0.99
22:00	4.79	4.79	4.1	0.69	0.69	0.69	0.69
23:00	4.28	4.27	4	0.28	0.27	0.28	0.27
0:00	3.49	3.48	3.8	0.31	0.32	-0.31	-0.32
1:00	2.75	2.75	3.6	0.85	0.85	-0.85	-0.85
2:00	2.57	2.57	3.3	0.73	0.73	-0.73	-0.73
3:00	2.35	2.35	3.1	0.75	0.75	-0.75	-0.75
4:00	2.58	2.58	3.2	0.62	0.62	-0.62	-0.62
5:00	3.27	3.27	3.8	0.53	0.53	-0.53	-0.53
6:00	4.02	4.02	3.7	0.32	0.32	0.32	0.32
7:00	4.34	4.34	4.3	0.04	0.04	0.04	0.04
8:00	4.63	4.63	4.1	0.53	0.53	0.53	0.53
9:00	4.8	4.8	4.9	0.10	0.10	-0.10	-0.10
10:00	4.89	4.89	4.8	0.09	0.09	0.09	0.09
11:00	5.07	5.07	4.7	0.37	0.37	0.37	0.37
12:00	5.24	5.24	4.8	0.44	0.44	0.44	0.44
				IFM	IFMP	Lat	
Mean Absolute Error				0.53	0.58	Lerwick (LE061)	60.13 N
Mean Residual				0.21	0.25	960710/11	Lon
Correlation				0.91	0.90		358.82 E

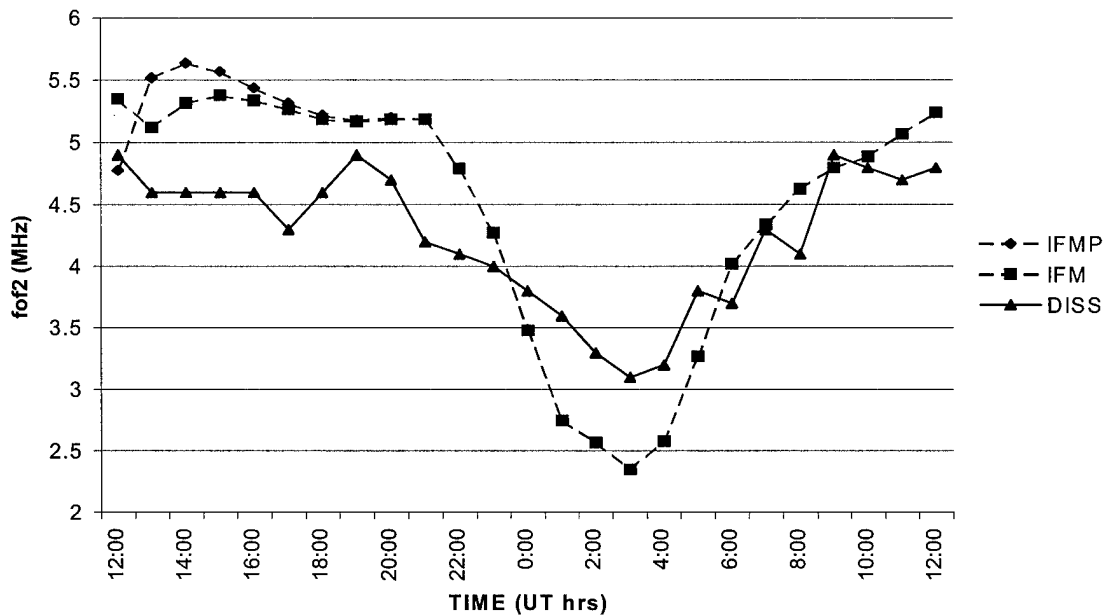


Figure 8. Lerwick 10-11 July foF2 data

The model output for these stations is in good agreement with observations. The average absolute errors are again, barely significant, and the residuals are too small to indicate any strong bias in the model. The correlation was very good, and essentially identical for the IFM and the IFMP runs.

The worst agreement for this period was from Chung-Li and Hobart. The average absolute error for these stations for this period was 2.03 for IFM and 1.81 for IFMP. The average residual was 1.45 for IFM and 1.11 for IFMP. The average correlation was 0.75 for IFM and 0.81 for IFMP. The large absolute error and positive residual indicate a very strong tendency for the model to overestimate the foF2 values. The correlation shows a greater difference between the IFM and IFMP runs with IFMP showing much better correlation to the observed data. Figure 9 and Table 11 show the 9-10 July Chung-Li data.

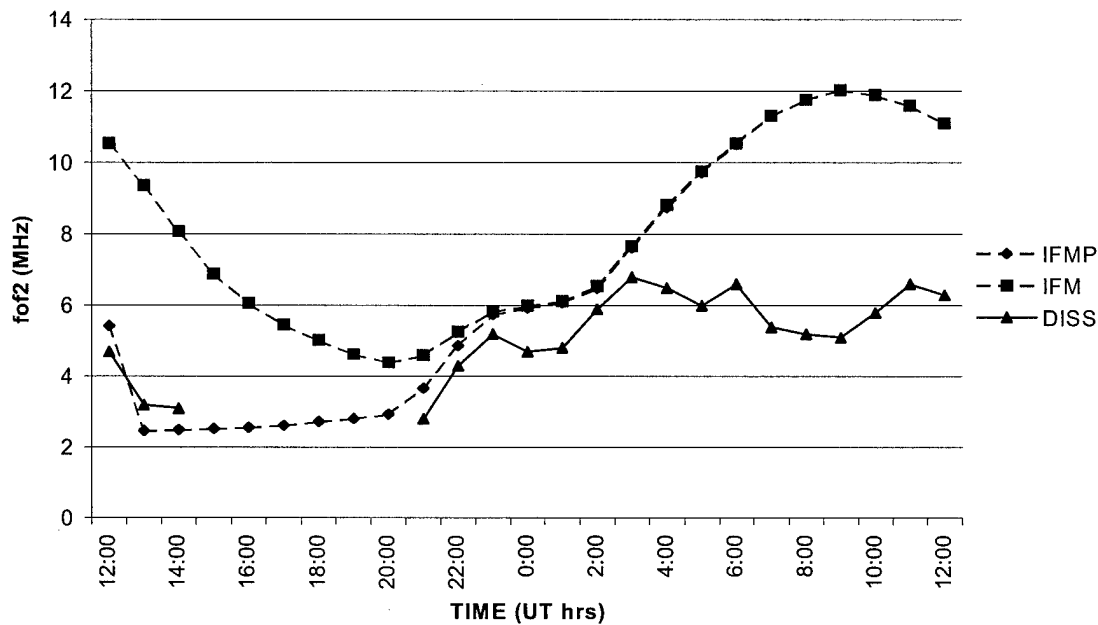


Figure 9. Chung-Li 9-10 July foF2 data

Table 11. Chung-Li 9-10 July foF2 data

TIME	Data (foF2 in MHz)			Absolute Error		Residual	
	IFMP	IFM	DISS	IFMP	IFM	IFMP	IFM
12:00	5.43	10.55	4.7	0.73	5.85	0.73	5.85
13:00	2.47	9.37	3.2	0.73	6.17	-0.73	6.17
14:00	2.5	8.08	3.1	0.60	4.98	-0.60	4.98
15:00	2.53	6.9					
16:00	2.56	6.07					
17:00	2.62	5.46					
18:00	2.73	5.02					
19:00	2.81	4.64					
20:00	2.94	4.4					
21:00	3.67	4.59	2.8	0.87	1.79	0.87	1.79
22:00	4.88	5.26	4.3	0.58	0.96	0.58	0.96
23:00	5.75	5.83	5.2	0.55	0.63	0.55	0.63
0:00	5.94	6	4.7	1.24	1.30	1.24	1.30
1:00	6.08	6.12	4.8	1.28	1.32	1.28	1.32
2:00	6.49	6.55	5.9	0.59	0.65	0.59	0.65
3:00	7.62	7.68	6.8	0.82	0.88	0.82	0.88
4:00	8.76	8.82	6.5	2.26	2.32	2.26	2.32
5:00	9.73	9.77	6	3.73	3.77	3.73	3.77
6:00	10.52	10.55	6.6	3.92	3.95	3.92	3.95
7:00	11.31	11.32	5.4	5.91	5.92	5.91	5.92
8:00	11.76	11.77	5.2	6.56	6.57	6.56	6.57
9:00	12.04	12.04	5.1	6.94	6.94	6.94	6.94
10:00	11.91	11.91	5.8	6.11	6.11	6.11	6.11
11:00	11.6	11.6	6.6	5.00	5.00	5.00	5.00
12:00	11.11	11.11	6.3	4.81	4.81	4.81	4.81
				IFM	IFMP	Lat Chung-Li (CL424) 24.91 N 960709/10 Lon 121.24 E	
Mean Absolute Error				3.56	2.92		
Mean Residual				3.56	2.77		
Correlation				0.45	0.74		

Again, the IFM generally did a good job of forecasting foF2 during period three. The model performed reasonably well at mid and high latitudes, but the results were mixed at low latitudes. The averaged statistics for this period were very similar to those from period two. Again, the model seems to be forecasting well overall, but is over estimating the foF2 values.

4.1.5 Period 4 foF2. The best agreement between forecast and observed foF2 occurred at, Tashkent and Chilton. At these stations, the average absolute error for the period was 0.55 for IFM and 0.57 for IFMP. The average residual was 0.33 for IFM and 0.28 for IFMP. The average correlation was 0.89 for IFM and for IFMP. Figure 10 shows the September 16-17 data for Tashkent, and Table 12 lists the corresponding data.

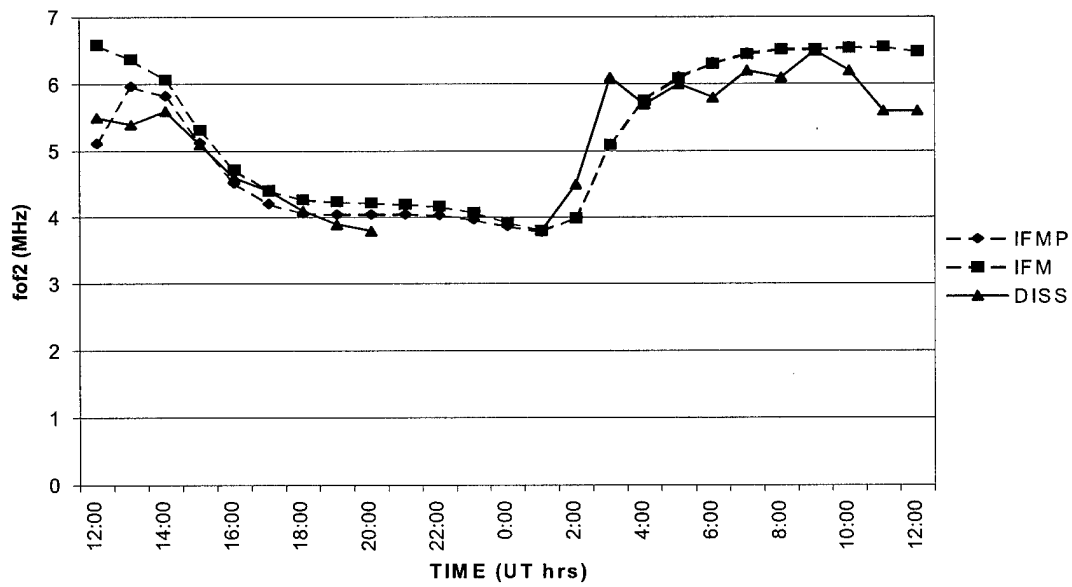


Figure 10. Tashkent 16-17 September foF2 data

Table 12. Tashkent 16-17 September foF2 data

TIME	Data (foF2 in MHz)			Absolute Error		Residual	
	IFMP	IFM	DISS	IFMP	IFM	IFMP	IFM
12:00	5.12	6.59	5.5	0.38	1.09	-0.38	1.09
13:00	5.97	6.38	5.4	0.57	0.98	0.57	0.98
14:00	5.83	6.07	5.6	0.23	0.47	0.23	0.47
15:00	5.13	5.32	5.1	0.03	0.22	0.03	0.22
16:00	4.52	4.72	4.6	0.08	0.12	-0.08	0.12
17:00	4.21	4.41	4.4	0.19	0.01	-0.19	0.01
18:00	4.07	4.27	4.1	0.03	0.17	-0.03	0.17
19:00	4.05	4.24	3.9	0.15	0.34	0.15	0.34
20:00	4.05	4.22	3.8	0.25	0.42	0.25	0.42
21:00	4.05	4.2					
22:00	4.04	4.17					
23:00	3.97	4.08					
0:00	3.87	3.93					
1:00	3.79	3.81	3.8	0.01	0.01	-0.01	0.01
2:00	4	3.99	4.5	0.50	0.51	-0.50	-0.51
3:00	5.1	5.1	6.1	1.00	1.00	-1.00	-1.00
4:00	5.77	5.76	5.7	0.07	0.06	0.07	0.06
5:00	6.11	6.09	6	0.11	0.09	0.11	0.09
6:00	6.32	6.31	5.8	0.52	0.51	0.52	0.51
7:00	6.47	6.45	6.2	0.27	0.25	0.27	0.25
8:00	6.53	6.52	6.1	0.43	0.42	0.43	0.42
9:00	6.53	6.52	6.5	0.03	0.02	0.03	0.02
10:00	6.55	6.54	6.2	0.35	0.34	0.35	0.34
11:00	6.56	6.56	5.6	0.96	0.96	0.96	0.96
12:00	6.49	6.49	5.6	0.89	0.89	0.89	0.89
		IFM	IFMP			Lat	
Mean Absolute Error		0.39	0.33	Tashkent (TQ241)		41.33 N	
Mean Residual		0.24	0.15	960916/17		Lon	
Correlation		0.90	0.92	69.62 E			

The model output for this station is in good agreement with observations. The average absolute error and the average residual are statistically very small, but do indicate that the IFM is again consistently overestimating foF2 values. The correlation is still reasonably good.

The worst agreement for this period was from Chung-Li and Hobart. The average absolute error for the period was 1.86 for IFM and 1.71 for IFMP. The average residual was 1.77 for IFM and 1.33 for IFMP. The average correlation was 0.90 for IFM and 0.91 for IFMP. The absolute error and positive residual of nearly the same value indicates a strong tendency for the model to overestimate the foF2 values. The correlation is almost identical for the IFM and IFMP, and is quite good which indicates that the model is forecasting the trend of the ionosphere well, but is over forecasting the values. Figure 11 and Table 13 show the 16-17 September Chung-Li data.

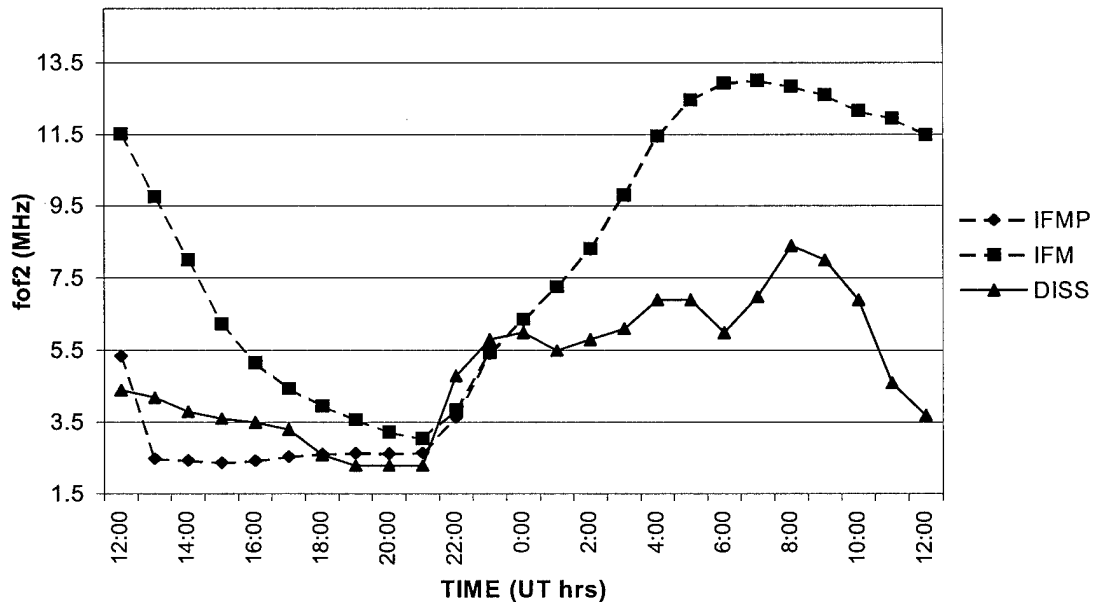


Figure 11. Chung-Li 16-17 September foF2 data

Table 13. Chung-Li 16-17 September foF2 data

Data (foF2 in MHz)				Absolute Error		Residual	
TIME	IFMP	IFM	DISS	IFMP	IFM	IFMP	IFM
12:00	5.35	11.52	4.4	0.95	7.12	0.95	7.12
13:00	2.49	9.77	4.2	1.71	5.57	-1.71	5.57
14:00	2.45	8.01	3.8	1.35	4.21	-1.35	4.21
15:00	2.38	6.24	3.6	1.22	2.64	-1.22	2.64
16:00	2.44	5.17	3.5	1.06	1.67	-1.06	1.67
17:00	2.55	4.45	3.3	0.75	1.15	-0.75	1.15
18:00	2.62	3.96	2.6	0.02	1.36	0.02	1.36
19:00	2.65	3.58	2.3	0.35	1.28	0.35	1.28
20:00	2.63	3.23	2.3	0.33	0.93	0.33	0.93
21:00	2.66	3.05	2.3	0.36	0.75	0.36	0.75
22:00	3.64	3.85	4.8	1.16	0.95	-1.16	-0.95
23:00	5.41	5.44	5.8	0.39	0.36	-0.39	-0.36
0:00	6.35	6.37	6	0.35	0.37	0.35	0.37
1:00	7.26	7.27	5.5	1.76	1.77	1.76	1.77
2:00	8.3	8.32	5.8	2.50	2.52	2.50	2.52
3:00	9.79	9.81	6.1	3.69	3.71	3.69	3.71
4:00	11.45	11.46	6.9	4.55	4.56	4.55	4.56
5:00	12.46	12.47	6.9	5.56	5.57	5.56	5.57
6:00	12.93	12.94	6	6.93	6.94	6.93	6.94
7:00	13.01	13.01	7	6.01	6.01	6.01	6.01
8:00	12.85	12.85	8.4	4.45	4.45	4.45	4.45
9:00	12.61	12.61	8	4.61	4.61	4.61	4.61
10:00	12.17	12.17	6.9	5.27	5.27	5.27	5.27
11:00	11.96	11.96	4.6	7.36	7.36	7.36	7.36
12:00	11.49	11.49	3.7	7.79	7.79	7.79	7.79
				IFM	IFMP	Lat	
Mean Absolute Error				3.41	2.90	Chung-Li (CL424)	
Mean Residual				3.30	2.26	960916/17	
Correlation				0.77	0.81	Lon	
				121.24 E			

Again, the IFM generally did a good job of forecasting foF2 during period four.

There was no clear latitudinal bias in how well the model performed. The average residual again showed an indication that the model was over forecasting foF2 values for many locations. The correlation was generally around 0.8.

4.1.6 Period 5 foF2. The best agreement between forecast and observed foF2 occurred at, Learmonth and Tashkent. At these stations, the average absolute error for the period was 0.66 for IFM and 0.65 for IFMP. The average residual was 0.03 for IFM

and -0.12 for IFMP. The average correlation was 0.74 for IFM and 0.72 for IFMP.

Figure 12 displays the December 14-15 data for Learmonth, and Table 14 lists the corresponding data.

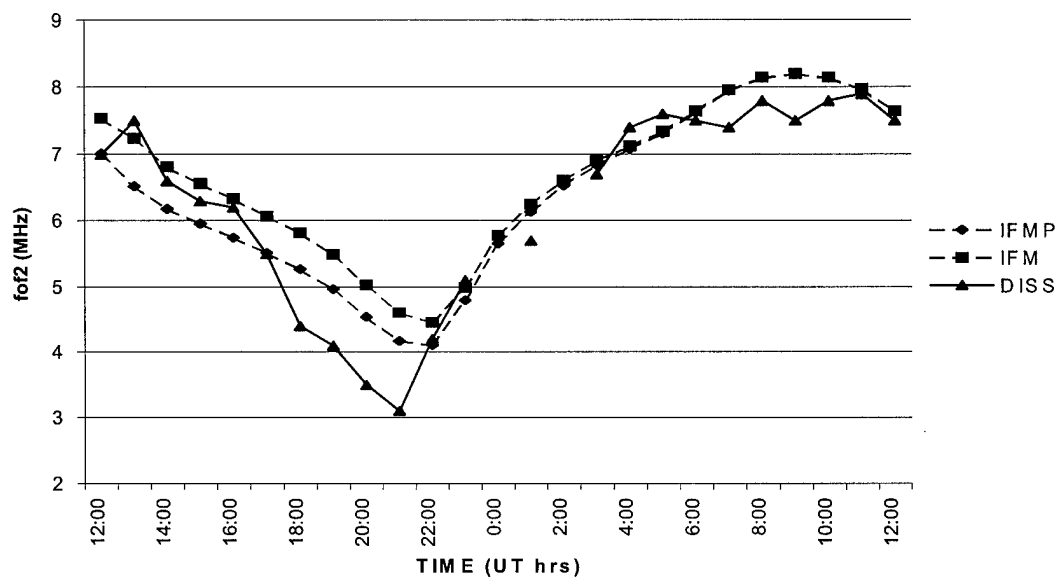


Figure 12. Learmonth 14-15 December foF2 data

Table 14. Learmonth 14-15 December foF2 data

Data (foF2 in MHz)				Absolute Error		Residual	
TIME	IFMP	IFM	DISS	IFMP	IFM	IFMP	IFM
12:00	7.01	7.54	7	0.01	0.54	0.01	0.54
13:00	6.52	7.24	7.5	0.98	0.26	-0.98	-0.26
14:00	6.18	6.81	6.6	0.42	0.21	-0.42	0.21
15:00	5.96	6.56	6.3	0.34	0.26	-0.34	0.26
16:00	5.75	6.33	6.2	0.45	0.13	-0.45	0.13
17:00	5.52	6.07	5.5	0.02	0.57	0.02	0.57
18:00	5.27	5.82	4.4	0.87	1.42	0.87	1.42
19:00	4.97	5.49	4.1	0.87	1.39	0.87	1.39
20:00	4.54	5.03	3.5	1.04	1.53	1.04	1.53
21:00	4.17	4.61	3.1	1.07	1.51	1.07	1.51
22:00	4.11	4.46	4.2	0.09	0.26	-0.09	0.26
23:00	4.8	4.99	5.1	0.30	0.11	-0.30	-0.11
0:00	5.66	5.78					
1:00	6.14	6.25	5.7	0.44	0.55	0.44	0.55
2:00	6.53	6.61					
3:00	6.84	6.9	6.7	0.14	0.20	0.14	0.20
4:00	7.08	7.12	7.4	0.32	0.28	-0.32	-0.28
5:00	7.31	7.34	7.6	0.29	0.26	-0.29	-0.26
6:00	7.62	7.64	7.5	0.12	0.14	0.12	0.14
7:00	7.95	7.96	7.4	0.55	0.56	0.55	0.56
8:00	8.14	8.15	7.8	0.34	0.35	0.34	0.35
9:00	8.2	8.2	7.5	0.70	0.70	0.70	0.70
10:00	8.14	8.15	7.8	0.34	0.35	0.34	0.35
11:00	7.97	7.98	7.9	0.07	0.08	0.07	0.08
12:00	7.64	7.64	7.5	0.14	0.14	0.14	0.14
				IFM	IFMP	Lat	
Mean Absolute Error		0.51	0.45	Learmonth (LM42B)		-21.90 S	
Mean Residual		0.43	0.16	961214/15		Lon	
Correlation		0.95	0.94	114.00 E			

The model output for these stations is in good agreement with observations. The average absolute error is higher than for previous periods, and the average residual is statistically insignificant. The correlation is good for Learmonth, but is rather poor for Tashkent.

The worst agreement for this period was from Eglin AFB and Chung-Li. The average absolute error for the period was 2.04 for IFM and 1.82 for IFMP. The average residual was 0.39 for IFM and 0.18 for IFMP. The average correlation was 0.74 for IFM and 0.76 for IFMP. The absolute error is quite large while the residuals are rather modest

indicating model inaccuracy not attributable to an over or under forecasting bias.

Correlation is still moderately good for both the IFM and the IFMP. Figure 13 and Table 15 show the 13-14 December Eglin AFB data.

Table 15. Eglin AFB 13-14 December foF2 data

Data (foF2 in MHz)				Absolute Error		Residual	
TIME	IFMP	IFM	DISS	IFMP	IFM	IFMP	IFM
12:00	3.18	1.11	3.1	0.08	1.99	0.08	-1.99
13:00	2.68	1.27	5.5	2.82	4.23	-2.82	-4.23
14:00	3.85	3.42	6.2	2.35	2.78	-2.35	-2.78
15:00	5.68	5.53					
16:00	6.37	6.29	6.5	0.13	0.21	-0.13	-0.21
17:00	6.68	6.64	6.4	0.28	0.24	0.28	0.24
18:00	6.76	6.74	7.3	0.54	0.56	-0.54	-0.56
19:00	6.72	6.71					
20:00	6.65	6.65	7	0.35	0.35	-0.35	-0.35
21:00	6.69	6.68	6.2	0.49	0.48	0.49	0.48
22:00	6.66	6.66	5.2	1.46	1.46	1.46	1.46
23:00	6.39	6.39	4.5	1.89	1.89	1.89	1.89
0:00	5.36	5.36	4.3	1.06	1.06	1.06	1.06
1:00	4.4	4.4	3.2	1.20	1.20	1.20	1.20
2:00	3.71	3.71	3.5	0.21	0.21	0.21	0.21
3:00	3.13	3.13	4.2	1.07	1.07	-1.07	-1.07
4:00	2.64	2.63	4.1	1.46	1.47	-1.46	-1.47
5:00	2.26	2.26	4	1.74	1.74	-1.74	-1.74
6:00	2.02	2.02	4	1.98	1.98	-1.98	-1.98
7:00	1.83	1.83	3.9	2.07	2.07	-2.07	-2.07
8:00	1.67	1.67	4.3	2.63	2.63	-2.63	-2.63
9:00	1.51	1.51	4.1	2.59	2.59	-2.59	-2.59
10:00	1.36	1.36	4.4	3.04	3.04	-3.04	-3.04
11:00	1.21	1.21	3	1.79	1.79	-1.79	-1.79
12:00	1.11	1.11					
				IFM	IFMP	Lat	
Mean Absolute Error				1.57	1.48	Eglin AFB (EG931) 30.40 N	
Mean Residual				-0.95	-0.86	961213/14 Lon	
Correlation				0.65	0.70	273.20 E	

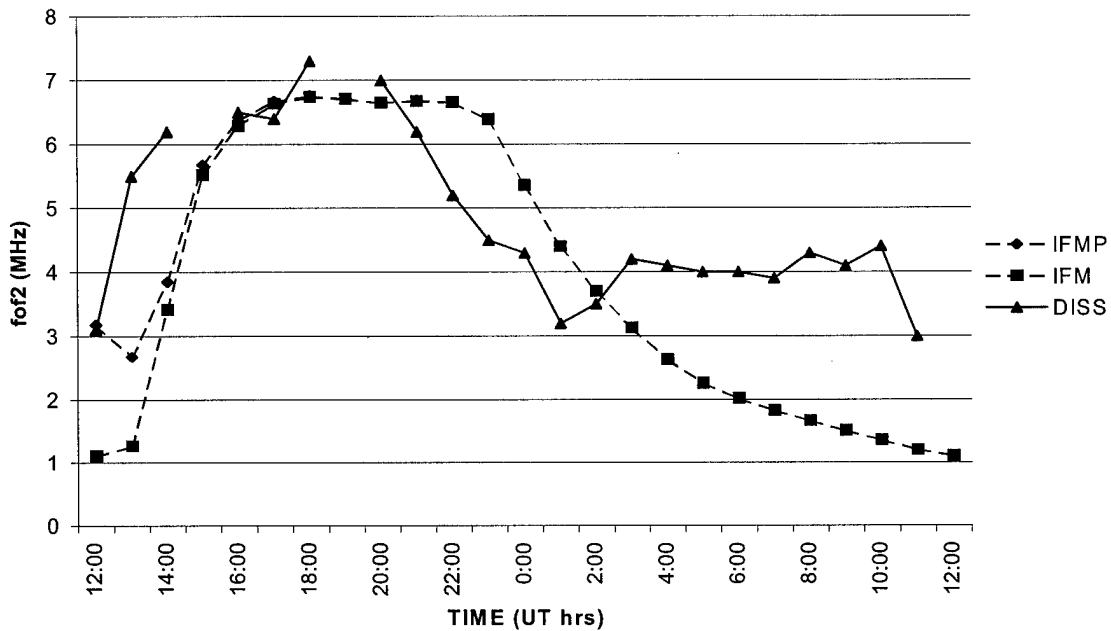


Figure 13. Eglin AFB 13-14 December foF2 data

The IFM performed worse for this period than for any of the others. Enhanced solar activity, though still at very modest levels, seems the most likely explanation for this difference since no clear latitudinal or seasonal bias was consistently detected in the data. The correlation as well as the absolute errors seem to have been effected by the increased solar activity.

4.1.7 IFM vs. IFMP Error. Based on analysis of the graphs produced during this study, it appeared that the IFM diverged from real-time input values rather rapidly and converged to the cold start solution. In an attempt to quantify this observation, the average absolute error for all stations and periods was calculated separately for IFM and IFMP. The results are displayed in Figure 14. It is apparent that after the first three hours, there is no significant difference between IFM and IFMP.

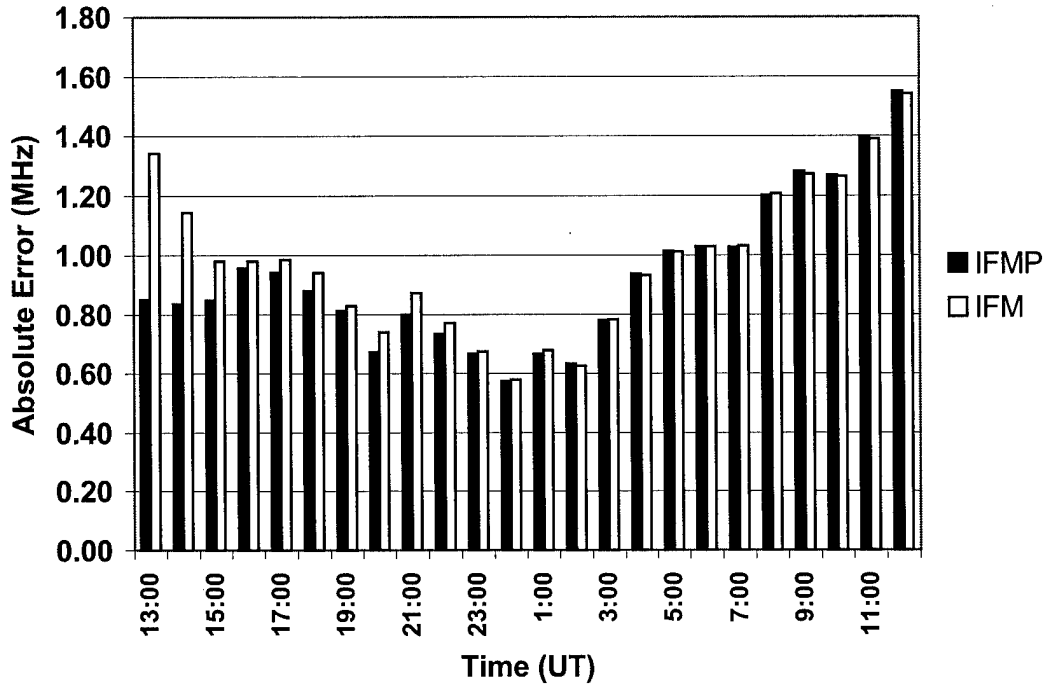


Figure 14. Average Absolute Errors (IFM vs. IFMP)

The tendency for IFM to converge to a common solution is a byproduct of the IFM's design to compensate for bad initialization data (Schunk et al, 1997). However, this feature severely limits the usefulness of real-time data to bias the IFM toward a more realistic representation of the ionosphere. To further test this tendency, the IFM was run twice with the global indices for day 076. The model was initialized with PRISM output which was generated at the extremes of the allowable real-time data input values. The first PRISM run was conducted with foF2 values of 0.0 MHz and hmF2 values of 200 km. The second run was conducted with foF2 values of 28.4 MHz and hmF2 values of 1000 km. These extreme values were input at each of the 50 station locations used

throughout this research. The output of the IFM with the minimum inputs from PRISM was convergent with the IFM without PRISM solution at all times and for all stations. The output of the IFM with the maximum inputs for PRISM was more variable. Three stations showed a flat line output, three stations showed a high-amplitude chaotic pattern, and the remaining four stations showed an initial difference with a convergence through time similar to the pattern seen in the runs conducted with realistic inputs. The IFM documentation (Schunk et al, 1997) suggests that given enough time, all stations would converge to the solution achieved without PRISM input. It appears that errors that tend to minimize $foF2$ and $hmF2$ will converge rapidly, while errors that overestimate $foF2$ and $hmF2$ will converge more slowly.

4.2 Analysis of $hmF2$

Table 16 presents the results averaged over all stations for each period. Table 17 shows the average statistical comparison results for each station and each period. Only 6 stations had sufficient data to plot and analyze. Because of the small sample size, and the fact that most stations didn't have data for all time periods, an analysis of seasonal and geographic trends was not attempted. The data suggests that unlike the $foF2$, the $hmF2$ is underestimated by the IFM. Poor correlation in every time period further suggests that the IFM failed to capture the trend of the ionosphere. Finally, the absolute errors are large enough to be statistically significant in every time period, and, like the $foF2$ analysis, initializing the model with PRISM offered no improvement in the results. Data is examined within each time period in the paragraphs which follow. Additional charts and tables for each period can be found in appendix F.

Table 16. hmF2 Statistics (averaged over each period for all stations)

Period	Period Averages						
	IFM			IFMP			Correlation
	Abs Error	Residual	Correlation	Abs Error	Residual		
March	37.60	-11.17	0.22	37.70	-10.97	0.22	
May	43.71	-19.41	0.01	44.04	-19.44	0.03	
July	61.40	-46.77	0.07	60.95	-46.07	0.12	
September	27.71	8.94	0.35	27.16	8.38	0.36	
December	23.47	-4.66	0.22	23.92	-5.78	0.21	

Table 17. hmF2 Statistics (averaged over each period for each station)

Station	Period	IFM			IFMP		
		Abs Error	Residual	Correlation	Abs Error	Residual	Correlation
Chilton	March	42.40	-40.52		42.40	-40.52	
	May	59.51	-57.55	0.28	59.51	-57.55	0.28
	July	94.85	-94.19	-0.45	92.52	-91.85	-0.30
	September						
	December						
Chung-Li	March	32.80	18.19	0.22	33.00	18.59	0.22
	May	26.11	8.33	0.77	26.11	8.33	0.77
	July	35.70	-11.78	0.51	35.70	-11.78	0.51
	September	32.26	27.10	0.54	32.26	27.10	0.54
	December	15.31	9.06	-0.12	15.31	9.06	-0.12
Dixon Is	March						
	May	50.83	-10.32	-0.34	50.62	-10.53	-0.33
	July						
	September	18.89	3.33	0.37	16.67	1.11	0.42
	December						
Eglin AFB	March						
	May						
	July						
	September						
	December						
Grahamsto	March						
	May	20.56	-4.44		22.81	-6.94	0.03
	July	28.94	-28.31		28.94	-28.31	
	September	21.75	-12.32	0.64	21.75	-12.32	0.64
	December	37.98	-27.59	0.61	39.31	-30.93	0.60
Hobart	March						
	May						
	July						
	September						
	December						
Learmouth	March						
	May						
	July						
	September						
	December						
Lerwick	March						
	May	69.19	-67.77	-0.39	68.46	-67.04	-0.32
	July	103.31	-102.69	0.54	103.31	-102.69	0.54
	September						
	December						
Tashkent	March						
	May	36.08	15.31	-0.26	36.73	17.10	-0.24
	July	44.21	3.10	-0.31	44.28	4.28	-0.27
	September	37.95	17.63	-0.15	37.96	17.64	-0.15
	December	17.13	4.54	0.16	17.13	4.54	0.16
Townsville	March						
	May						
	July						
	September						
	December						

4.2.1 Period 1 hmF2. The best agreement between forecast and observed hmF2 occurred Chung-Li. The average absolute error was 32.80 for IFM and 33.00 for IFMP. The average residual was 18.19 for IFM and 18.59 for IFMP. The average correlation was 0.22 for both IFM and IFMP. Figure 15 and Table 18 shows the data for Chung-Li for 18-19 March.

Table 18. Chung-Li 18-19 March hmF2 data

TIME	Data (hmF2 in km)			Absolute Error		Residual	
	IFMP	IFM	DISS	IFMP	IFM	IFMP	IFM
12:00	350	290					
13:00	310	290					
14:00	270	270					
15:00	290	290					
16:00	290	290					
17:00	290	290					
18:00	290	290					
19:00	290	290					
20:00	270	270					
21:00	270	270					
22:00	250	250					
23:00	250	250					
0:00	270	270	275	5.00	5.00	-5.00	-5.00
1:00	290	290	300	10.00	10.00	-10.00	-10.00
2:00	290	290	340	50.00	50.00	-50.00	-50.00
3:00	330	330	350	20.00	20.00	-20.00	-20.00
4:00	330	330	335	5.00	5.00	-5.00	-5.00
5:00	330	330	315	15.00	15.00	15.00	15.00
6:00	330	330	290	40.00	40.00	40.00	40.00
7:00	330	330	265	65.00	65.00	65.00	65.00
8:00	310	310	240	70.00	70.00	70.00	70.00
9:00	290	290					
10:00	290	290					
11:00	310	310					
12:00	290	290					
		IFM	IFMP			Lat Chung-Li (CL424) 24.91 N 960318/19 Lon 121.24 E	
Mean Absolute Error		31.11	31.11				
Mean Residual		11.11	11.11				
Correlation		0.18	0.18				

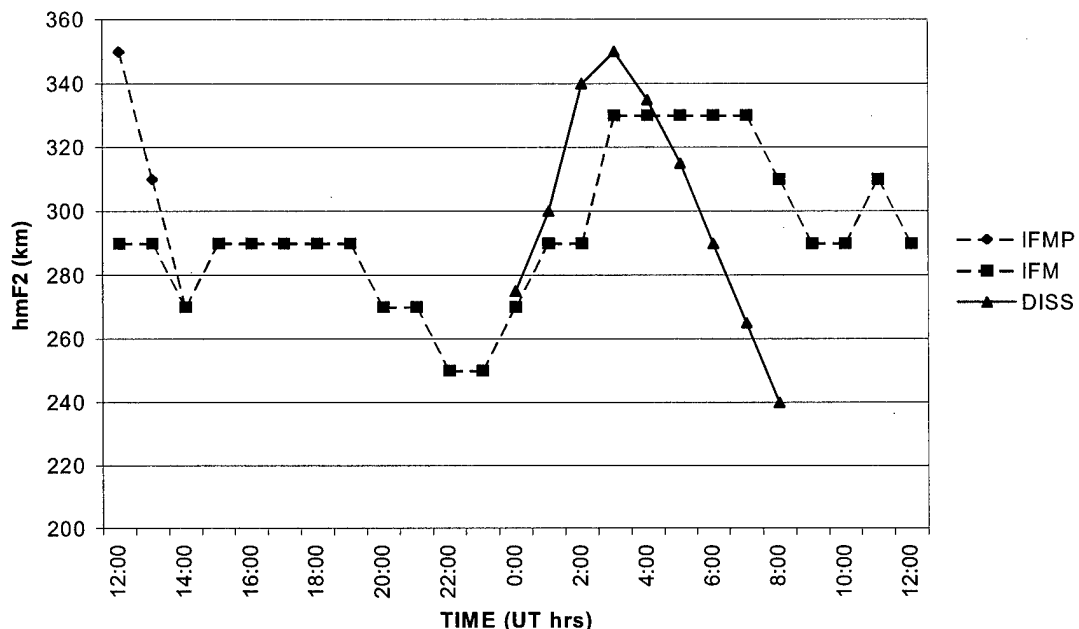


Figure 15. Chung-Li 18-19 March hmF2 data

The model output for this station is rather poor. The average error is nearly double the uncertainty in the ionosonde measurement. The poor correlation indicates that the model and the ionosphere are tracking almost independently and have very little in common.

The worst agreement for this period was from Chilton. The average absolute error for the period was 42.40 for both IFM and IFMP. The average residual was -40.52 for both the IFM and IFMP. The correlation was undefined. Figure 16 and Table 19 show the 19-20 March Chilton hmF2 data. Overall, the IFM did a poor job of forecasting hmF2 during period one. There was little relation between the IFM's forecast and the actual state of the ionosphere.

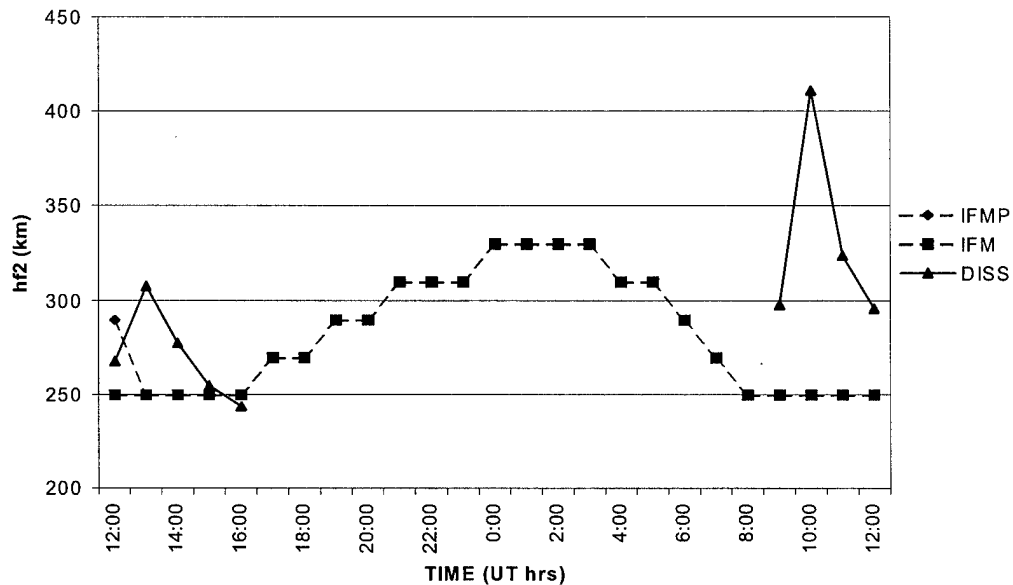


Figure 16. Chilton 19-20 March hmF2 data

Table 19. Chilton 19-20 March hmF2 data

TIME	Data (hmF2 in km)			Absolute Error		Residual	
	IFMP	IFM	DISS	IFMP	IFM	IFMP	IFM
12:00	290	250	268	22.00	18.00	22.00	-18.00
13:00	250	250	308	58.00	58.00	-58.00	-58.00
14:00	250	250	278	28.00	28.00	-28.00	-28.00
15:00	250	250	255	5.00	5.00	-5.00	-5.00
16:00	250	250	244	6.00	6.00	6.00	6.00
17:00	270	270					
18:00	270	270					
19:00	290	290					
20:00	290	290					
21:00	310	310					
22:00	310	310					
23:00	310	310					
0:00	330	330					
1:00	330	330					
2:00	330	330					
3:00	330	330					
4:00	310	310					
5:00	310	310					
6:00	290	290					
7:00	270	270					
8:00	250	250					
9:00	250	250	298	48.00	48.00	-48.00	-48.00
10:00	250	250	411	161.00	161.00	-161.00	-161.00
11:00	250	250	324	74.00	74.00	-74.00	-74.00
12:00	250	250	296	46.00	46.00	-46.00	-46.00
				IFM	IFMP	Lat	
Mean Absolute Error				53.25	53.25	Chilton (RL052) 51.60 N	
Mean Residual				-51.75	-51.75	960319/20 Lon	
Correlation				#DIV/0!	#DIV/0!	358.70 E	

4.2.2 Period 2 hmF2. The best agreement between forecast and observed foF2 occurred at Grahamstown. At this station, the average absolute error for the period was 20.56 for IFM and 22.81 for IFMP. The average residual was -4.44 for IFM and -6.94 for IFMP. The correlation was undefined for IFM and was 0.03 for IFMP. Figure 17 and Table 20 show the May 11-12 Data for Grahamstown.

Table 20. Grahamstown 11-12 May hmF2 data

Data (hF2 in km)				Absolute Error		Residual	
TIME	IFMP	IFM	DISS	IFMP	IFM	IFMP	IFM
12:00	270	250	278	8.00	28.00	-8.00	-28.00
13:00	250	250	267	17.00	17.00	-17.00	-17.00
14:00	250	250					
15:00	250	250					
16:00	270	270					
17:00	270	270					
18:00	290	290					
19:00	290	290					
20:00	270	270					
21:00	270	270					
22:00	270	270					
23:00	270	270					
0:00	270	270					
1:00	270	270					
2:00	270	270					
3:00	270	270					
4:00	270	270					
5:00	250	250					
6:00	250	250					
7:00	250	250	228	22.00	22.00	22.00	22.00
8:00	250	250	245	5.00	5.00	5.00	5.00
9:00	250	250	249	1.00	1.00	1.00	1.00
10:00	250	250	255	5.00	5.00	-5.00	-5.00
11:00	250	250	251	1.00	1.00	-1.00	-1.00
12:00	250	250	225	25.00	25.00	25.00	25.00
		IFM	IFMP			Lat	
Mean Absolute Error		10.86	10.86	Grahamstown (GR13L)		-33.30 N	
Mean Residual		4.29	4.29			960511/12	Lon
Correlation		#DIV/0!	#DIV/0!				26.50 E

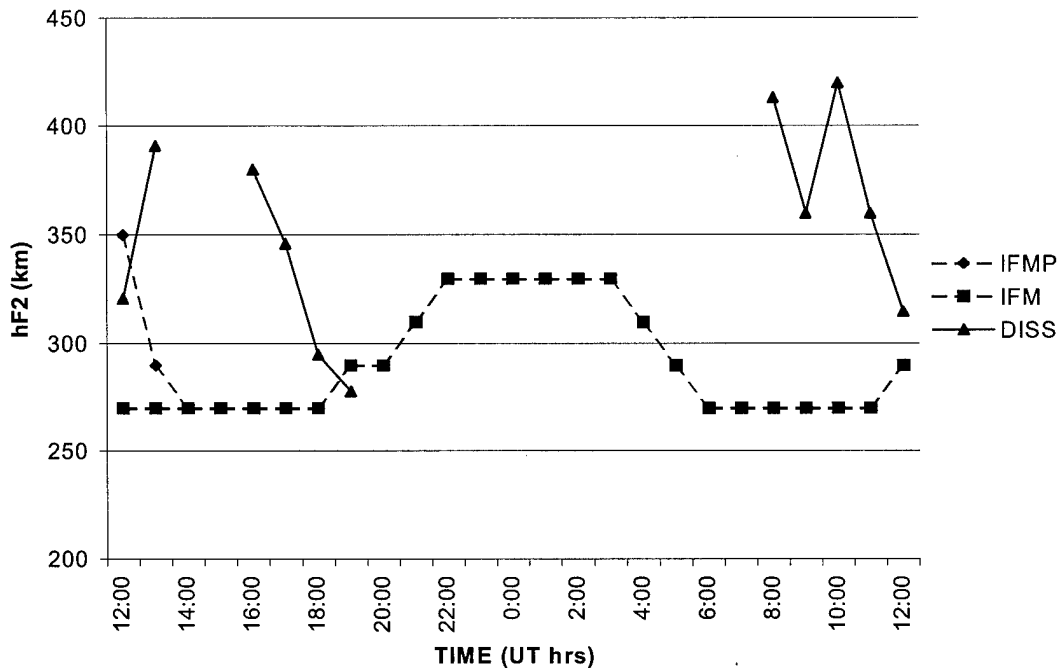


Figure 17. Grahamstown 11-12 May hmF2 data

The model output for this station is better than in period one. The mean absolute error is within the measurement error. However, the negative correlation raises doubts as to whether the model is capturing the physics of what is actually shaping the ionosphere.

The worst agreement for this period was from Lerwick. The average absolute error for the period was 69.19 for IFM and 68.46 for IFMP. The average residual was -67.77 for IFM and -67.04 for IFMP. The average correlation was -0.39 for IFM and -0.32 for IFMP. The absolute error and positive residual of nearly the same value indicates a strong tendency for the model to under forecast the hmF2 values. The small, negative correlation values indicate a chaotic relationship between the model and the ionosphere. Figure 18 and Table 21 show the 13-14 May Lerwick hmF2 data.

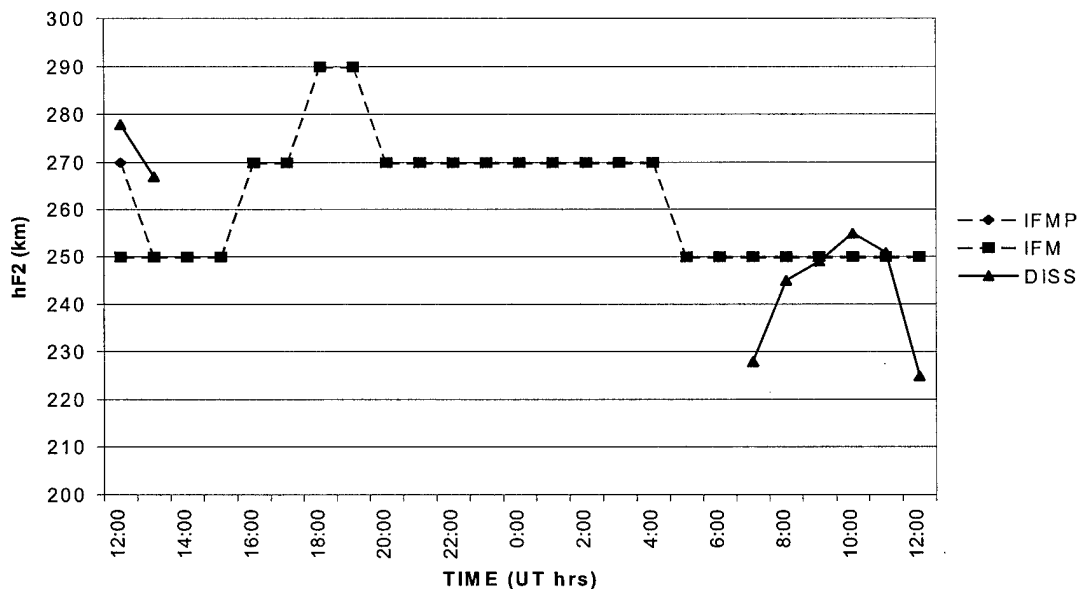


Figure 18. Lerwick 13-14 May hmF2 data

Table 21. Lerwick 13-14 May hmF2 data

TIME	Data (hF2 in km)			Absolute Error		Residual	
	IFMP	IFM	DISS	IFMP	IFM	IFMP	IFM
12:00	350	270	321	29.00	51.00	29.00	-51.00
13:00	290	270	391	101.00	121.00	-101.00	-121.00
14:00	270	270					
15:00	270	270					
16:00	270	270	380	110.00	110.00	-110.00	-110.00
17:00	270	270	346	76.00	76.00	-76.00	-76.00
18:00	270	270	295	25.00	25.00	-25.00	-25.00
19:00	290	290	278	12.00	12.00	12.00	12.00
20:00	290	290					
21:00	310	310					
22:00	330	330					
23:00	330	330					
0:00	330	330					
1:00	330	330					
2:00	330	330					
3:00	330	330					
4:00	310	310					
5:00	290	290					
6:00	270	270					
7:00	270	270					
8:00	270	270	413	143.00	143.00	-143.00	-143.00
9:00	270	270	360	90.00	90.00	-90.00	-90.00
10:00	270	270	420	150.00	150.00	-150.00	-150.00
11:00	270	270	360	90.00	90.00	-90.00	-90.00
12:00	290	290	315	25.00	25.00	-25.00	-25.00
				IFM	IFMP	Lat	
						Lerwick (LE061)	60.13 N
						960513/14	Lon
							358.82 E

Overall, the IFM did a poor job of forecasting hmF2 during period two. The error was over twice as large as the measurement uncertainty, the residual indicated a strong tendency to under forecast hmF2, and there was very little correlation between the IFM forecast and the ionosonde observations

4.2.3 Period 3 hmF2. The best agreement between forecast and observed foF2 occurred Grahamstown. At this station, the average absolute error for the period was 28.94 for both IFM and for IFMP. The average residual was -28.31 for both IFM and IFMP. The correlation was undefined. Figure 19 and Table 22 show the July 10-11 data for Grahamstown.

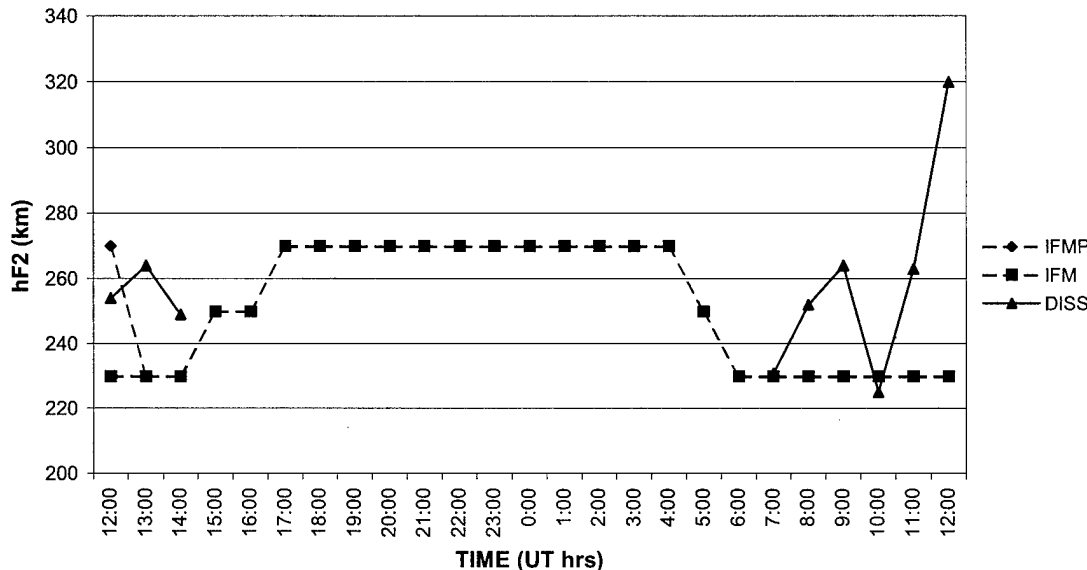


Figure 19. Grahamstown 10-11 July hmF2 data

Table 22. Grahamstown 10-11 July hmF2 data

TIME	Data (hmF2 in km)			Absolute Error		Residual	
	IFMP	IFM	DISS	IFMP	IFM	IFMP	IFM
12:00	270	230	254	16.00	24.00	16.00	-24.00
13:00	230	230	264	34.00	34.00	-34.00	-34.00
14:00	230	230	249	19.00	19.00	-19.00	-19.00
15:00	250	250					
16:00	250	250					
17:00	270	270					
18:00	270	270					
19:00	270	270					
20:00	270	270					
21:00	270	270					
22:00	270	270					
23:00	270	270					
0:00	270	270					
1:00	270	270					
2:00	270	270					
3:00	270	270					
4:00	270	270					
5:00	250	250					
6:00	230	230					
7:00	230	230	231	1.00	1.00	-1.00	-1.00
8:00	230	230	252	22.00	22.00	-22.00	-22.00
9:00	230	230	264	34.00	34.00	-34.00	-34.00
10:00	230	230	225	5.00	5.00	5.00	5.00
11:00	230	230	263	33.00	33.00	-33.00	-33.00
12:00	230	230	320	90.00	90.00	-90.00	-90.00
		IFM	IFMP			Lat	
Mean Absolute Error		29.75	29.75	Grahamstown (GR13L)		-33.30 N	
Mean Residual		-28.50	-28.50	960710/11		Lon	
Correlation		#DIV/0!	#DIV/0!			26.50 E	

The model output for this station is again poor. The Large error with the nearly equal negative residual will result in under forecast hmF2 values. While the correlation is undefined, the graph indicates little relation between the forecast values and the observed values.

The worst agreement for this period was from Lerwick. The average absolute error for the period was 103.31 for both IFM and IFMP. The average residual was -102.69 for both IFM and IFMP. The average correlation was 0.54 for both modes of the IFM. The error and residual are huge, and the correlation is poor. The IFM is grossly

under estimating the height of the F2 layer peak. Figure 20 and Table 23 show the 10-11 July Lerwick data.

Table 23. Lerwick 10-11 July hmF2 data

Data (hmF2 in km)				Absolute Error		Residual	
TIME	IFMP	IFM	DISS	IFMP	IFM	IFMP	IFM
12:00	350	270	294	56.00	24.00	56.00	-24.00
13:00	270	270	410	140.00	140.00	-140.00	-140.00
14:00	270	270	436	166.00	166.00	-166.00	-166.00
15:00	270	270	385	115.00	115.00	-115.00	-115.00
16:00	270	270	323	53.00	53.00	-53.00	-53.00
17:00	270	270	365	95.00	95.00	-95.00	-95.00
18:00	270	270	327	57.00	57.00	-57.00	-57.00
19:00	270	270	273	3.00	3.00	-3.00	-3.00
20:00	270	270					
21:00	290	290					
22:00	310	310					
23:00	310	310					
0:00	310	310					
1:00	310	310					
2:00	310	310					
3:00	310	310					
4:00	290	290					
5:00	270	270					
6:00	270	270					
7:00	270	270	478	208.00	208.00	-208.00	-208.00
8:00	270	270					
9:00	270	270	300	30.00	30.00	-30.00	-30.00
10:00	270	270	330	60.00	60.00	-60.00	-60.00
11:00	270	270	386	116.00	116.00	-116.00	-116.00
12:00	270	270	355	85.00	85.00	-85.00	-85.00
				IFM	IFMP	Lat Lerwick (LE061) 60.13 N 960710/11 Lon 358.82 E	
Mean Absolute Error				94.00	94.00		
Mean Residual				-94.00	-94.00		
Correlation				#DIV/0!	#DIV/0!		

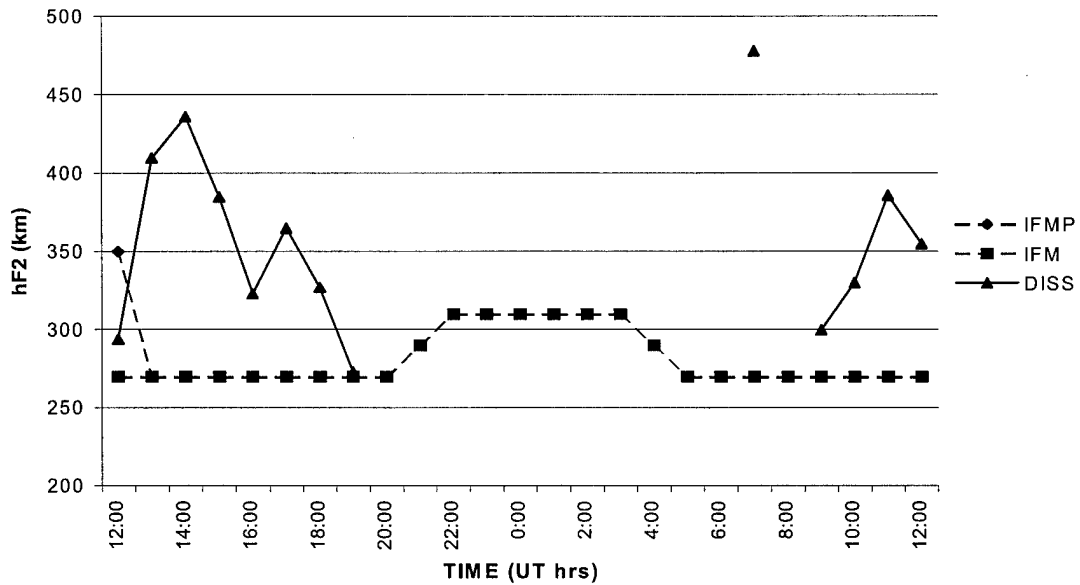


Figure 20. Lerwick 10-11 July hmF2 data

Again, the IFM preformed poorly. The large error and residual indicate a consistent under forecasting of the hmF2. Correlation, though undefined numerically, appears very poor as well from the graph.

4.2.4 Period 4 hmF2. The best agreement between forecast and observed foF2 occurred at, Dixon Island. At this station, the average absolute error for the period was 18.89 for IFM and 16.67 for IFMP. The average residual was 3.33 for IFM and 1.11 for IFMP. The average correlation was 0.37 for IFM and 0.42 for IFMP. Figure 21 and Table 24 show the September 18-19 data for Dixon Island.

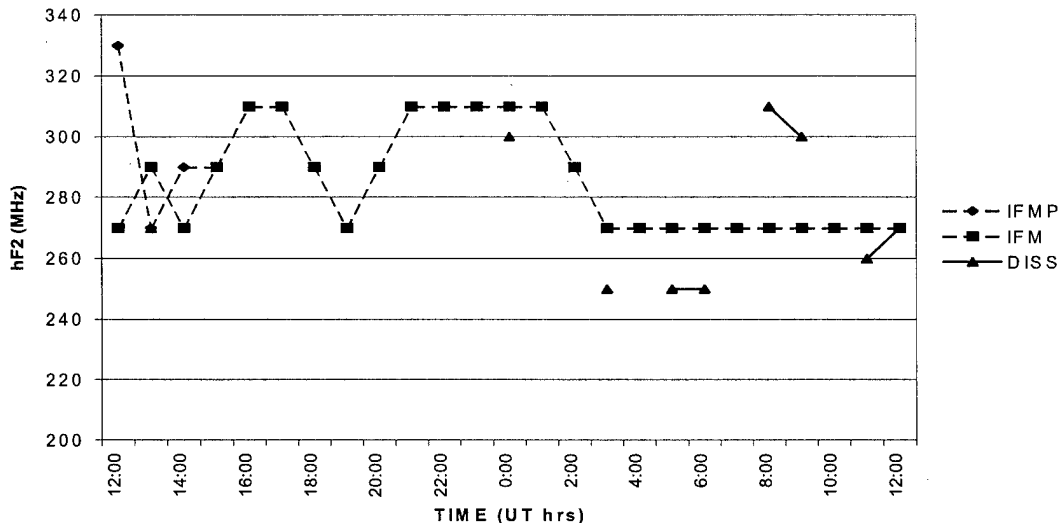


Figure 21. Dixon Island 18-19 September hmF2 data

Table 24. Dixon Island 18-19 September hmF2 data

TIME	Data (hmF2 in km)			Absolute Error		Residual	
	IFMP	IFM	DISS	IFMP	IFM	IFMP	IFM
12:00	330	270					
13:00	270	290	270	0.00	20.00	0.00	20.00
14:00	290	270					
15:00	290	290					
16:00	310	310					
17:00	310	310					
18:00	290	290					
19:00	270	270					
20:00	290	290					
21:00	310	310					
22:00	310	310					
23:00	310	310					
0:00	310	310	300	10.00	10.00	10.00	10.00
1:00	310	310					
2:00	290	290					
3:00	270	270	250	20.00	20.00	20.00	20.00
4:00	270	270					
5:00	270	270	250	20.00	20.00	20.00	20.00
6:00	270	270	250	20.00	20.00	20.00	20.00
7:00	270	270					
8:00	270	270	310	40.00	40.00	-40.00	-40.00
9:00	270	270	300	30.00	30.00	-30.00	-30.00
10:00	270	270					
11:00	270	270	260	10.00	10.00	10.00	10.00
12:00	270	270	270	0.00	0.00	0.00	0.00
	IFM	IFMP				Lat	
Mean Absolute Error		18.89	16.67	Dixon Island (DI373)		73.50 N	
Mean Residual		3.33	1.11	960918/19		Lon	
Correlation		0.37	0.42	80.40 E			

The model output for this station is much better than in previous cases. However, 18-19 September was the only Dixon Island run in this period with enough observed data to be included in the average statistics, so the data is a single run and not a sample of several runs. Still, the error is approximately equal to the observational uncertainty, and the residual is small enough not to indicate any bias in the forecast. The correlation is still poor, but the forecast values are much more reasonable compared to observed values.

The worst agreement for this period was from Tashkent. The average absolute error for the period was 37.95 for IFM and 37.96 for IFMP. The average residual was 17.63 for IFM and 17.64 for IFMP. The average correlation was -0.15 for both the IFM and IFMP. The absolute error is again large, and the residual indicates some positive bias in the model causing it to over forecast the hmF2 values. The correlation remains very poor. Figure 22 and Table 25 show hmF2 data for 17-18 September for Tashkent.

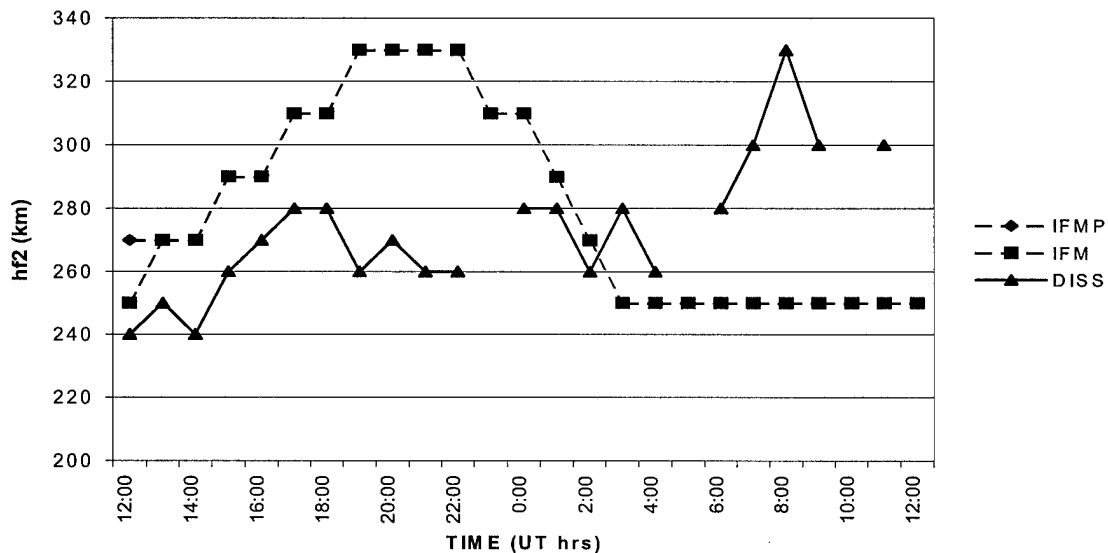


Figure 22. Tashkent 17-18 September hmF2 data

Table 25. Tashkent 17-18 September hmF2 data

TIME	Data (hmF2 in km)			Absolute Error		Residual	
	IFMP	IFM	DISS	IFMP	IFM	IFMP	IFM
12:00	270	250	240	30.00	10.00	30.00	10.00
13:00	270	270	250	20.00	20.00	20.00	20.00
14:00	270	270	240	30.00	30.00	30.00	30.00
15:00	290	290	260	30.00	30.00	30.00	30.00
16:00	290	290	270	20.00	20.00	20.00	20.00
17:00	310	310	280	30.00	30.00	30.00	30.00
18:00	310	310	280	30.00	30.00	30.00	30.00
19:00	330	330	260	70.00	70.00	70.00	70.00
20:00	330	330	270	60.00	60.00	60.00	60.00
21:00	330	330	260	70.00	70.00	70.00	70.00
22:00	330	330	260	70.00	70.00	70.00	70.00
23:00	310	310					
0:00	310	310	280	30.00	30.00	30.00	30.00
1:00	290	290	280	10.00	10.00	10.00	10.00
2:00	270	270	260	10.00	10.00	10.00	10.00
3:00	250	250	280	30.00	30.00	-30.00	-30.00
4:00	250	250	260	10.00	10.00	-10.00	-10.00
5:00	250	250					
6:00	250	250	280	30.00	30.00	-30.00	-30.00
7:00	250	250	300	50.00	50.00	-50.00	-50.00
8:00	250	250	330	80.00	80.00	-80.00	-80.00
9:00	250	250	300	50.00	50.00	-50.00	-50.00
10:00	250	250					
11:00	250	250	300	50.00	50.00	-50.00	-50.00
12:00	250	250					
	IFM	IFMP		Lat Tashkent (TQ241) 960917/18 Lon 69.62 E			
Mean Absolute Error	39.00	39.00					
Mean Residual	9.00	9.00					
Correlation	-0.41	-0.41					

The IFM, though still not forecasting well, produced much better results for this period than for others. However, one must keep in mind that the best results were from a single model run and not an average of several runs. Also worth noting is the extremely low solar activity occurring during this period.

4.2.5 Period 5 hmF2. The best agreement between forecast and observed hmF2 occurred at, Chung-Li. At this station the average absolute error for the period was 15.31 for both IFM and IFMP. The average residual was 9.06 for both IFM and IFMP. The average correlation was -0.12 for both IFM and IFMP. These are the best results obtained, but the averages only included 2 days of the 5 day period, and though the error and residual are not statistically significant, the correlation is still very poor. Figure 23 and Table 26 show the December 13-14 data for Chung-Li.

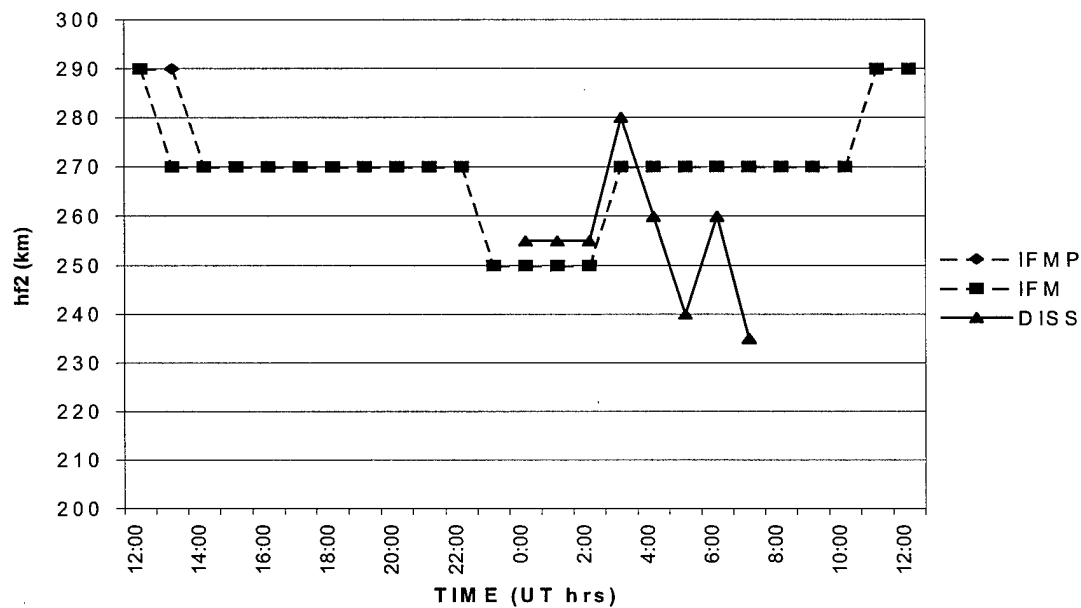


Figure 23. Chung-Li 13-14 December hmF2 data

Table 26. Chung-Li 13-14 December hmF2 data

Data (hmF2 in km)				Absolute Error		Residual	
TIME	IFMP	IFM	DISS	IFMP	IFM	IFMP	IFM
12:00	290	290					
13:00	290	270					
14:00	270	270					
15:00	270	270					
16:00	270	270					
17:00	270	270					
18:00	270	270					
19:00	270	270					
20:00	270	270					
21:00	270	270					
22:00	270	270					
23:00	250	250					
0:00	250	250	255	5.00	5.00	-5.00	-5.00
1:00	250	250	255	5.00	5.00	-5.00	-5.00
2:00	250	250	255	5.00	5.00	-5.00	-5.00
3:00	270	270	280	10.00	10.00	-10.00	-10.00
4:00	270	270	260	10.00	10.00	10.00	10.00
5:00	270	270	240	30.00	30.00	30.00	30.00
6:00	270	270	260	10.00	10.00	10.00	10.00
7:00	270	270	235	35.00	35.00	35.00	35.00
8:00	270	270					
9:00	270	270					
10:00	270	270					
11:00	290	290					
12:00	290	290					
		IFM	IFMP	Lat Chung-Li (CL42424.91 N 961213/14 Lon Correlation 121.24 E			
Mean Absolute Error		13.75	13.75				
Mean Residual		7.50	7.50				
Correlation		0.00	0.00				

The worst agreement for this period was from Grahamstown. The average absolute error for the period was 37.98 for IFM and 39.31 for IFMP. The average residual was -27.59 for IFM and -30.93 for IFMP. The average correlation was 0.61 for IFM and 0.60 for IFMP. The absolute error and large negative residual indicates a strong tendency for the model to underestimate the hmF2 values. The correlation, though still poor, is much better than for other periods and locations. Additionally, all 5 days in the period had 12 to 13 data points to compare, so the correlation is not a result of an unrepresentative sampling. Figure 24 and Table 27 show the 12-13 December Grahamstown data.

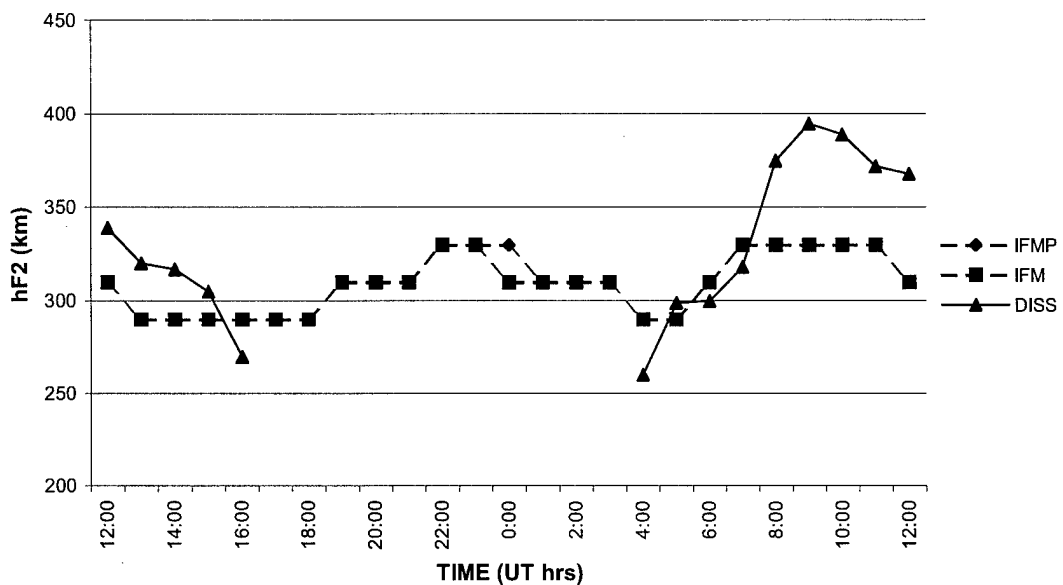


Figure 24. Grahamstown 12-13 December hmF2 data

Table 27. Grahamstown 12-13 December hmF2 data

TIME	Data (hmF2 in km)			Absolute Error		Residual			
	IFMP	IFM	DISS	IFMP	IFM	IFMP	IFM		
12:00	310	310	339	29.00	29.00	-29.00	-29.00		
13:00	290	290	320	30.00	30.00	-30.00	-30.00		
14:00	290	290	317	27.00	27.00	-27.00	-27.00		
15:00	290	290	305	15.00	15.00	-15.00	-15.00		
16:00	290	290	270	20.00	20.00	20.00	20.00		
17:00	290	290							
18:00	290	290							
19:00	310	310							
20:00	310	310							
21:00	310	310							
22:00	330	330							
23:00	330	330							
0:00	330	310							
1:00	310	310							
2:00	310	310							
3:00	310	310							
4:00	290	290	260	30.00	30.00	30.00	30.00		
5:00	290	290	299	9.00	9.00	-9.00	-9.00		
6:00	310	310	300	10.00	10.00	10.00	10.00		
7:00	330	330	318	12.00	12.00	12.00	12.00		
8:00	330	330	375	45.00	45.00	-45.00	-45.00		
9:00	330	330	395	65.00	65.00	-65.00	-65.00		
10:00	330	330	389	59.00	59.00	-59.00	-59.00		
11:00	330	330	372	42.00	42.00	-42.00	-42.00		
12:00	310	310	368	58.00	58.00	-58.00	-58.00		
		IFM	IFMP			Lat			
Mean Absolute Error		32.46	32.46	Grahamstown (GR13 -33.30 N					
Mean Residual		-21.38	-21.38	961212/13 Lon					
Correlation		0.79	0.79	26.50 E					

The IFM performed reasonably well. Results were comparable to period 4. Interestingly, since period 4 experienced a minimum of solar activity, and period 5 had the most active solar indices of the study, there seems little correlation between solar activity and IFM performance. Though this is too limited a case to draw that conclusion with great confidence, since even the most active solar and geomagnetic indices are still very minimal, it does provide impetus for further study. Due to the overall poor results for the hmF2 forecasts, a more detailed analysis was not attempted.

5. Conclusions and Recommendations

5.1 Conclusions

5.1.1 Summary. An increasing dependence on technology within the military demands a better understanding and a robust capability to forecast the environmental conditions effecting that technology. The ionosphere has a potentially huge impact on communications, navigation and intelligence gathering to name just a few. The Ionospheric Forecast Model represents an important first step in moving beyond specifying the current state of the ionosphere or speculating on its future state based on climatology toward forecasting on the basis of the physical principles that actually govern its evolution.

This study has focused on evaluating the IFM's ability to forecast the height and critical frequency of the F2 layer of the ionosphere. The model was run twice for each of the five 5-day periods encompassed in this study. First the model was run by specifying the initial ionosphere using the IRI climatological model and allowing the output from IFM to specify subsequent runs, and second, it was run using the PRISM model with real-time ionosonde data as the initial specification. The research included fifty ionosonde stations as inputs to the PRISM, and used 10 of the 50 ionosonde stations as data points to compare the IFM output against. The time period included March through December of 1996.

5.1.2 Validation of foF2 Forecasts. The IFM does a good job of forecasting foF2. There is a consistent tendency to forecast values higher than what is actually

observed. Typically, forecast values are about 1 MHz above what is observed. The over forecasting of foF2 values seems to be most pronounced in the *ifm_equ* core model, and less pronounced in *ifm_south* and *ifm_north* models. The IFM foF2 output correlates very well with the observed data. The correlation coefficient is around 0.80 on average. There is some evidence, though not conclusive, that the correlation is poorest during the winter season, especially in the northern hemisphere. It seems odd that the IFM does not do a better job during the hemisphere's respective winter seasons since solar radiation is incident on the ionosphere for shorter periods of time. The most unexpected result of this study is that using real-time ionosonde data through PRISM to specify the initial ionosphere produced no better results than cold starting the IFM with an IRI specification. It appeared from the graphical analysis that the real-time data only effected the first 2 to 12 hours of the IFM's output, and in most cases the IFMP solution rapidly converged to the IFM solution. Based on that analysis, the absolute errors were for IFM vs. IFMP were calculated and graphed to determine if there was a more significant difference between methods before the solutions converged. In a few cases this calculation resulted in a significant improvement in the IFMP absolute error versus the IFM absolute error, but on average, the improvement was very marginal, and not statistically significant. The IFM's foF2 forecasts have a consistent positive bias, but are reasonably accurate and correlate well with observations. This analysis is likely the best possible scenario for obtaining an accurate forecast since the output stations analyzed coincided with real-time input data locations. Significantly different results might be obtained if the output stations are excluded from the input pool. If implemented, the Fof2 forecasting capability would be a useful operational tool.

5.1.3 Validation of hmF2 Forecasts. On average, the IFM does a poor job of forecasting hmF2. Though there were only 6 stations with sufficient data for comparisons, and the data was much more sparse than that available to validate the foF2 forecasts, the hmF2 forecasts were consistently poor with few exceptions. The hmF2 forecasts had an average error of about 40 km, which exceeds the 20 km error established as a "good" forecast criteria, even when measurement error is considered. In most cases the forecasts under predicted the observed values. If the under forecasting were consistent and predictable, the output might still be of value, but the error varies greatly. The correlation between the forecast output and the observations was consistently poor with few exceptions. The limited vertical spatial resolution and the sparse observational data likely contributed to the poor results. The IFM's hmF2 forecasting capability would not be a useful operational tool in its present form.

5.2 Recommendations

The IFM requires further validation under a much greater variety of conditions to evaluate its potential and capabilities. Additional studies that would be useful include:

- A study of the other output parameters of the IFM, especially the TEC
- Another study with cold start versus PRISM start using other data sources such as TEC, satellite or backscatter radar data
- A study comparing cold start for every run versus initial cold start and initializations with IFM output for subsequent runs versus PRISM initialization runs or some combination of these

- A thorough study of seasonal or geographic dependencies
- A study under more active solar or geomagnetic conditions
- A more detailed evaluation of the temporal influence (through the course of a 24-hour forecast) of ingesting real-time data versus cold starting

Finally, the IFM appears to lessen the importance of the real-time inputs rather rapidly and revert to the cold start solution. While this is certainly advantageous if the model happens to be initialized with bad data, it also abandons the potential accuracy that could be gained with reliable data input, and a strong model dependence on the initial data. In many of the graphs produced during this study, there was a persistence in the foF2 value from 1200 UT at the start of the run to 1200 UT at the end of the forecast. If the models had retained the initial, real-time data biased solution, and taken persistence into account, it seems that the accuracy of the model might be dramatically improved. This, of course, would leave the model at the mercy of bad data, but thorough data validation prior to model input could alleviate that concern.

Appendix A: Space Environment Corporation Validation Results

The information in this appendix is summarized from AFRL-VS-HA-TR-98-0001 which is contained in the bibliography. Space Environment Corporation, as part of their contract to upgrade and support the IFM, have conducted a broad range of validations. These validations have covered all versions of the model, and have resulted in several changes and improvements. This appendix only contains that information most relevant to the research reported in this thesis.

In a validation relevant to mid-latitudes, and comparing to ionosonde and incoherent scatter radar data, the following conclusions were found. During solar minimum Summer, both NmF2 and hmF2 were in good agreement with measurements. However, during solar minimum winter, IFM failed to reproduce a pre-dawn secondary maximum in NmF2, but otherwise was in good agreement with NmF2 measurements. Also during the winter, hmF2 values were approximately 20 km too high compared to measurements.

In a validation comparing IFM forecasts with DMSP *in situ* electron density measurements, variations were in good agreement, but measured densities were about 10 to 25% greater than forecasted. IFM forecasts correlate well with high latitude features. A weak storm during one day of the validation was modeled as an increased electron density by IFM in agreement with DMSP measurements.

Another extensive validation with ionosonde data revealed that nighttime density variations are not modeled well by IFM. Observations showed a distinct variation from one night to another, while the IFM was more consistent from night to night.

During a second validation phase conducted for the southern hemisphere in and around Australia, it was found that in the low latitudes to lower mid latitudes that NmF2 agrees within about 20%, and hmF2 agrees with measurements within +/- 20 km during the day but is too high by 20 to 80 km at night.

Appendix B: The Ionosphere

This appendix is intended to provide a broad overview of some of the key processes of the ionosphere, and to establish an appreciation for the formidable task that is represented in trying to forecast the ionosphere globally. This appendix is based on (Kelley, 1989; Rees, 1989 and Tascione, 1994)

The ionosphere is that region of the atmosphere that consists of a partially ionized gas due to solar radiation and particle precipitation. Three main processes vie for control of the ionosphere's composition and structure. Those processes are ionization, recombination and transport. As stated earlier, ionization occurs due to incident solar radiation and particle collisions. Recombination occurs through recombination of electrons and ions and is a very dependent on density, which dictates that the probability of recombination increases as density (and thus collision frequency) increases. Transport is the final player in determining how the ions and electrons of the ionosphere will be distributed. Unlike the lower, neutral atmosphere where fluid dynamics primarily dictate the motions of the winds, the ionosphere is also subject to electric and magnetic fields influencing motions. It is primarily the ionosphere's electromagnetic properties that makes it so rich in structure and so difficult to easily forecast. These three important processes are substantially described by three equations: the continuity equation (equation 9), the energy equation (equation 10), and the momentum equation (equation 11).

$$\frac{\partial \rho_i}{\partial t} = (P_i - L_i) M_i - \nabla \cdot (\rho_i \mathbf{V}_i) \quad (9)$$

The term on the left-hand side is the time-rate-of change of the i^{th} constituent. ρ_i is the density. The first term on the right-hand side is the local production and loss term, and M_i is the mass of the constituent. This first term represents the photochemical, chemical and collisional processes adding and removing ion-electron pairs to the ionosphere. The second term on the right is the transport term, and describes the transport of the constituent into or out of the volume. V_i is the drift velocity of the ions or electrons. A similar continuity equation applies to the neutral species in the atmosphere, but since the number of neutrals is much greater than the number of ions and electrons, local production and loss terms are not used, and the velocity is the neutral wind speed.

$$\rho_i k \frac{d_i T_i}{dt} = Q_i - L_i^T - n_i k T_i \nabla \cdot v_i - \nabla \cdot q_i + \sum_{\text{in } i} F_i \cdot v_i \quad (10)$$

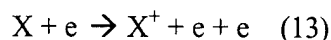
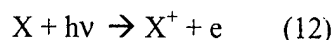
The energy equation represents the time rate of change of energy. The convective derivative on the left is the net time rate of change of energy per unit volume. The terms on the right hand side represent: the local heating rate, the heat loss rate, compressional heating, divergence of heat flow, and the work done on the i^{th} constituent respectively.

$$\rho \frac{d\mathbf{v}}{dt} = \mathbf{J} \times \mathbf{B} - \nabla p + \rho \mathbf{g} \quad (11)$$

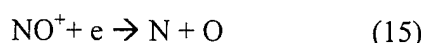
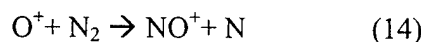
The momentum equation describes the motion of a plasma. The term on the left is the time rate of change of momentum. It is balanced on the right by the external forces due to electromagnetic forces, pressure gradient and gravity.

These are the three equations that are solved numerically within the IFM core programs.

Production and loss mechanisms are many and varied in the ionosphere. Photoionization represented by equation 12 is the primary ionization source though impact ionization represented by equation 13 also contributes, especially in the polar regions.



The major ion present in the F2 layer is O^+ produced by photoionization of atomic oxygen. The recombination process is not straight forward. A process call ion atom interchange (equation 14) is responsible for removing the O^+ from the F2 region. A dissociative recombination process (equation 15) can then convert the ion and an electron back into neutral species.



Transport of ions and electrons is an extremely complex topic. Unlike a neutral gas where one must consider only gravity, diffusion, coriolis and the neutral wind flow, charged particles are also influenced by electric fields and magnetic fields. Additionally, once the plasma is set in motion, it often produces additional electric and magnetic fields which in turn alter the plasmas motion again. The zonal electric field along the equator is one example of how plasma transport differs from a neutral gas. This field is directed

from the dawn terminator toward the dusk terminator. In combination with the earth's magnetic field, an **E** X **B** force causes the plasma to drift up during the day and down at night. Just prior to the reversal of the field at dusk, the field's strength is enhanced. High conductivity along the magnetic field lines allows the plasma from the equatorial F layer to move to the high latitude E layer regions. To further complicate matters, not all of the variables influencing plasma motions in the ionosphere are contained within the ionosphere. The solar wind flowing past the earth's dipole magnetic field at great distances above the equator induce an electric field between magnetic field lines. This electric field is then mapped along the field lines to where they converge in the polar regions and induce currents in the ionosphere. The ionosphere is energetically coupled to the magnetosphere and to space. It is not an isolated system.

Appendix C: PRISM

The Parameterized Real-Time Ionospheric Specification Model (PRISM) is a computer model designed to specify the state of the ionosphere. As inputs, the PRISM requires the K_p value, the y and z components of the IMF, the F10.7 cm flux and the sun spot number. PRISM can produce an output with only these parameters. This part of the model is referred to as the Parameterized Ionospheric Model (PIM). This output is the result of a climatological database processed by four different physics-based ionospheric models contained within the PIM model. The intended method for using the model is to input additional real-time observational data to enhance the accuracy of the specification. PRISM accepts a wide variety of inputs such as DISS data, TEC data from GPS and from the Ionospheric Monitoring System, and *in situ* measurements from satellites. The input data is weighted based on its location and is used to adjust the output from the PIM.

Results of validations of PRISM have been mixed. A validation of an earlier version of the model by Computational Physics Inc., the designer of the model, showed that the model performed much better than previous ionospheric specification models. A subsequent validation (Coxwell, 1996) indicated that the model often performed better with no observational data input than with DISS input.

Appendix D: Diss Station Information

Data from the following DISS stations were used as input to the PRISM model. Stations preceded by a * are the ground truth stations which IFM output was compared against. Not all stations had data available for all times used in the PRISM input files. All available data was used with a time of the model hour +/- one hour. Latitude and longitude are in geographic coordinates with positive latitude being north, negative latitude being south, and positive longitude being measured from 0 to 360 degrees in an eastward direction from the zero degree prime meridian.

Ashkhabad (AS237)	37.900N, 58.300E
Beijing (BP440)	39.900N, 116.500E
Bermuda (BJJ32)	32.400N, 295.300E
Boulder (BC840)	40.000N, 254.700E
Camden (CN53L)	-34.000S, 150.700E
*Chilton (RL052)	51.600N, 358.700E
Chongqing (09429)	29.500N, 106.400E
*Chung-Li (CL424)	24.910N, 121.240E
Churchill (CH958)	58.800N, 265.800E
College (CO764)	64.800N, 212.200E
*Dixon Island (DI373)	73.500N, 80.400E
Dumont d'Urville/Terre Adelie (DU56O)	-66.660S, 140.020E
Dyess (DS932)	32.400N, 260.300E

*Eglin AFB (EG931)	30.400N, 273.200E
El Arenosillo (EA036)	37.100N, 353.270E
Goose Bay (GSJ53)	54.300N, 299.670E
*Grahamstown (GR13L)	-33.300S, 26.500E
Guangzhou (GU421)	23.100N, 113.400E
*Hobart (HO54K)	-42.920S, 147.320E
Irkutsk (IR352)	52.500N, 104.000E
Juliusruh/Rugen (JR055)	54.600N, 13.400E
Kiruna (KI167)	67.840N, 20.420E
Lannion (LN047)	48.450N, 356.730E
*Learmonth (LM42B)	-21.900S, 114.000E
Leningrad (LD160)	59.950N, 30.700E
*Lerwick (LE061)	60.130N, 358.820E
Lycksele (LY164)	64.620N, 18.760E
Magadan (MG560)	60.000N, 151.000E
Manzhouli (ML449)	49.600N, 117.500E
Moscow (MO155)	55.500N, 37.300E
Nicosia (NC136)	35.100N, 33.200E
Novosibirsk (NS355)	54.600N, 83.200E
Okinawa (OK426)	26.300N, 127.800E
Ottawa (OT945)	45.400N, 284.100E
Petroplavsk (PK553)	53.020N, 158.650E
Point Arguello (PA836)	35.600N, 239.400E

Poitiers (PT046)	46.570N, 0.350E
Resolute Bay (RB974)	74.700N, 265.100E
Rome (RO041)	41.900N, 12.520E
Rostov-on-Don (RV149)	47.200N, 39.680E
Salekhard (SD266)	66.500N, 66.700E
Sofia (SQ143)	42.700N, 23.400E
Stanley (PSJ5J)	-51.700S, 302.200E
*Tashkent (TQ241)	41.330N, 69.620E
Tokyo (TO535)	35.700N, 139.500E
*Townsville (TV51R)	-19.630S, 146.850E
Tunguska (TZ362)	61.600N, 90.000E
Uppsala (UP158)	59.800N, 17.600E
Wakkai (WK545)	45.400N, 141.700E
Wallops Island (WP937)	37.900N, 284.500E

Appendix E: Additional Charts and Tables

This appendix contains additional charts and tables from individual runs of the IFM. It does not contain all of the data produced for this study, but only a representative sample of some of the more interesting results. Charts and tables showing foF2 data are first followed by hmF2 data.

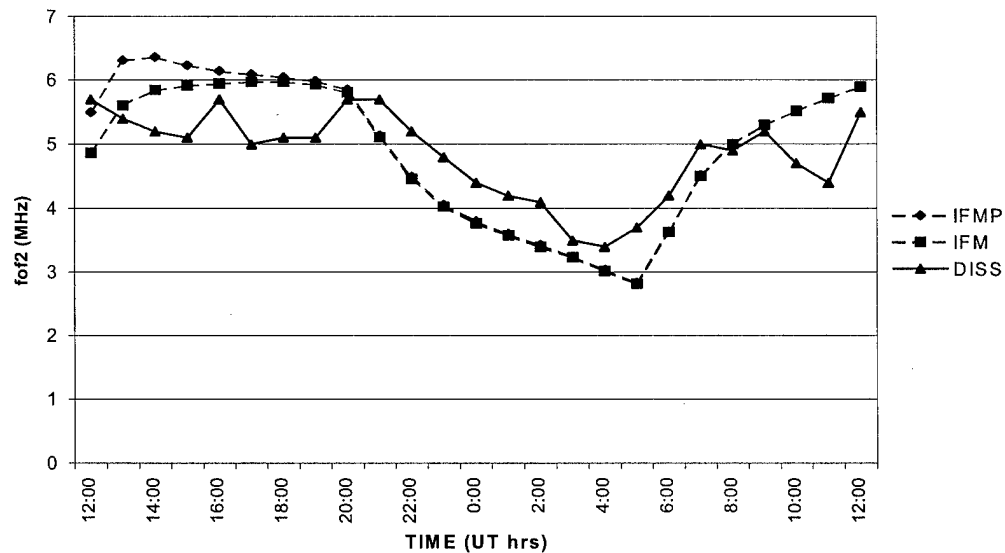


Figure 25. Chilton 10-11 May foF2 data

Table 28. Chilton 10-11 May foF2 data

TIME	Data (foF2 in MHz)			Absolute Error		Residual	
	IFMP	IFM	DISS	IFMP	IFM	IFMP	IFM
12:00	5.5	4.87	5.7	0.20	0.83	-0.20	-0.83
13:00	6.32	5.61	5.4	0.92	0.21	0.92	0.21
14:00	6.37	5.85	5.2	1.17	0.65	1.17	0.65
15:00	6.24	5.92	5.1	1.14	0.82	1.14	0.82
16:00	6.15	5.95	5.7	0.45	0.25	0.45	0.25
17:00	6.1	5.98	5	1.10	0.98	1.10	0.98
18:00	6.05	5.98	5.1	0.95	0.88	0.95	0.88
19:00	5.99	5.94	5.1	0.89	0.84	0.89	0.84
20:00	5.86	5.81	5.7	0.16	0.11	0.16	0.11
21:00	5.14	5.11	5.7	0.56	0.59	-0.56	-0.59
22:00	4.5	4.46	5.2	0.70	0.74	-0.70	-0.74
23:00	4.06	4.03	4.8	0.74	0.77	-0.74	-0.77
0:00	3.8	3.77	4.4	0.60	0.63	-0.60	-0.63
1:00	3.6	3.58	4.2	0.60	0.62	-0.60	-0.62
2:00	3.43	3.4	4.1	0.67	0.70	-0.67	-0.70
3:00	3.25	3.23	3.5	0.25	0.27	-0.25	-0.27
4:00	3.04	3.02	3.4	0.36	0.38	-0.36	-0.38
5:00	2.84	2.82	3.7	0.86	0.88	-0.86	-0.88
6:00	3.64	3.63	4.2	0.56	0.57	-0.56	-0.57
7:00	4.52	4.51	5	0.48	0.49	-0.48	-0.49
8:00	5.01	5	4.9	0.11	0.10	0.11	0.10
9:00	5.3	5.3	5.2	0.10	0.10	0.10	0.10
10:00	5.52	5.52	4.7	0.82	0.82	0.82	0.82
11:00	5.72	5.72	4.4	1.32	1.32	1.32	1.32
12:00	5.9	5.9	5.5	0.40	0.40	0.40	0.40
		IFM	IFMP			Lat	
Mean Absolute Error		0.59	0.66	Chilton (RL052)	51.60 N		
Mean Residual		0.04	0.13	960510/11	Lon		
Correlation		0.82	0.82		358.70 E		

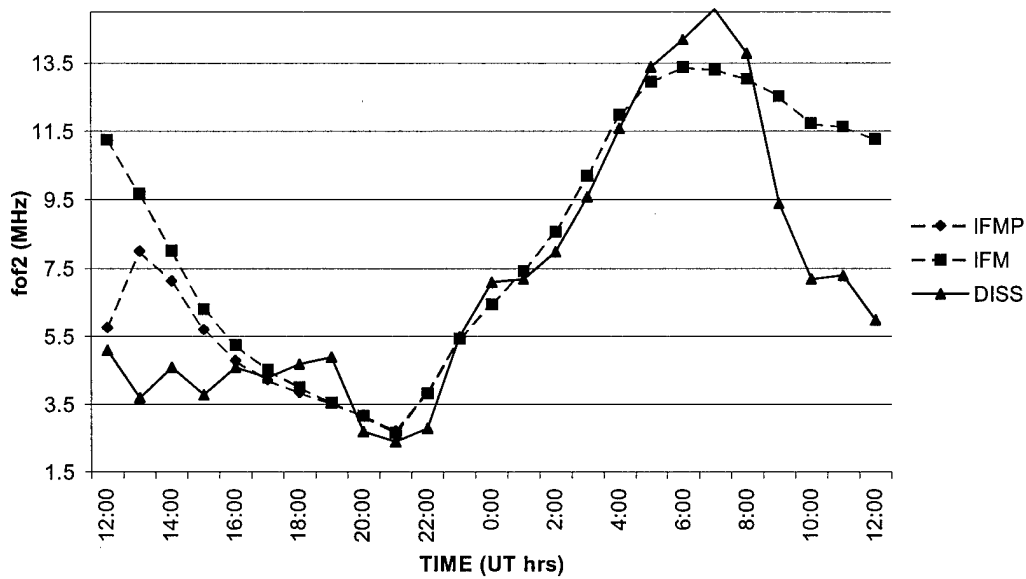


Figure 26. Chung-Li 18-19 March foF2 data

Table 29. Chung-Li 18-19 March foF2 data

TIME	Data (foF2 in MHz)			Absolute Error		Residual	
	IFMP	IFM	DISS	IFMP	IFM	IFMP	IFM
12:00	5.77	11.27	5.1	0.67	6.17	0.67	6.17
13:00	8.02	9.68	3.7	4.32	5.98	4.32	5.98
14:00	7.14	8.03	4.6	2.54	3.43	2.54	3.43
15:00	5.72	6.32	3.8	1.92	2.52	1.92	2.52
16:00	4.81	5.26	4.6	0.21	0.66	0.21	0.66
17:00	4.23	4.53	4.3	0.07	0.23	-0.07	0.23
18:00	3.86	4.02	4.7	0.84	0.68	-0.84	-0.68
19:00	3.53	3.56	4.9	1.37	1.34	-1.37	-1.34
20:00	3.19	3.17	2.7	0.49	0.47	0.49	0.47
21:00	2.72	2.67	2.4	0.32	0.27	0.32	0.27
22:00	3.86	3.84	2.8	1.06	1.04	1.06	1.04
23:00	5.44	5.44	5.5	0.06	0.06	-0.06	-0.06
0:00	6.46	6.45	7.1	0.64	0.65	-0.64	-0.65
1:00	7.43	7.43	7.2	0.23	0.23	0.23	0.23
2:00	8.57	8.57	8	0.57	0.57	0.57	0.57
3:00	10.21	10.21	9.6	0.61	0.61	0.61	0.61
4:00	11.99	11.99	11.6	0.39	0.39	0.39	0.39
5:00	12.96	12.96	13.4	0.44	0.44	-0.44	-0.44
6:00	13.4	13.4	14.2	0.80	0.80	-0.80	-0.80
7:00	13.32	13.32	15.1	1.78	1.78	-1.78	-1.78
8:00	13.05	13.05	13.8	0.75	0.75	-0.75	-0.75
9:00	12.53	12.53	9.4	3.13	3.13	3.13	3.13
10:00	11.75	11.75	7.2	4.55	4.55	4.55	4.55
11:00	11.65	11.65	7.3	4.35	4.35	4.35	4.35
12:00	11.29	11.29	6	5.29	5.29	5.29	5.29
				IFM	IFMP	Lat	
Mean Absolute Error				1.68	1.53	Chung-Li (CL424) 24.91 N	
Mean Residual				1.13	0.97	960318/19 Lon	
Correlation				0.84	0.86	121.24 E	

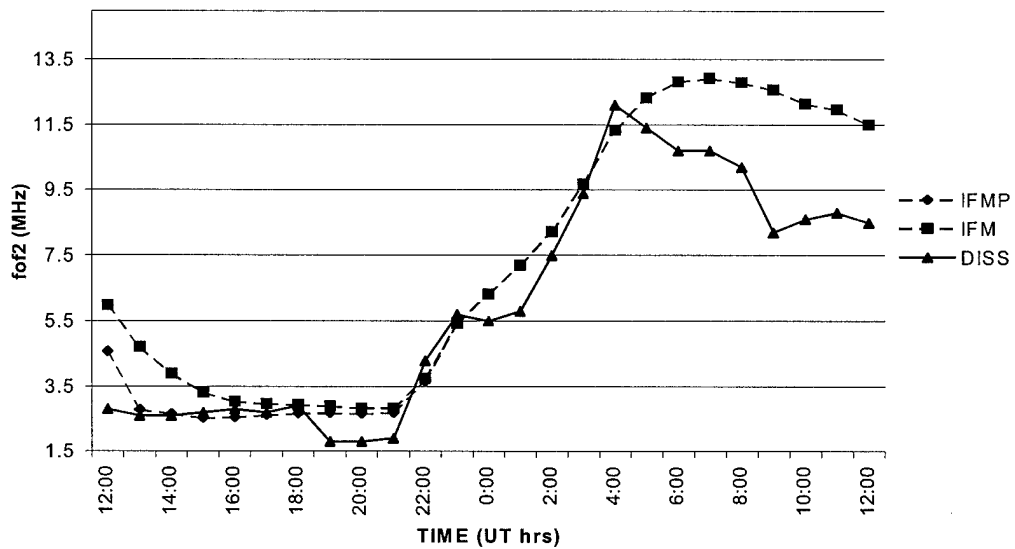


Figure 27. Chung-Li 14-15 September foF2 data

Table 30 Chung-Li 14-15 September foF2 data

TIME	Data (foF2 in MHz)			Absolute Error		Residual	
	IFMP	IFM	DISS	IFMP	IFM	IFMP	IFM
12:00	4.58	5.99	2.8	1.78	3.19	1.78	3.19
13:00	2.79	4.72	2.6	0.19	2.12	0.19	2.12
14:00	2.67	3.91	2.6	0.07	1.31	0.07	1.31
15:00	2.53	3.32	2.7	0.17	0.62	-0.17	0.62
16:00	2.55	3.04	2.8	0.25	0.24	-0.25	0.24
17:00	2.63	2.98	2.7	0.07	0.28	-0.07	0.28
18:00	2.68	2.94	2.9	0.22	0.04	-0.22	0.04
19:00	2.69	2.9	1.8	0.89	1.10	0.89	1.10
20:00	2.67	2.84	1.8	0.87	1.04	0.87	1.04
21:00	2.7	2.84	1.9	0.80	0.94	0.80	0.94
22:00	3.66	3.75	4.3	0.64	0.55	-0.64	-0.55
23:00	5.42	5.43	5.7	0.28	0.27	-0.28	-0.27
0:00	6.32	6.33	5.5	0.82	0.83	0.82	0.83
1:00	7.21	7.22	5.8	1.41	1.42	1.41	1.42
2:00	8.22	8.23	7.5	0.72	0.73	0.72	0.73
3:00	9.69	9.69	9.4	0.29	0.29	0.29	0.29
4:00	11.32	11.33	12.1	0.78	0.77	-0.78	-0.77
5:00	12.34	12.34	11.4	0.94	0.94	0.94	0.94
6:00	12.83	12.83	10.7	2.13	2.13	2.13	2.13
7:00	12.93	12.93	10.7	2.23	2.23	2.23	2.23
8:00	12.8	12.8	10.2	2.60	2.60	2.60	2.60
9:00	12.58	12.58	8.2	4.38	4.38	4.38	4.38
10:00	12.15	12.15	8.6	3.55	3.55	3.55	3.55
11:00	11.97	11.97	8.8	3.17	3.17	3.17	3.17
12:00	11.51	11.51	8.5	3.01	3.01	3.01	3.01
		IFM	IFMP			Lat	
Mean Absolute Error				1.44	1.27	Chung-Li (CL424)	24.91 N
Mean Residual				1.31	1.07	960914/15	Lon
Correlation				0.95	0.96		121.24 E

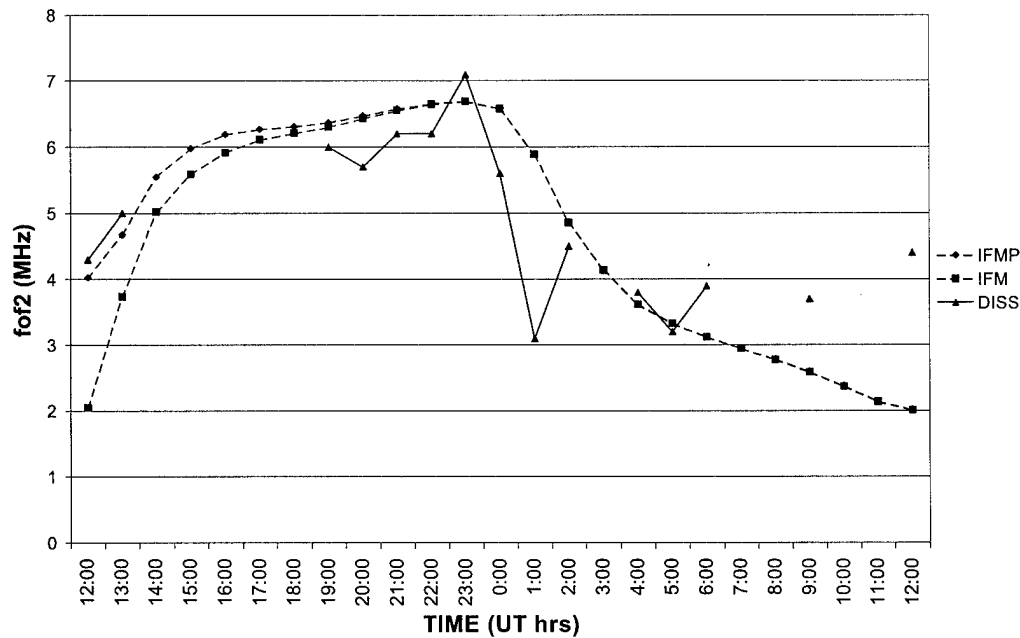


Figure 28. Eglin AFB 15-16 September foF2 data

Table 31. Eglin AFB 15-16 September foF2 data

TIME	Data (foF2 in MHz)			Absolute Error		Residual	
	IFMP	IFM	DISS	IFMP	IFM	IFMP	IFM
12:00	4.03	2.05	4.3	0.27	2.25	-0.27	-2.25
13:00	4.68	3.74	5	0.32	1.26	-0.32	-1.26
14:00	5.55	5.02					
15:00	5.98	5.59					
16:00	6.19	5.92					
17:00	6.27	6.11					
18:00	6.31	6.21					
19:00	6.37	6.3	6	0.37	0.30	0.37	0.30
20:00	6.47	6.43	5.7	0.77	0.73	0.77	0.73
21:00	6.58	6.55	6.2	0.38	0.35	0.38	0.35
22:00	6.66	6.65	6.2	0.46	0.45	0.46	0.45
23:00	6.7	6.69	7.1	0.40	0.41	-0.40	-0.41
0:00	6.59	6.58	5.6	0.99	0.98	0.99	0.98
1:00	5.9	5.89	3.1	2.80	2.79	2.80	2.79
2:00	4.87	4.86	4.5	0.37	0.36	0.37	0.36
3:00	4.15	4.14					
4:00	3.63	3.62	3.8	0.17	0.18	-0.17	-0.18
5:00	3.33	3.33	3.2	0.13	0.13	0.13	0.13
6:00	3.13	3.12	3.9	0.77	0.78	-0.77	-0.78
7:00	2.95	2.95					
8:00	2.79	2.78					
9:00	2.6	2.59	3.7	1.10	1.11	-1.10	-1.11
10:00	2.38	2.37					
11:00	2.15	2.14					
12:00	2.02	2.01	4.4	2.38	2.39	-2.38	-2.39
				IFM	IFMP	Lat	
Mean Absolute Error				0.87	0.82	Eglin AFB (EG931)	
Mean Residual				0.00	0.08	960915/16	
Correlation				0.72	0.73	Lon	
						273.20 E	

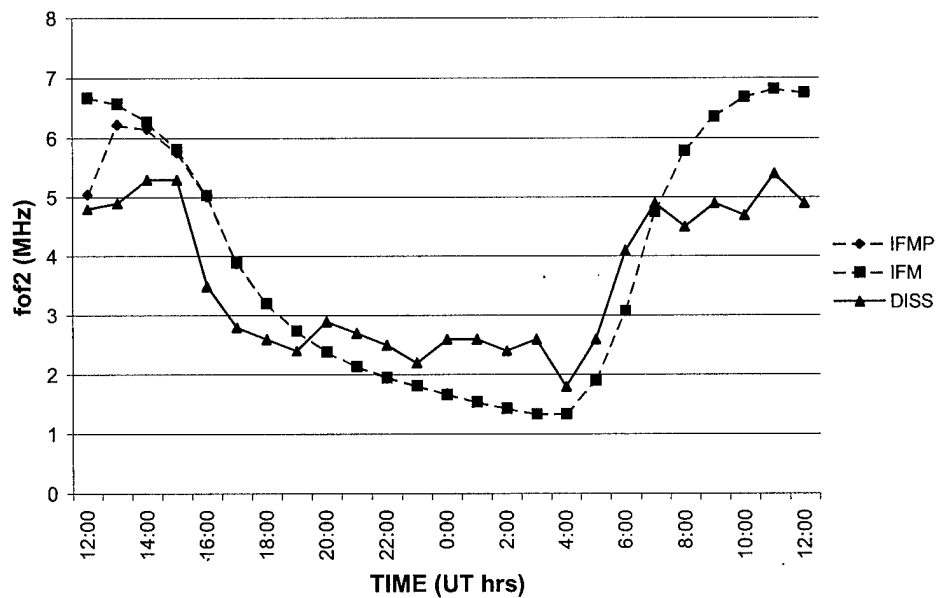


Figure 29. Grahamstown 10-11 July foF2 data

Table 32. Grahamstown 10-11 July foF2 data

TIME	Data (foF2 in MHz)			Absolute Error		Residual	
	IFMP	IFM	DISS	IFMP	IFM	IFMP	IFM
12:00	5.05	6.68	4.8	0.25	1.88	0.25	1.88
13:00	6.23	6.58	4.9	1.33	1.68	1.33	1.68
14:00	6.16	6.28	5.3	0.86	0.98	0.86	0.98
15:00	5.76	5.82	5.3	0.46	0.52	0.46	0.52
16:00	5.01	5.04	3.5	1.51	1.54	1.51	1.54
17:00	3.88	3.9	2.8	1.08	1.10	1.08	1.10
18:00	3.21	3.21	2.6	0.61	0.61	0.61	0.61
19:00	2.74	2.74	2.4	0.34	0.34	0.34	0.34
20:00	2.39	2.39	2.9	0.51	0.51	-0.51	-0.51
21:00	2.14	2.14	2.7	0.56	0.56	-0.56	-0.56
22:00	1.96	1.95	2.5	0.54	0.55	-0.54	-0.55
23:00	1.81	1.81	2.2	0.39	0.39	-0.39	-0.39
0:00	1.68	1.67	2.6	0.92	0.93	-0.92	-0.93
1:00	1.54	1.54	2.6	1.06	1.06	-1.06	-1.06
2:00	1.43	1.43	2.4	0.97	0.97	-0.97	-0.97
3:00	1.34	1.34	2.6	1.26	1.26	-1.26	-1.26
4:00	1.34	1.34	1.8	0.46	0.46	-0.46	-0.46
5:00	1.9	1.9	2.6	0.70	0.70	-0.70	-0.70
6:00	3.08	3.08	4.1	1.02	1.02	-1.02	-1.02
7:00	4.75	4.75	4.9	0.15	0.15	-0.15	-0.15
8:00	5.79	5.79	4.5	1.29	1.29	1.29	1.29
9:00	6.36	6.36	4.9	1.46	1.46	1.46	1.46
10:00	6.69	6.69	4.7	1.99	1.99	1.99	1.99
11:00	6.82	6.82	5.4	1.42	1.42	1.42	1.42
12:00	6.76	6.76	4.9	1.86	1.86	1.86	1.86
				IFM	IFMP	Lat	
Mean Absolute Error				0.97	0.95	Grahamstown (GR13L)	
Mean Residual				0.26	0.24	-33.30 N	
Correlation				0.92	0.92	960710/11	
				Lon		26.50 E	

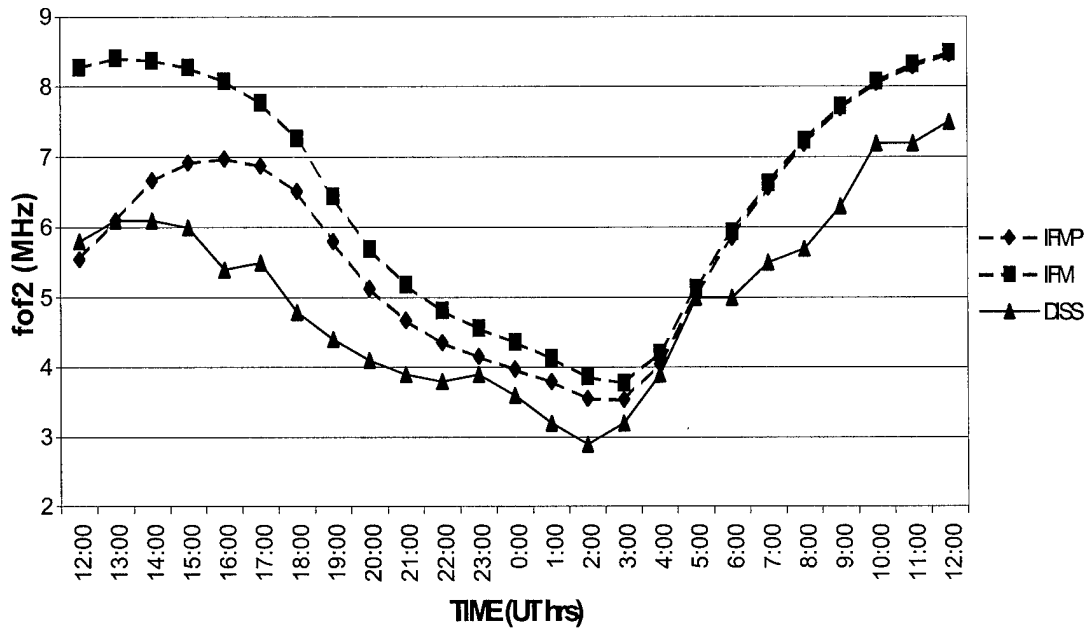


Figure 30. Grahamstown 13-14 December foF2 data

Table 33. Grahamstown 13-14 December foF2 data

TIME	Data (foF2 in MHz)			Absolute Error		Residual	
	IFMP	IFM	DSS	IFMP	IFM	IFMP	IFM
12:00	5.55	8.28	5.8	0.25	2.48	-0.25	2.48
13:00	6.1	8.41	6.1	0.00	2.31	0.00	2.31
14:00	6.67	8.38	6.1	0.57	2.28	0.57	2.28
15:00	6.92	8.28	6	0.92	2.28	0.92	2.28
16:00	6.98	8.09	5.4	1.58	2.69	1.58	2.69
17:00	6.88	7.78	5.5	1.38	2.28	1.38	2.28
18:00	6.52	7.27	4.8	1.72	2.47	1.72	2.47
19:00	5.8	6.45	4.4	1.40	2.05	1.40	2.05
20:00	5.13	5.7	4.1	1.03	1.60	1.03	1.60
21:00	4.68	5.19	3.9	0.78	1.29	0.78	1.29
22:00	4.36	4.82	3.8	0.56	1.02	0.56	1.02
23:00	4.16	4.57	3.9	0.26	0.67	0.26	0.67
0:00	3.98	4.37	3.6	0.38	0.77	0.38	0.77
1:00	3.8	4.14	3.2	0.60	0.94	0.60	0.94
2:00	3.56	3.87	2.9	0.66	0.97	0.66	0.97
3:00	3.54	3.78	3.2	0.34	0.58	0.34	0.58
4:00	4.05	4.21	3.9	0.15	0.31	0.15	0.31
5:00	5.04	5.14	5	0.04	0.14	0.04	0.14
6:00	5.86	5.94	5	0.86	0.94	0.86	0.94
7:00	6.57	6.64	5.5	1.07	1.14	1.07	1.14
8:00	7.19	7.24	5.7	1.49	1.54	1.49	1.54
9:00	7.69	7.73	6.3	1.39	1.43	1.39	1.43
10:00	8.05	8.09	7.2	0.85	0.89	0.85	0.89
11:00	8.3	8.33	7.2	1.10	1.13	1.10	1.13
12:00	8.46	8.49	7.5	0.96	0.99	0.96	0.99

	IFM	IFMP	Lat
Mean Absolute Error	1.36	0.84	Grahamstown (GR13L) -33.30 N
Mean Residual	1.36	0.84	961213/14 Lon
Correlation	0.92	0.95	26.50 E

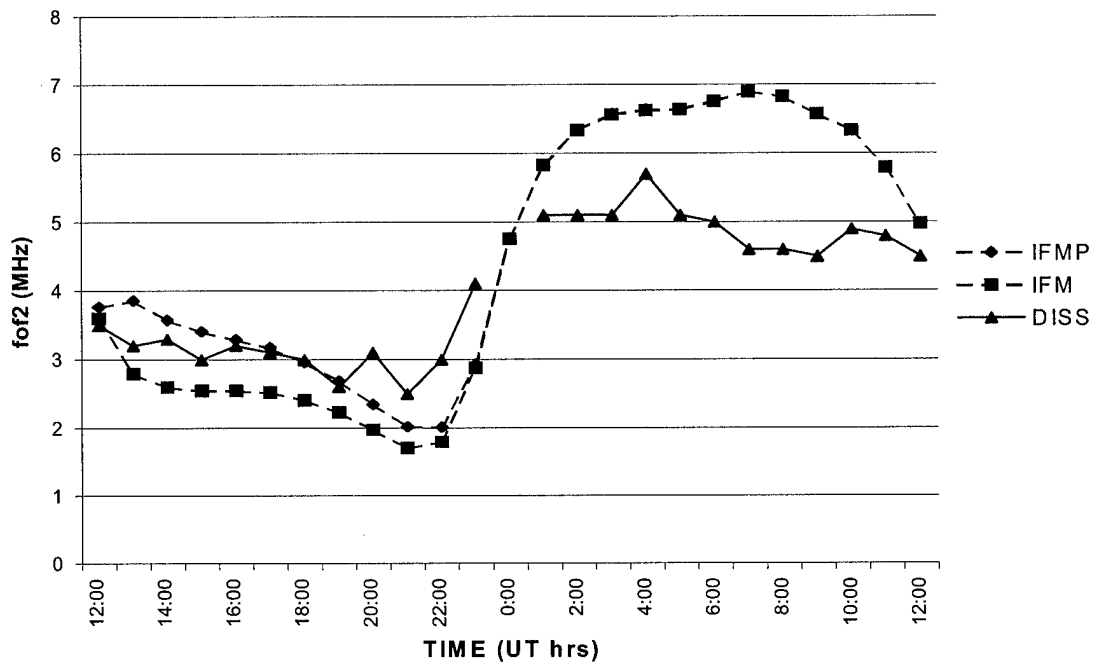


Figure 31. Learmonth 14-15 September foF2 data

Table 34. Learmonth 14-15 September foF2 data

TIME	Data (foF2 in MHz)			Absolute Error		Residual	
	IFMP	IFM	DISS	IFMP	IFM	IFMP	IFM
12:00	3.77	3.6	3.5	0.27	0.10	0.27	0.10
13:00	3.86	2.8	3.2	0.66	0.40	0.66	-0.40
14:00	3.58	2.6	3.3	0.28	0.70	0.28	-0.70
15:00	3.41	2.55	3	0.41	0.45	0.41	-0.45
16:00	3.29	2.55	3.2	0.09	0.65	0.09	-0.65
17:00	3.18	2.53	3.1	0.08	0.57	0.08	-0.57
18:00	2.96	2.41	3	0.04	0.59	-0.04	-0.59
19:00	2.69	2.23	2.6	0.09	0.37	0.09	-0.37
20:00	2.35	1.98	3.1	0.75	1.12	-0.75	-1.12
21:00	2.02	1.71	2.5	0.48	0.79	-0.48	-0.79
22:00	2.01	1.8	3	0.99	1.20	-0.99	-1.20
23:00	2.93	2.88	4.1	1.17	1.22	-1.17	-1.22
0:00	4.77	4.76					
1:00	5.84	5.83	5.1	0.74	0.73	0.74	0.73
2:00	6.35	6.34	5.1	1.25	1.24	1.25	1.24
3:00	6.58	6.57	5.1	1.48	1.47	1.48	1.47
4:00	6.64	6.63	5.7	0.94	0.93	0.94	0.93
5:00	6.65	6.64	5.1	1.55	1.54	1.55	1.54
6:00	6.77	6.76	5	1.77	1.76	1.77	1.76
7:00	6.9	6.9	4.6	2.30	2.30	2.30	2.30
8:00	6.83	6.83	4.6	2.23	2.23	2.23	2.23
9:00	6.58	6.58	4.5	2.08	2.08	2.08	2.08
10:00	6.34	6.34	4.9	1.44	1.44	1.44	1.44
11:00	5.8	5.8	4.8	1.00	1.00	1.00	1.00
12:00	4.98	4.98	4.5	0.48	0.48	0.48	0.48
		IFM	IFMP			Lat	
Mean Absolute Error		1.10	0.97	Learmonth (LM42B)		-21.9	
Mean Residual		0.40	0.67	960914/15		Lon	
Correlation		0.94	0.92	114.00 E			

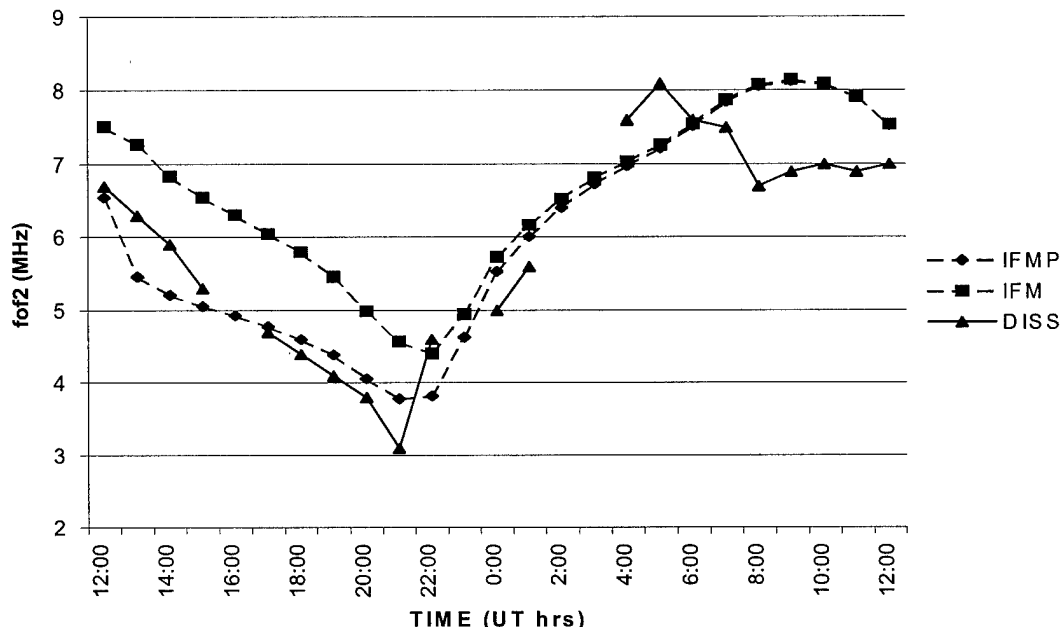


Figure 32. Learmonth 13-14 December foF2 data

Table 35. Learmonth 13-14 December foF2 data

TIME	Data (foF2 in MHz)			Absolute Error		Residual	
	IFMP	IFM	DISS	IFMP	IFM	IFMP	IFM
12:00	6.55	7.51	6.7	0.15	0.81	-0.15	0.81
13:00	5.46	7.27	6.3	0.84	0.97	-0.84	0.97
14:00	5.21	6.84	5.9	0.69	0.94	-0.69	0.94
15:00	5.06	6.55	5.3	0.24	1.25	-0.24	1.25
16:00	4.93	6.31					
17:00	4.78	6.05	4.7	0.08	1.35	0.08	1.35
18:00	4.6	5.8	4.4	0.20	1.40	0.20	1.40
19:00	4.39	5.46	4.1	0.29	1.36	0.29	1.36
20:00	4.06	4.99	3.8	0.26	1.19	0.26	1.19
21:00	3.78	4.57	3.1	0.68	1.47	0.68	1.47
22:00	3.82	4.41	4.6	0.78	0.19	-0.78	-0.19
23:00	4.63	4.95					
0:00	5.53	5.73	5	0.53	0.73	0.53	0.73
1:00	6.01	6.17	5.6	0.41	0.57	0.41	0.57
2:00	6.41	6.53					
3:00	6.73	6.82					
4:00	6.98	7.04	7.6	0.62	0.56	-0.62	-0.56
5:00	7.22	7.26	8.1	0.88	0.84	-0.88	-0.84
6:00	7.52	7.55	7.6	0.08	0.05	-0.08	-0.05
7:00	7.85	7.88	7.5	0.35	0.38	0.35	0.38
8:00	8.06	8.08	6.7	1.36	1.38	1.36	1.38
9:00	8.13	8.15	6.9	1.23	1.25	1.23	1.25
10:00	8.09	8.1	7	1.09	1.10	1.09	1.10
11:00	7.91	7.92	6.9	1.01	1.02	1.01	1.02
12:00	7.53	7.54	7	0.53	0.54	0.53	0.54
		IFM	IFMP			Lat	
Mean Absolute Error		0.93	0.61	Learmonth (LM 42B) -21.9			
Mean Residual		0.76	0.19	961213/14 Lon			
Correlation		0.88	0.90	114.00 E			

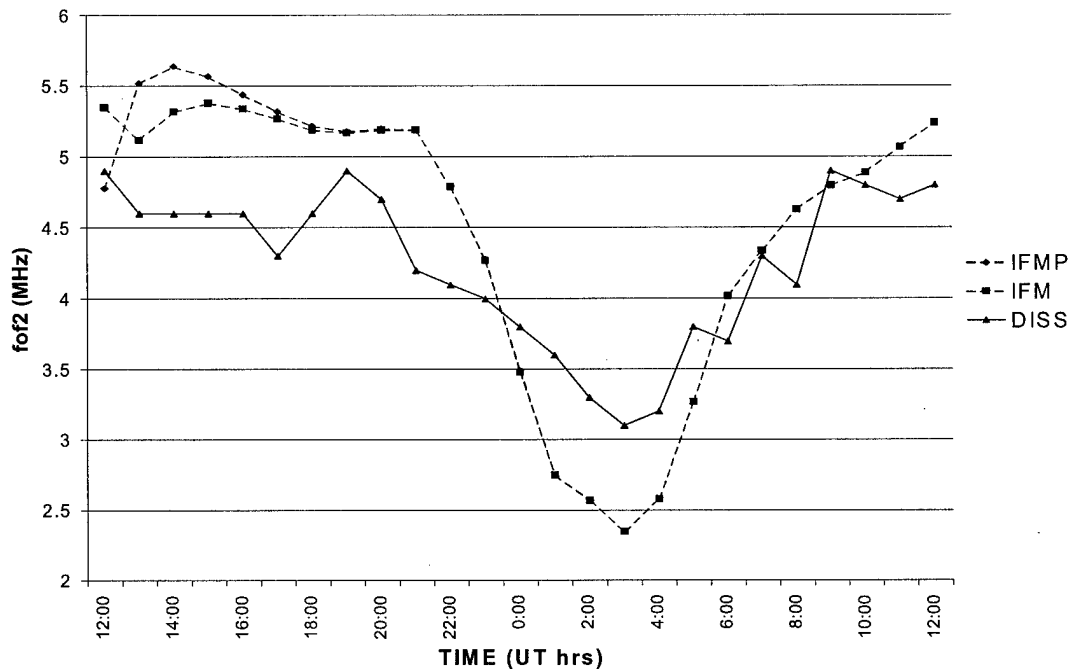


Figure 33. Lerwick 10-11 July foF2 data

Table 36. Lerwick 10-11 July foF2 data

TIME	Data (foF2 in MHz)			Absolute Error		Residual	
	IFMP	IFM	DISS	IFMP	IFM	IFMP	IFM
12:00	4.78	5.35	4.9	0.12	0.45	-0.12	0.45
13:00	5.52	5.12	4.6	0.92	0.52	0.92	0.52
14:00	5.64	5.32	4.6	1.04	0.72	1.04	0.72
15:00	5.57	5.38	4.6	0.97	0.78	0.97	0.78
16:00	5.44	5.34	4.6	0.84	0.74	0.84	0.74
17:00	5.32	5.27	4.3	1.02	0.97	1.02	0.97
18:00	5.22	5.19	4.6	0.62	0.59	0.62	0.59
19:00	5.18	5.17	4.9	0.28	0.27	0.28	0.27
20:00	5.2	5.19	4.7	0.50	0.49	0.50	0.49
21:00	5.19	5.19	4.2	0.99	0.99	0.99	0.99
22:00	4.79	4.79	4.1	0.69	0.69	0.69	0.69
23:00	4.28	4.27	4	0.28	0.27	0.28	0.27
0:00	3.49	3.48	3.8	0.31	0.32	-0.31	-0.32
1:00	2.75	2.75	3.6	0.85	0.85	-0.85	-0.85
2:00	2.57	2.57	3.3	0.73	0.73	-0.73	-0.73
3:00	2.35	2.35	3.1	0.75	0.75	-0.75	-0.75
4:00	2.58	2.58	3.2	0.62	0.62	-0.62	-0.62
5:00	3.27	3.27	3.8	0.53	0.53	-0.53	-0.53
6:00	4.02	4.02	3.7	0.32	0.32	0.32	0.32
7:00	4.34	4.34	4.3	0.04	0.04	0.04	0.04
8:00	4.63	4.63	4.1	0.53	0.53	0.53	0.53
9:00	4.8	4.8	4.9	0.10	0.10	-0.10	-0.10
10:00	4.89	4.89	4.8	0.09	0.09	0.09	0.09
11:00	5.07	5.07	4.7	0.37	0.37	0.37	0.37
12:00	5.24	5.24	4.8	0.44	0.44	0.44	0.44
	IFM	IFMP		Lat Lerwick (LE061) 60.13 N 960710/11		Lon 358.82 E	
Mean Absolute Error		0.53	0.58				
Mean Residual		0.21	0.25				
Correlation		0.91	0.90				

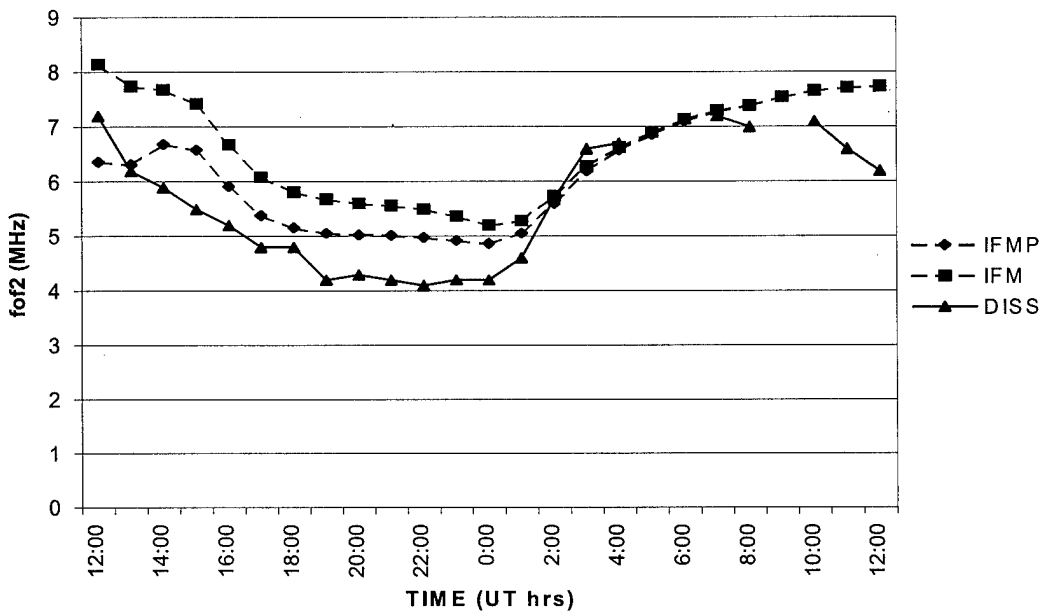


Figure 34. Tashkent 13-14 May foF2 data

Table 37. Tashkent 13-14 May foF2 data

TIME	Data (foF2 in MHz)			Absolute Error		Residual	
	IFMP	IFM	DISS	IFMP	IFM	IFMP	IFM
12:00	6.37	8.15	7.2	0.83	0.95	-0.83	0.95
13:00	6.32	7.75	6.2	0.12	1.55	0.12	1.55
14:00	6.69	7.69	5.9	0.79	1.79	0.79	1.79
15:00	6.59	7.43	5.5	1.09	1.93	1.09	1.93
16:00	5.92	6.68	5.2	0.72	1.48	0.72	1.48
17:00	5.39	6.09	4.8	0.59	1.29	0.59	1.29
18:00	5.16	5.82	4.8	0.36	1.02	0.36	1.02
19:00	5.06	5.69	4.2	0.86	1.49	0.86	1.49
20:00	5.03	5.61	4.3	0.73	1.31	0.73	1.31
21:00	5.02	5.57	4.2	0.82	1.37	0.82	1.37
22:00	4.98	5.51	4.1	0.88	1.41	0.88	1.41
23:00	4.92	5.37	4.2	0.72	1.17	0.72	1.17
0:00	4.87	5.21	4.2	0.67	1.01	0.67	1.01
1:00	5.06	5.29	4.6	0.46	0.69	0.46	0.69
2:00	5.6	5.75	5.7	0.10	0.05	-0.10	0.05
3:00	6.2	6.29	6.6	0.40	0.31	-0.40	-0.31
4:00	6.58	6.63	6.7	0.12	0.07	-0.12	-0.07
5:00	6.86	6.9					
6:00	7.11	7.14					
7:00	7.28	7.3	7.2	0.08	0.10	0.08	0.10
8:00	7.39	7.39	7	0.39	0.39	0.39	0.39
9:00	7.55	7.55					
10:00	7.66	7.66	7.1	0.56	0.56	0.56	0.56
11:00	7.72	7.72	6.6	1.12	1.12	1.12	1.12
12:00	7.74	7.74	6.2	1.54	1.54	1.54	1.54
				IFM	IFMP	Lat	
Mean Absolute Error				1.03	0.62	Tashkent (TQ241 41.33 N	
Mean Residual				0.99	0.57	960513/14 Lon	
Correlation				0.82	0.91	69.62 E	

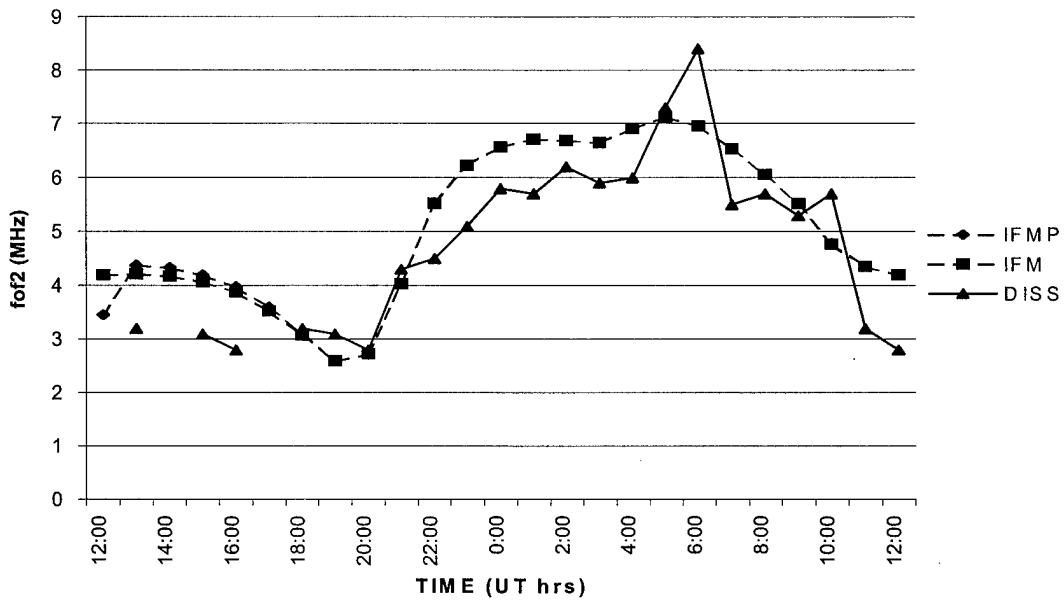


Figure 35. Townsville 17-18 September foF2 data

Table 38. Townsville 17-18 September foF2 data

TIME	Data (foF2 in MHz)			Absolute Error		Residual	
	IFMP	IFM	DISS	IFMP	IFM	IFMP	IFM
12:00	3.46	4.2					
13:00	4.38	4.22	3.2	1.18	1.02	1.18	1.02
14:00	4.33	4.18					
15:00	4.2	4.07	3.1	1.10	0.97	1.10	0.97
16:00	3.98	3.88	2.8	1.18	1.08	1.18	1.08
17:00	3.6	3.53					
18:00	3.11	3.08	3.2	0.09	0.12	-0.09	-0.12
19:00	2.6	2.6	3.1	0.50	0.50	-0.50	-0.50
20:00	2.72	2.73	2.8	0.08	0.07	-0.08	-0.07
21:00	4.04	4.04	4.3	0.26	0.26	-0.26	-0.26
22:00	5.54	5.53	4.5	1.04	1.03	1.04	1.03
23:00	6.24	6.23	5.1	1.14	1.13	1.14	1.13
0:00	6.57	6.57	5.8	0.77	0.77	0.77	0.77
1:00	6.72	6.72	5.7	1.02	1.02	1.02	1.02
2:00	6.69	6.69	6.2	0.49	0.49	0.49	0.49
3:00	6.65	6.65	5.9	0.75	0.75	0.75	0.75
4:00	6.91	6.91	6	0.91	0.91	0.91	0.91
5:00	7.13	7.13	7.3	0.17	0.17	-0.17	-0.17
6:00	6.96	6.96	8.4	1.44	1.44	-1.44	-1.44
7:00	6.54	6.54	5.5	1.04	1.04	1.04	1.04
8:00	6.06	6.06	5.7	0.36	0.36	0.36	0.36
9:00	5.52	5.52	5.3	0.22	0.22	0.22	0.22
10:00	4.78	4.77	5.7	0.92	0.93	-0.92	-0.93
11:00	4.36	4.36	3.2	1.16	1.16	1.16	1.16
12:00	4.2	4.2	2.8	1.40	1.40	1.40	1.40
		IFM	IFMP			Lat	
Mean Absolute Error		0.77	0.78	Townsville (TV51F -19.63 N			
Mean Residual		0.45	0.47	960917/18 Lon			
Correlation		0.88	0.88	146.85 E			

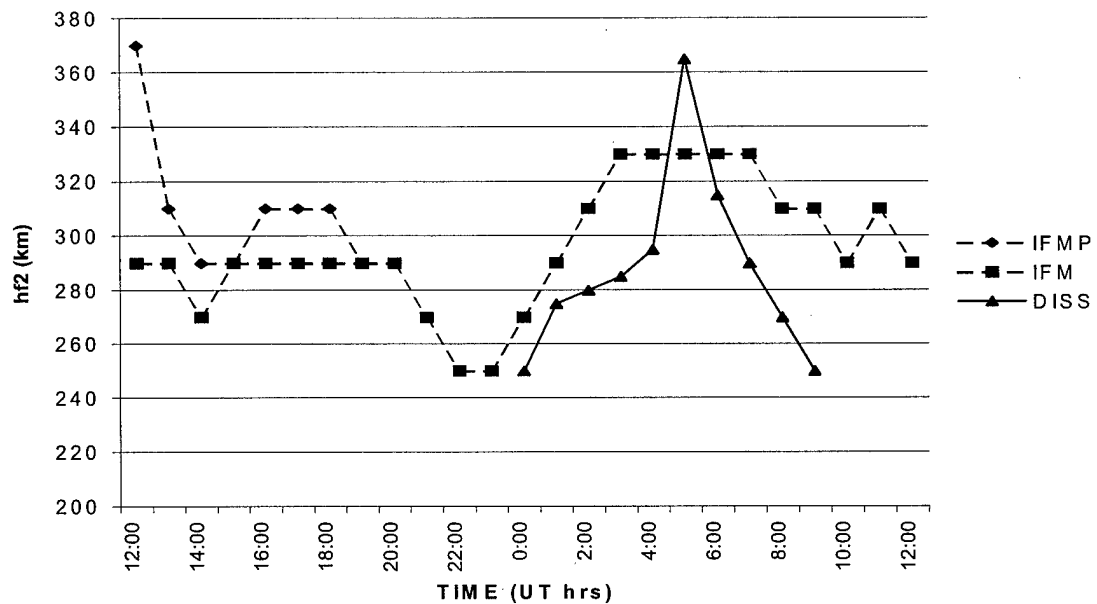


Figure 36. Chung-Li 18-19 September hmF2 data

Table 39. Chung-Li 18-19 September hmF2 data

TIME	Data (hmF2 in km)			Absolute Error		Residual		
	IFMP	IFM	DISS	IFMP	IFM	IFMP	IFM	
12:00	370	290						
13:00	310	290						
14:00	290	270						
15:00	290	290						
16:00	310	290						
17:00	310	290						
18:00	310	290						
19:00	290	290						
20:00	290	290						
21:00	270	270						
22:00	250	250						
23:00	250	250						
0:00	270	270	250	20.00	20.00	20.00	20.00	
1:00	290	290	275	15.00	15.00	15.00	15.00	
2:00	310	310	280	30.00	30.00	30.00	30.00	
3:00	330	330	285	45.00	45.00	45.00	45.00	
4:00	330	330	295	35.00	35.00	35.00	35.00	
5:00	330	330	365	35.00	35.00	-35.00	-35.00	
6:00	330	330	315	15.00	15.00	15.00	15.00	
7:00	330	330	290	40.00	40.00	40.00	40.00	
8:00	310	310	270	40.00	40.00	40.00	40.00	
9:00	310	310	250	60.00	60.00	60.00	60.00	
10:00	290	290						
11:00	310	310						
12:00	290	290						
	IFM	IFMP	Lat					
Mean Absolute Error		33.50	33.50	Chung-Li (CL 42.49 N				
Mean Residual		26.50	26.50	960918/19 Lon				
Correlation		0.64	0.64	121.24 E				

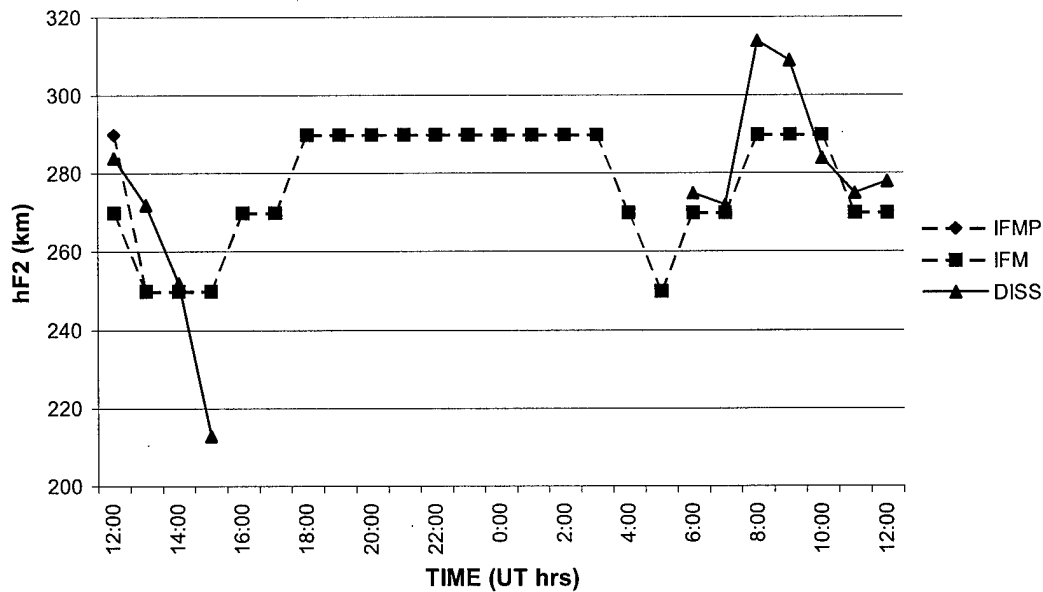


Figure 37. Grahamstown 18-19 September hmF2 data

Table 40. Grahamstown 18-19 September hmF2 data

TIME	Data (hmF2 in km)			Absolute Error		Residual	
	IFMP	IFM	DISS	IFMP	IFM	IFMP	IFM
12:00	290	270	284	6.00	14.00	6.00	-14.00
13:00	250	250	272	22.00	22.00	-22.00	-22.00
14:00	250	250	252	2.00	2.00	-2.00	-2.00
15:00	250	250	213	37.00	37.00	37.00	37.00
16:00	270	270					
17:00	270	270					
18:00	290	290					
19:00	290	290					
20:00	290	290					
21:00	290	290					
22:00	290	290					
23:00	290	290					
0:00	290	290					
1:00	290	290					
2:00	290	290					
3:00	290	290					
4:00	270	270					
5:00	250	250					
6:00	270	270	275	5.00	5.00	-5.00	-5.00
7:00	270	270	272	2.00	2.00	-2.00	-2.00
8:00	290	290	314	24.00	24.00	-24.00	-24.00
9:00	290	290	309	19.00	19.00	-19.00	-19.00
10:00	290	290	284	6.00	6.00	6.00	6.00
11:00	270	270	275	5.00	5.00	-5.00	-5.00
12:00	270	270	278	8.00	8.00	-8.00	-8.00
		IFM	IFMP			Lat	
Mean Absolute Error		13.00	13.00			Grahamstown (GF -33.30	
Mean Residual		-4.40	-4.40			960918/19 Lon	
Correlation		0.82	0.82			26.50 E	

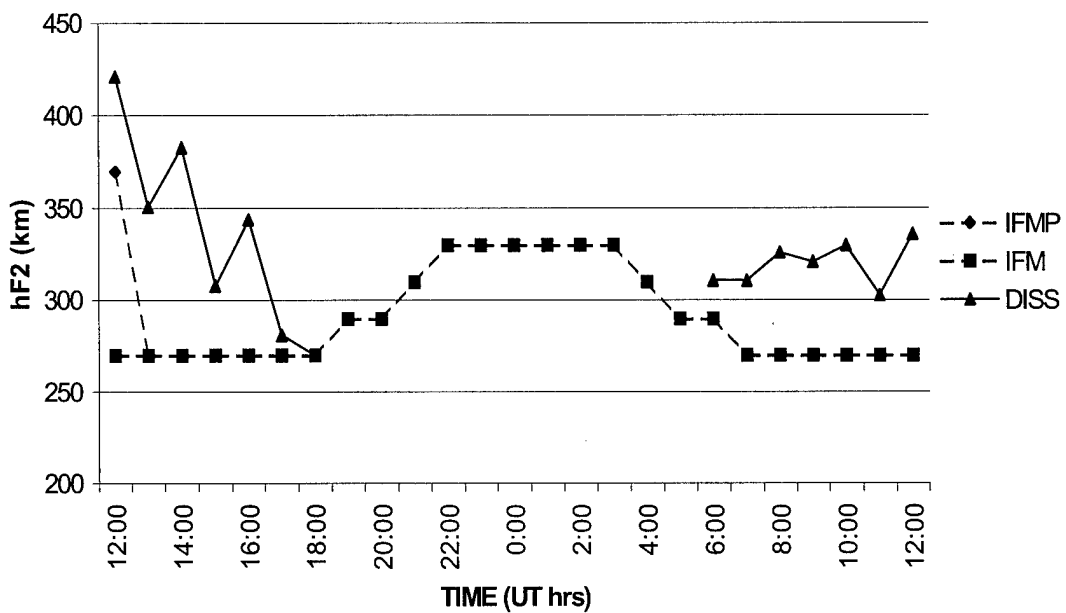


Figure 38. Lerwick 11-12 May hmF2 data

Table 41. Lerwick 11-12 May hmF2 data

Data (hF2 in km)				Absolute Error		Residual	
TIME	IFMP	IFM	DISS	IFMP	IFM	IFMP	IFM
12:00	370	270	421	51.00	151.00	-51.00	-151.00
13:00	270	270	351	81.00	81.00	-81.00	-81.00
14:00	270	270	383	113.00	113.00	-113.00	-113.00
15:00	270	270	308	38.00	38.00	-38.00	-38.00
16:00	270	270	344	74.00	74.00	-74.00	-74.00
17:00	270	270	281	11.00	11.00	-11.00	-11.00
18:00	270	270	270	0.00	0.00	0.00	0.00
19:00	290	290					
20:00	290	290					
21:00	310	310					
22:00	330	330					
23:00	330	330					
0:00	330	330					
1:00	330	330					
2:00	330	330					
3:00	330	330					
4:00	310	310					
5:00	290	290					
6:00	290	290	311	21.00	21.00	-21.00	-21.00
7:00	270	270	311	41.00	41.00	-41.00	-41.00
8:00	270	270	326	56.00	56.00	-56.00	-56.00
9:00	270	270	321	51.00	51.00	-51.00	-51.00
10:00	270	270	330	60.00	60.00	-60.00	-60.00
11:00	270	270	303	33.00	33.00	-33.00	-33.00
12:00	270	270	336	66.00	66.00	-66.00	-66.00
				IFM	IFMP	Lat	
Mean Absolute Error				49.62	49.62		
Mean Residual				-49.62	-49.62		
Correlation				-0.10	-0.10		
						Lon	
Lerwick (LE06160.13 N							
960511/12							
358.82 E							

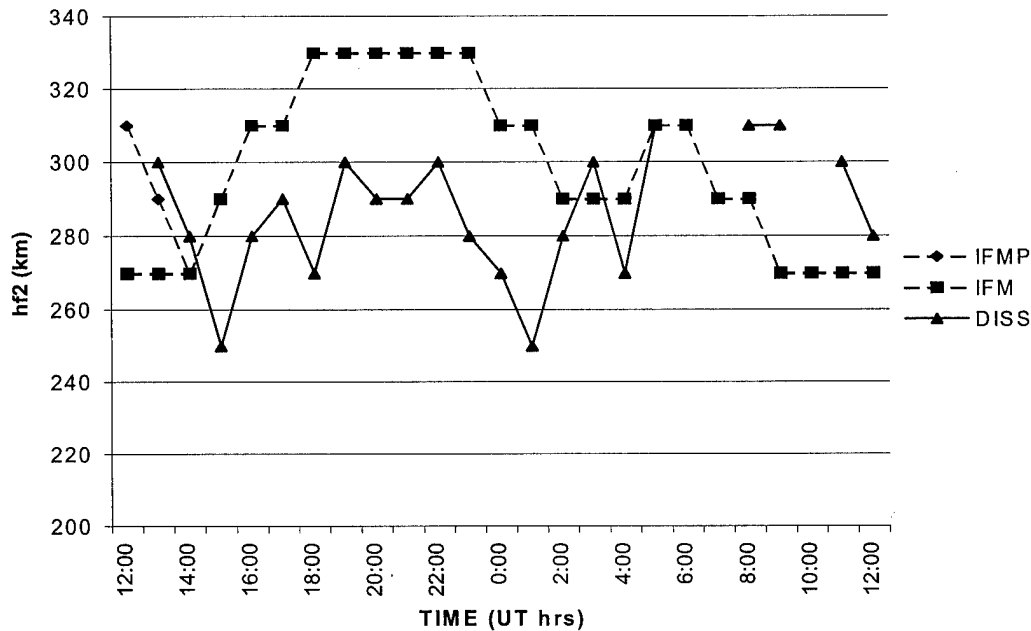


Figure 39. Tashkent 11-12 May hmF2 data

Table 42. Tashkent 11-12 May hmF2 data

TIME	Data (hmF2 in km)			Absolute Error		Residual	
	IFMP	IFM	DISS	IFMP	IFM	IFMP	IFM
12:00	310	270					
13:00	290	270	300	10.00	30.00	-10.00	-30.00
14:00	270	270	280	10.00	10.00	-10.00	-10.00
15:00	290	290	250	40.00	40.00	40.00	40.00
16:00	310	310	280	30.00	30.00	30.00	30.00
17:00	310	310	290	20.00	20.00	20.00	20.00
18:00	330	330	270	60.00	60.00	60.00	60.00
19:00	330	330	300	30.00	30.00	30.00	30.00
20:00	330	330	290	40.00	40.00	40.00	40.00
21:00	330	330	290	40.00	40.00	40.00	40.00
22:00	330	330	300	30.00	30.00	30.00	30.00
23:00	330	330	280	50.00	50.00	50.00	50.00
0:00	310	310	270	40.00	40.00	40.00	40.00
1:00	310	310	250	60.00	60.00	60.00	60.00
2:00	290	290	280	10.00	10.00	10.00	10.00
3:00	290	290	300	10.00	10.00	-10.00	-10.00
4:00	290	290	270	20.00	20.00	20.00	20.00
5:00	310	310	310	0.00	0.00	0.00	0.00
6:00	310	310					
7:00	290	290					
8:00	290	290	310	20.00	20.00	-20.00	-20.00
9:00	270	270	310	40.00	40.00	-40.00	-40.00
10:00	270	270					
11:00	270	270	300	30.00	30.00	-30.00	-30.00
12:00	270	270	280	10.00	10.00	-10.00	-10.00
				IFM	IFMP	Lat	
Mean Absolute Error				29.52	28.57	Tashkent (TQ 241 41.33 N	
Mean Residual				15.24	16.19	960511/12 Lon	
Correlation				-0.11	-0.08	69.62 E	

Appendix F: Glossary of Terms

DISS – Digital Ionospheric Sounding System – Surface remote sensing equipment that takes periodic observations of the ionosphere detecting such quantities as plasma frequency, electron density and heights of peak density layers.

DMSP – Defense Meteorological Satellite Program – meteorological satellites capable of taking *in situ* measurements of plasma parameters in the ionosphere.

E X B drift – The force on a charged particle (regardless of charge polarity) which causes it to accelerate in the **E X B** direction normal to both the **E** and **B** vectors.

F10.7 – An index of solar activity based on measurements of the 10.7 cm radio wave emissions from the sun.

foF2 – The plasma frequency at the density peak of the F2 layer of the ionosphere.

GPS – Global Positioning System – a constellation of satellites with provide precise navigational information. TEC data can be derived from them as well.

HF – High Frequency – refers to the portion of the electromagnetic spectrum between about 2 and 30 MHz. Used for long range communications by reflecting the signal off the ionosphere to points below the horizon.

hmF2 – the height of the density peak in the F2 layer of the ionospheres.

IMF – Interplanetary Magnetic Field – The magnetic field originating at the sun and carried out by the solar wind.

Kp – a global geomagnetic activity index. A value of 0 indicates undisturbed conditions while a value of 9 represents very disturbed conditions.

PRISM – Parameterized Real-Time Ionospheric Specification Model

PIM – Parameterized Ionospheric Model

SSN – Sunspot Number – An indicator of solar activity representing the number of sunspots on the visible disk with adjustments made for observer error.

TEC – Total Electron Content – The height integrated number of electrons in a column one square meter at its base.

Bibliography

1. Coxwell, R. D., Validation of the Parameterized Real-Time Ionospheric Specification Model (PRISM) Version 1.6b Using TOPEX Total Electron Content (TEC) Data, MS Thesis, AFIT/ENP/GAP/96D. School of Engineering, Air Force Institute of Technology (AETC), Wright-Patterson AFB OH, 1996
2. Fejer, B. G., E. R. de Paula, R. A. Heelis, and W. B. Hanson, "Global Equatorial Ionospheric Plasma Drifts Measured by the AE-E Satellite", J. Geophys. Res., 100: 5769-5776, 1995
3. Hardy, D. A., M. S. Gussenhoven, and E. Holeman, "A Statistical Model of Auroral Electron Precipitation", J. Geophys. Res., 90: 4229-4238, 1985
4. Heppner, J. P., and N. C. Maynard, "Empirical High-latitude Electric Field Models", J. Geophys. Res., 92: 4467-4489, 1987
5. Kelley, Michael C. The Earth's Ionosphere Plasma Physics and Electrodynamics, San Diego CA: Academic Press, Inc, 1989
6. McClave, J. T. and F.H. Dietrich II, Statistics, San Francisco CA: Dellen Publishing Company, 1991
7. Rees, M. H. Physics and Chemistry of the Upper Atmosphere. Cambridge: Cambridge University Press, 1989.
8. Schunk, R.W. et al. Expanded Capabilities for the Ionospheric Forecast Model: Final Report, 12 May 1994-30 September 1997. Contract F19628-94-C-0046. Logan UT: Space Environment Corporation, December 1997 (AFRL-VS-HA-TR-98-0001)
9. Shea, M. A. and D. F. Smart. "Space Weather: The Effects on Operations in Space" Advances in Space Research, 22: 29-38, 1998
10. Tascione, Thomas F. Introduction to the Space Environment. Malabar FL: Krieger Publishing Company, 1994.
11. Titheridge, J. E., "Aeronomical Calculations of Valley Size in the Ionosphere", Advances in Space Research, 10: 21-24, 1990.

Vita

Captain Michael D. Scott was born on 19 January 1964 in Joplin, Missouri. He graduated from Lawrence D. Bell High School in Hurst, Texas in May 1982. He enlisted in the Air Force in August 1982 and had numerous assignments until January 1994 when he entered Florida State University in Tallahassee, Florida. He graduated from Florida State University in August 1995 with a Bachelor of Science Degree in Meteorology. He was commissioned through Officer Training School at Maxwell AFB, Alabama in November 1995.

Captain Scott's initial assignment upon commissioning was to the 3d Weather Squadron at Fort Hood, Texas. He served as the Garrison Flight Commander, and as the Staff Weather Officer to the 1st Cavalry Division. He participated in numerous exercises and supported the Division's preparations for peacekeeping duties in Bosnia. In September 1998, he entered the Graduate Applied Physics program, School of Engineering, Air Force Institute of Technology. Upon Graduation, he will be assigned to Offutt AFB, Nebraska.

Permanent Address: 205 Arthur Dr.
Hurst, Texas 76053

REPORT DOCUMENTATION PAGE			Form Approved OMB No. 0704-0188
<p>Public reporting burden for this collection of information is estimated to average 1 hour per response, including the time for reviewing instructions, searching existing data sources, gathering and maintaining the data needed, and completing and reviewing the collection of information. Send comments regarding this burden estimate or any other aspect of this collection of information, including suggestions for reducing this burden, to Washington Headquarters Services, Directorate for Information Operations and Reports, 1215 Jefferson Davis Highway, Suite 1204, Arlington, VA 22202-4302, and to the Office of Management and Budget, Paperwork Reduction Project (0704-0188), Washington, DC 20503.</p>			
1. AGENCY USE ONLY (Leave blank)	2. REPORT DATE	3. REPORT TYPE AND DATES COVERED	Master's Thesis
4. TITLE AND SUBTITLE		Validation of the Ionospheric Forecast Model (IFM) Version 3	
6. AUTHOR(S)		Michael D. Scott, Captain, USAF	
7. PERFORMING ORGANIZATION NAME(S) AND ADDRESS(ES)		8. PERFORMING ORGANIZATION REPORT NUMBER	
Air Force Institute of Technology Graduate School of Engineering and Management (AFIT/EN) 2950 P Street, Building 640 WPAFB, OH 45433-7765		AFIT/GAP/ENP/00M-04	
9. SPONSORING/MONITORING AGENCY NAME(S) AND ADDRESS(ES)		10. SPONSORING/MONITORING AGENCY REPORT NUMBER	
SMC DET11/CID 1050 East Stewart Avenue, Building 2025 Peterson AFB, CO 80914-2902			
11. SUPPLEMENTARY NOTES			
Prof. David E. Weeks, ENP, DSN: 785-3636 ext. 4561			
12a. DISTRIBUTION AVAILABILITY STATEMENT		12b. DISTRIBUTION CODE	
APPROVED FOR PUBLIC RELEASE; DISTRIBUTION UNLIMITED			
13. ABSTRACT (Maximum 200 words)			
<p>The purpose of this research was to validate the Ionospheric Forecast Model (IFM) Version 3 to assess its usefulness as an operational tool. The IFM is a first principles computer model designed to forecast the state of the global ionosphere to 24 hours. The scope was limited to a comparison of the F2 layer critical frequency ($foF2$) and height of peak electron density ($hmF2$) against observed ionosonde data. The model was run with global solar and geomagnetic indices and Information from Digital Ionospheric Sounding System (DISS) observations as inputs. The IFM was run for a total of 25 days spread throughout 1996. It was run twice for each 24-hour period: once without any DISS input, and again, with data from as many as 50 DISS stations. The output from the IFM was compared against the observations from 10 stations. Analysis of $foF2$ showed the IFM did well with a slight bias to over forecast the values, but a small absolute error and good correlation. Analysis of the $hmF2$ showed a tendency for the model to under forecast values. $hmF2$ forecasts had large errors and very poor correlation. There was surprisingly little difference between the results with DISS input and without.</p>			
14. SUBJECT TERMS		15. NUMBER OF PAGES	
Ionosphere, Ionospheric Forecast Model, Space Environment, Space Physics, Space Forecast Models, SETT Models		108	
16. PRICE CODE			
17. SECURITY CLASSIFICATION OF REPORT	18. SECURITY CLASSIFICATION OF THIS PAGE	19. SECURITY CLASSIFICATION OF ABSTRACT	20. LIMITATION OF ABSTRACT
UNCLASSIFIED	UNCLASSIFIED	UNCLASSIFIED	UL